Dominik Huber, Bsc

Improving Soluble Periplasmic Antibody Fragment Production in *Escherichia coli* by Folding-Modulator Gene Co-Expression

MASTER'S THESIS

to achieve the university degree of

Diplom-Ingenieur

Master's degree programme: Biotechnology

submitted to

Graz University of Technology

SUPERVISORS

Univ.-Prof. Dipl.-Ing. Dr.techn. Bernd Nidetzky
Instutite of Biotechnology and Bioprocess Engineering

Dr. Simon Stammen
Boehringer Ingelheim RCV Process Science - Molecular Biology & Expression Systems

Graz, January 2016

Affidavit

I declare that I have authored this thesis independently, that I have not used other than the declared sources/resources, and that I have explicitly indicated all material which has been quoted either literally or by content from the sources used. The text document uploaded to TUGRAZonline is identical to the present master‘s thesis dissertation.

_____ _____

Date Signature

Die nachfolgende Arbeit enthält vertrauliche Daten des Unternehmens Boehringer Ingelheim RCV GmbH & Co KG.

Veröffentlichungen beziehungsweise Vervielfältigung der Arbeit, ganz oder auch nur teilweise, sind ohne ausdrückliche Genehmigung seitens Boehringer Ingelheim RCV GmbH & Co KG nicht gestattet.

Die Sperrung der Arbeit erstreckt sich zunächst über einen Zeitraum von zwei Jahren. Eine Verlängerung dieses Zeitraums um weitere drei Jahre ist vorgesehen. Nach Ablauf der Sperre ist die Masterarbeit nur der Bibliothek der Technischen Universität Graz zugänglich zu machen, und darf nicht online verfügbar sein.

Januar, 2016

Abstract

The production of soluble and properly folded disulfide-bond containing therapeutic proteins (e.g. antibody fragments) in the periplasm of *Escherichia coli* constitutes a reasonable alternative to the production as inclusion bodies and subsequent *in vitro* refolding. A strain for soluble production of the model antibody fragment FabZ was developed in a previous part of this project. Production experiments with this strain resulted in significant levels of periplasmic FabZ aggregates. Since several studies have shown a positive effect of co-production of folding modulators on the soluble periplasmic production of recombinant proteins, an appropriate co-expression system should be developed in this work to improve soluble FabZ yields. Due to lack of knowledge which level of folding modulator co-production is suitable, the system was based on various strength constitutive promoters. These control the expression of one of the six periplasmic folding modulator genes *dsbA*, *dsbC*, *fkpA*, *ppiD*, *skp* and *surA.* The system was tested for improved FabZ production in shake flask and fed-batch fermentation experiments.

Based on results of a promoter test three constitutive promoter modules with different synthesis rates were selected and used for the creation of folding modulator gene co-expression plasmids. It was shown in both production scales that the new basic co-expression system did not interfere noticeably with target gene expression. Co-expression of *fkpA*, *surA* and *skp* at each level exerted a positive influence on total soluble FabZ yields in shake flask experiments. Skp co-production controlled by promoter module C2 increased total soluble FabZ yields 4.6-fold. This increase constituted the strongest positive influence observed in shake flask experiments. Co-synthesis of DsbA, DsbC and PpiD had no effect on soluble FabZ production or even exerted a negative influence. The newly established co-expression system was also applied successfully in the fed-batch fermentation process. FkpA co-production controlled by promoter module Ci resulted in up to 1.5-fold enhanced FabZ product titres. In contrast to results from shake flask experiments, the other co-synthesis approaches did not reveal a positive effect on soluble FabZ yields in the fed-batch fermentation experiments.

The developed co-expression system turned out to be suitable for screening and production applications. Furthermore, the findings of this work revealed that results of the applied shake flask approach were not predictive for the outcome of the fermentation process. Thus, the optimization of the small-scale system with improved predictive power is advisable.

Zusammenfassung

Die lösliche Produktion von korrekt gefalteten therapeutischen Proteinen mit Disulfidbrücken (z.B. Antikörperfragmenten) im Periplasma von *Escherichia coli*, ist eine ökonomisch attraktive Alternative zur Produktion als „Inclusion Bodies“ mit anschließender *in vitro* Rückfaltung. In vorangegangenen Projektarbeiten wurde ein Stamm entwickelt, der für die lösliche Produktion des Model - Antikörperfragments FabZ verwendet werden kann. Produktionsversuche mit diesem Stamm führten zur Bildung signifikanter Mengen an periplasmatischen FabZ Aggregaten. Da mehreren Studien einen positiven Einfluss einer Co-Produktion von Faltungshelfern auf die lösliche periplasmatische Produktion von rekombinanten Proteinen gezeigt haben, sollte ein dieser Arbeit ein Co-Expressionssystem entwickelt werden, welches die löslichen Ausbeuten von FabZ steigern kann. Da man vorher nicht wusste, welches Level eines co-produzierten Faltungshelfers nützlich sein könnte, wurden verschieden starke konstitutive Promotoren für das System verwendet. Die Expression der einzelnen Faltungshelfergene *dsbA*, *dsbC*, *fkpA*, *ppiD*, *skp* und *surA* sollte durch diese unterschiedlich starken Promotoren kontrolliert werden. In Schüttelkolben- und Fermentationsexperimenten wurde anschließend der Einfluss des entwickelten Systems auf das Produktionsverhalten des FabZ-Produktionsstammes getestet.

In Promotortests wurden drei konstitutive Promotoren mit unterschiedlichen Stärken identifiziert, die anschließend zur Herstellung der Co-Expressionsplasmide verwendet wurden. In beiden Produktionsmaßstäben konnte gezeigt werden, dass das neue Grundplasmid ohne Faltungshelfer die Expression des Zielgenes kaum beeinflusste. In unterschiedlichem Maße gesteigerte zelluläre Level von FkpA, Skp und SurA führten in den Schüttelkolben-Versuchen zu teilweise erheblich gesteigerten Ausbeuten an löslichem FabZ. Die maximale Steigerung um den Faktor 4.6 wurde bei der durch den Promoter C2 gesteuerten Co-Produktion von Skp erreicht. Die Co-Synthese von DsbA, DsbC und PpiD hatte keine positiven Auswirkungen auf die gemessene Konzentration an löslichem FabZ. Das neue Co-Expressionssystem wurde auch erfolgreich im Fermentationsprozess angewandt. Eine durch den Promoter Ci gesteuerte FkpA Co-Produktion steigerte die Titer an löslichem FabZ im Fermentations-Versuch um das 1,5-fache. Im Gegensatz zu den Ergebnissen aus Schüttelkolben-Versuchen zeigten alle anderen Co-Synthese Versuche unter den Fermentationsbedingungen keinen positiven Einfluss auf die Ausbeuten an löslichem FabZ.

Die erfolgreiche Anwendung in Co-Produktionsversuchen legt nahe, dass das neue Co-Expressionssystem für Screening- und Produktionszwecke gut geeignet ist. Allerdings konnte auch festgestellt werden, dass anhand der Ergebnisse des verwendeten Schüttelkolbenansatzes die Resultate des Fermentationsprozesses nicht vorhergesagt werden können. Daher scheint es notwendig, den Schüttelkolbenansatz im Hinblick auf eine erhöhte Vorhersagekraft zu optimieren.

Table of Contents

List of Abbreviations

ADCC	Antibody-dependent cellular cytotoxicity
AGE	Agarose gel electrophoresis
ANOVA	Analysis of variance
bp	Base pairs
BSA	Bovine serum albumin
CDC	Complement-dependent cytotoxicity
CoV	Coefficient of variation
DCW	Dry cell weight
DO	Dissolved oxygen
ELISA	Enzyme linked immunosorbent assay
EoF	End of fermentation
Fab	Fragment antibody binding
Fc	Fragment crystallisable
FKBP	FK506-binding protein
FM	Folding modulator
GFP	Green fluorescent protein
GoI	Gene of interest
HC	Heavy chain
HRP	Horse reddish peroxidase
IB	Inclusion body
Ig	Immunglobulin
IPTG	Isopropyl-β-D-thiogalactopyranosid

LC	Light chain
MCS	Multiple cloning site
o/n	Over night
OD	Optical density
OD_{550}	Optical density measured at 550 nm
OmpA	Outer membrane protein A
Ori	Origin of replication
PCN	Plasmid copy number
PMF	Proton-motive force
PPIase	Peptidyl-prolyl isomerase
RBS	Ribosomal binding site
REN	Restriction endonuclease
RFU	Relative fluorescence unit
RO-H_2O	Reverse osmosis water
RT	Room temperature
scFv	Single chain fragment variable
SDS-PAGE	Sodium dodecyl sulfate polyacrylamide gel electrophoresis
SRP	Signal recognition particle
TAE	Tris-acetate-EDTA
TAT	Twin-arginine translocation
TE	Termination efficiency
TF	Trigger factor
UTR	Untranslated region

1. Introduction

1.1. Track Record of Biopharmaceuticals

In 1982 human insulin was approved for therapeutic use as the first pharmaceutical produced entirely by means of recombinant DNA technology in the bacterium *Escherichia coli* (*E. coli*) (FDA 1982). Subsequently, therapeutics produced by biotechnological techniques, termed biopharmaceuticals, captured the pharmaceutical market. In 2010 one third of all drugs under development were biopharmaceuticals (Sekhon 2010). For the production of biopharmaceuticals microbial cells (including bacteria and yeasts), insect cells, mammalian cells, plant cells as well as transgenic animals and plants can be applied (Sekhon 2010). For example, blood factors, hormones, thrombolytic agents, interferons, antibodies, haematopoietic growth factors, interleukin-based products, vaccines and therapeutic enzymes all belong to the class of biopharmaceuticals (Walsh 2003). These drugs have revolutionized the way in which cancer, diabetes, multiple sclerosis, hepatitis, viral infections and several other severe diseases are treated (Sekhon 2010). Until 2014 the number of approved biopharmaceuticals has reached 246 (Walsh 2014). The market value of biopharmaceuticals reached a total cumulative sales value of $ 140 billion in 2013 (Walsh 2014) and global revenues of $ 163 billion were gained in 2014 (Otto et al. 2014). In the next few years antibodies and antibody-derived products were predicted to constitute the most prominent and fastest growing class of biopharmaceuticals (Walsh 2014). It was reviewd that in 2010 antibody therapeutics comprised almost 50 % of the entire protein therapeutic market and led to total sales of approximately $ 81 billion (Jeong et al. 2011). Several therapeutic antibody products such as Avastin, Herceptin, Humira, Erbitux, Remicade and Rituxan have already reached blockbuster status (Spadiut et al. 2014).

1.2. Antibodies and Antibody Fragments

Antibodies are part of the immune system and belong to the protein class of immunoglobulins (Igs). They are responsible for the identification and neutralization of foreign substances like viruses or bacteria. Antibodies can bind to their corresponding antigens, which are specific parts of the foreign substance (Janeway et al. 2001). Upon binding of the antibody, the foreign substance is neutralized or marked for the following destruction by other defence systems such as phagocytes. As previously reviewed, antibodies are used for several therapeutic applications as well as in the research and diagnostic field (Frenzel et al. 2013). Potential medical applications of antibodies include the detection and treatment of bacterial infections, cardiovascular diseases, vein thrombosis, septic shocks, autoimmune disorders and cancer (Walsh 2003).

A typical antibody is Y-shaped (see Figure 1-1) and has two identical antigen binding sites at the end of the arms of the Y (Elgert 2009). Antibodies are composed of two identical heavy chains (HCs) of 50 - 70 kDa and two identical light chains (LCs) of approximately 25 kDa. In the hinge region the antibody molecule is stabilized by intermolecular disulfide bonds between the two HC monomers. Each HC is linked to an LC monomer by another intermolecular disulfide bond. For stabilization each monomer contains further intramolecular disulfide bonds. Two different types of LCs are present in antibodies, which are termed λ and κ, but do not confer a different function. There are five main types of HCs (μ, δ, γ, α and ε) which define the corresponding class of the Ig leading to the five isotypes IgM, IgD, IgG, IgA and IgE. The type of HC determines the functional properties and effector mechanism of the antibody. LC and HC consist of 2 and 4 similar 110 amino acid long immunoglobulin domains. Both are composed of variable and constant regions. The variable regions consist of the amino-terminal variable domain of the LC and HC (V_L and V_H) and determine the antigen binding sites. The remaining domains of the LC and HC are constant between antibodies of the same isotype and make up the C terminal constant region (C_L and C_H) (Janeway et al. 2001).

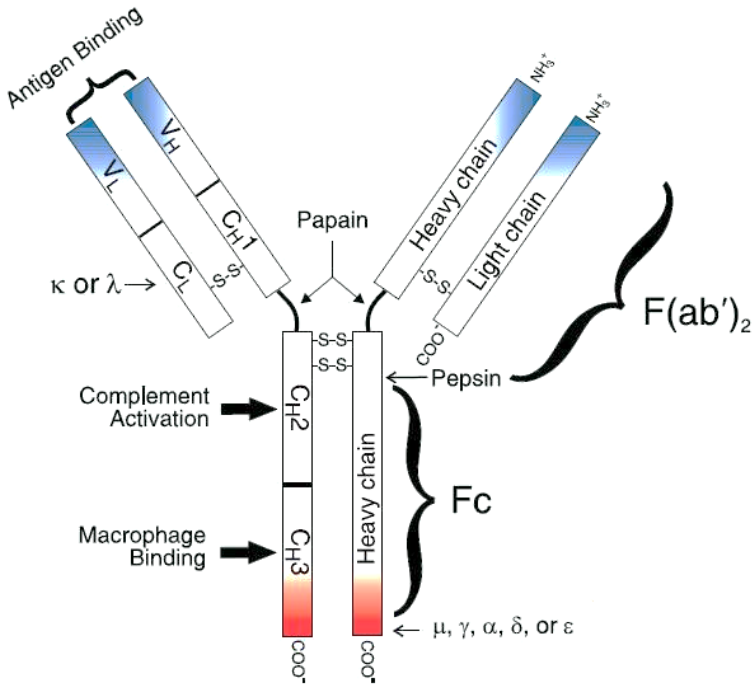

Figure 1-1: Schematic representation of an antibody molecule. The structure of a Y-shaped antibody with respective heavy chain (μ, δ, γ, α or ε) and light chain (λ or κ) is shown. Intermolecular disulfide bonds (S-S) and flexible hinge region are depicted. The amino terminal variable region is composed of V_L and V_H domains and is responsible for antigen binding. The constant region of the light chain is composed of the C_L domain and the constant region of the heavy chain is composed of the C_H1, C_H2 and C_H3 domains. Effector functions of the C_H2 and C_H3 domains are indicated. The cleavage site of the enzymes papain and pepsin are shown. Enzymatic digestion with papain yields two Fab fragments and one Fc fragment. Enzymatic digestion with pepsin yields one $F(ab')_2$ fragment. The figure was adapted from the Life Technologies Molecular Probes Handbook (LifeTechnologies 2010).

Different antibody fragments can be obtained by cleavage of the full-size antibody with different proteases. Enzymatic digestion with papain cleaves the antibody into two identical antigen-binding fragments (Fab) and a crystallisable fragment (Fc). The Fab fragments exhibit full antigen binding activity and consist of the complete LC and the V_H and C_H1 domains of the HC linked by an intermolecular disulfide bond (Janeway et al. 2001). The Fc fragment consists of the C_H2 and C_H3 domains and is glycosylated at position Asn^{297} (Jeong et al. 2011). It has no antigen-binding activity but can interact with cells and effector molecules (Janeway et al. 2001). A $F(ab')_2$ fragment is obtained upon enzymatic digestion with pepsin. Pepsin cuts on the carboxy-terminal side of the hinge region so that the two antigen-binding arms remain linked. The smallest antibody fragments with antigen binding capacity are the single V_L or V_H domains (Frenzel et al. 2013). By connecting the V_L and V_H domains by an artificial peptide linker, scFv (single chain fragment variable) molecules can be obtained (Janeway et al. 2001). In Figure 1-2 various antibody fragments are represented.

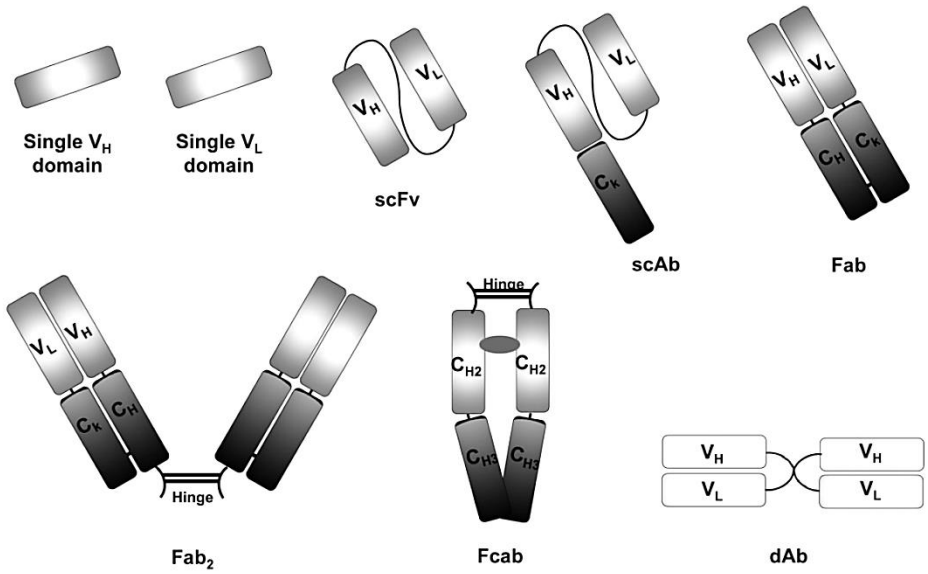

Figure 1-2: Schematic presentation of various antibody fragments. The smallest antibody fragments with antigen binding capacity are the single V_H and V_L domains. In scFv, scab and dAb molecules the variable domains are connected by artificial peptide linkers. In Fab, Fab_2 and Fcab molecules HC and LC are covalently linked by disulfide bonds. The Fcab molecule consists of the Fc region and thus requires glycosylation at position Asn^{297}. This figure was copied from a previously published review article (Jeong et al. 2011).

Like full-size antibodies, antibody fragments are most frequently used for the treatment of cancerous and immunological diseases but also to treat cardiovascular and infectious diseases and ophthalmic conditions (Nelson & Reichert 2009). However, most antibody fragments are mainly used in therapeutic application where the binding to the antigen is sufficient for the desired effect such as receptor blocking or pathogen neutralization (Frenzel et al. 2013). In addition to the therapeutic applications, antibody fragments can also be used for bioseparation, immunodetection and purification approaches (A. DeMarco 2011).

The inability to induce effector functions such as antibody-dependent cellular cytotoxicity (ADCC) and complement-dependent cytotoxicity (CDC) constitutes the main drawback of antibody fragments lacking the Fc-region (Sanz et al. 2005). Further potential drawbacks of antibody fragments compared to full-size antibodies include lower stability (Bird et al. 1988) and shorter circulating half-lives in humans due to a rapid blood clearance (Larson et al. 1983). However, the half-life of antibody fragments can for example be extended by strategies such as PEGylation (A. Jain & S. K. Jain 2008) and conjugation to albumin (Holt et al. 2008). On the other hand, there are some advantages of antibody fragments compared to the full-size molecules. Because of their smaller size, antibody fragments have more effective tissue penetration abilities (Nelson & Reichert 2009). Antibody fragments which lack the glycosylated Fc region also exhibit a reduced immunogenic potential compared to the full-size molecules (Ahmad et al. 2012). Small non-glycosylated antibody fragments (e.g. V_L and V_H domains, scFv, Fab or dAb molecules) can be produced using microbial expression systems. It was reviewed that the production of antibody fragments in microbial hosts could constitute an easy and economical alternative compared to mammalian cell culture systems which are usually used for the production of full-size antibodies and glycosylated antibody fragments (Holliger & Hudson 2005). Among microbial expression system, *E. coli* is most commonly used for the production of antibody fragments. Lucentis® and Cimza® are two previously approved Fab fragments which were produced in *E. coli*.

1.3. Production of Biopharmaceuticals in *Escherichia coli*

The gram-negative bacterium *E. coli* is to date the most commonly used organism for the production of recombinant proteins. Somatostatin was the first recombinant human therapeutic protein to be successfully generated in *E. coli* (Itakura et al. 1977). Since then, many biopharmaceuticals such as hormones, growth factors, thrombolytic agents, antibody fragments and interferons have been produced in *E. coli* (Walsh 2010). In January 2009 approximately 30 % of all recombinant proteins which were approved as biopharmaceuticals by the FDA and EMEA were produced in *E. coli* (Ferrer-Miralles et al. 2009).

E. coli has several advantages as a production organism. These were recently reviewed and include the availability of many molecular biology tools and protocols, the fast growth kinetics, the growth to high cell densities and the effortlessness of transformation with exogenous DNA (Rosano & Ceccarelli 2014). *E. coli's* appealing production host profile is completed by the simple process scale-up, the ability to grow on low cost media and thus the cost-effective production of recombinant proteins (Spadiut et al. 2014). On the contrary, recombinant protein production in *E. coli* is often limited by the inability to perform certain posttranslational modifications such as glycosylation. Further limitations include insufficiencies in disulfide bond formation and proteolytic protein maturation. Production of complex proteins of eukaryotic origin, which require adequate folding and glycosylation, is thus hardly feasible in *E. coli* (Kamionka 2011). Unbalanced production of recombinant

proteins can lead to high amounts of unfolded and misfolded proteins in the cytoplasm resulting in inclusion body (IB) formation (Marston 1986). Figure 1-3 illustrates advantages and disadvantages of using *E. coli* as general expression host and for cytoplasmic and periplasmic protein production.

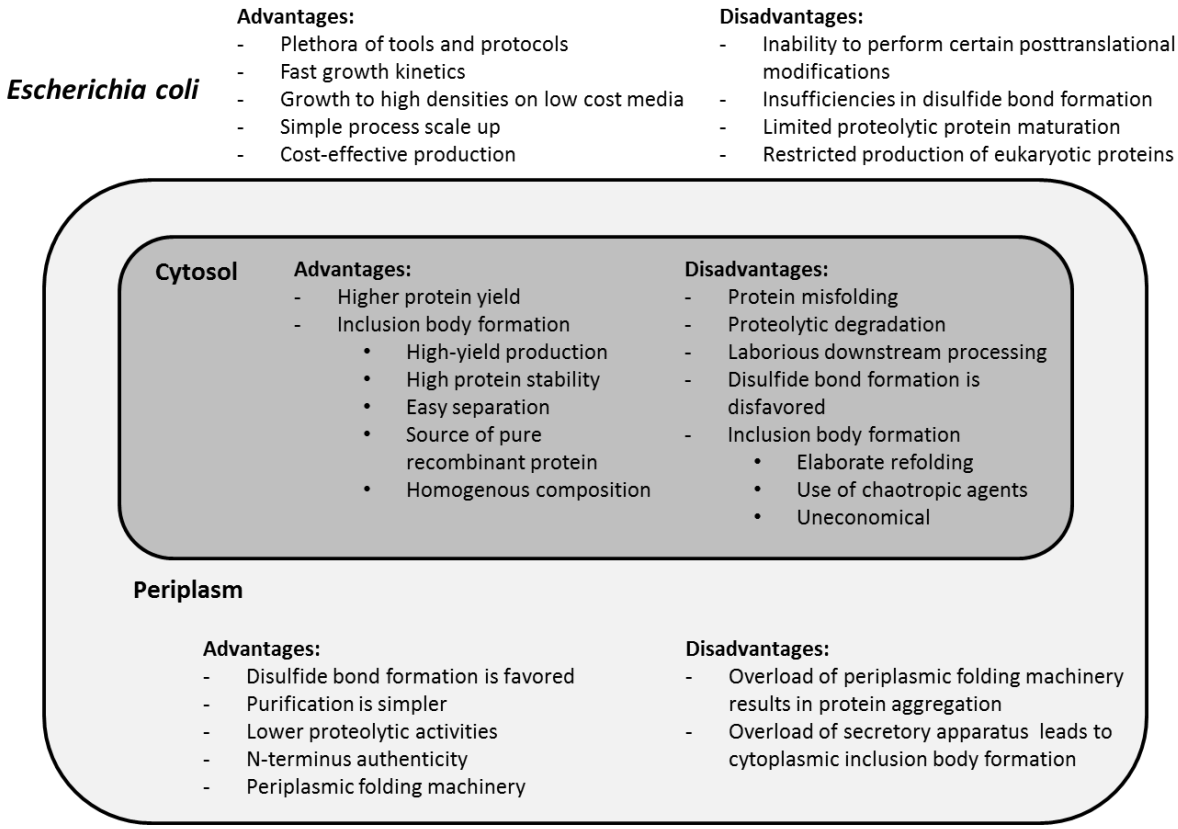

Figure 1-3: Advantages and disadvantages of *E. coli* for production of biopharmaceuticals. General advantages and disadvantages of using *E. coli* as a production organism are indicated. In addition, benefits and drawbacks of cytoplasmic and periplasmic production processes are listed.

Because of several advantages, IB formation is exploited for the production of certain biopharmaceuticals. For example, high-yield production and high stability of protein aggregates are advantages of the IB process and have been previously reviewed (Huang et al. 2012). Upon cell disruption, IBs can be easily separated from other bacterial components and can thus can be a source of relatively pure recombinant proteins (Singh & Panda 2005). In addition, IBs are relatively homogeneous in composition and more than 90 % of the total imbedded polypeptides can be constituted by the recombinant protein (Villaverde & Carrió 2003). However, IBs have to be fully denaturated and refolded *in vitro* to regain the biological functionality of the native protein (Lee et al. 2006). Refolding of IBs to active proteins is often challenging as refolding strategies have to be optimized for each target protein. In addition, chaotropic agents used for the resolubilisation of IBs often negatively affect the quality of the refolded proteins (Sahdev et al. 2008). The economic feasibility of an IB process has to be evaluated for each product (Lee et al. 2006). The refolding and

purification of proteins from IBs is in many cases more expensive and time consuming than the purification of soluble proteins (Sørensen & Mortensen 2005). For example, high-level cytoplasmic antibody fragment production in *E. coli* was investigated by expression both, LC and HC separately as IBs. However, the refolding process of the IBs was not efficient and not economically competitive (Harrison & Keshavarz-Moore 1996). Hence, soluble production of recombinant target proteins represents an appealing alternative to *in vitro* refolding procedures.

1.4. Soluble Protein Production in the Bacterial Periplasm

1.4.1. Advantages of the Periplasm and its Folding Modulators

As mentioned above the IB process can be affiliated with severe drawbacks for the production of therapeutic proteins. Thus, soluble protein production represents an interesting alternative compared to the IB process as cumbersome refolding strategies can be avoided. In *E. coli* soluble proteins can be produced in the cytoplasm or in the periplasm.

In the *E. coli* cytoplasm high levels of proteases, reductases and reducing agents are present. Due to the thioredoxin-thioredoxin reductase (trxB) and the glutaredoxin-glutaredoxin reductase (gor) systems the cytoplasm is maintained as a reducing environment and thus disulfide bond formation can barely be accomplished (Stewart et al. 1998). Hence, the cytoplasm of *E. coli* appears not suitable for the soluble production of most biopharmaceuticals. However, recent advances have facilitated the production of soluble and bioactive recombinant proteins in the *E. coli* cytoplasm and were previously reviewed (François Baneyx & Mujacic 2004; Sørensen & Mortensen 2005; Kolaj et al. 2009; Huang et al. 2012). The decrease of the synthesis rate of the target protein by growth temperature or expression rate reductions constitutes a potential strategy to improve the soluble cytoplasmic protein production. In addition, the cytoplasmic folding environment can be improved by co-expression of cytoplasmic folding modulators (GroEL/S and DnaK) or chaperones (IbpA/B and ClpB). Specific solubility enhancing peptide tags such as the maltose binding protein (MBP) and the N-utilizing substance A (NusA) can also be used to avoid IB formation (Overton 2014). Furthermore, mutated *E. coli* strains were developed which can be used for improved soluble production of disulfide bond-containing proteins in the cytoplasm. In these oxidizing strains (e.g. AD494 and Origami™) the reducing pathways of the cytoplasm have been partially or totally impaired, which may greatly enhance the formation of disulfide bonds (A. DeMarco 2009). AD494 cells carry a mutation in the *trxB* gene, while the Origami™ host strain have mutations in both the *trxB* and the *gor* gene (Novagen). Despite all of the progress made, soluble production of recombinant target proteins in the cytoplasm has several drawbacks. These were previously reviewed and include protein misfolding, low protein yield, high proteolytic degradation and laborious downstream processing (Graumann & Premstaller 2006). As previously reviewed, the use of

the oxidizing *E. coli* mutant strains did also not lead to the desired results as low soluble yields of the target protein were obtained and slow cell growth was observed (A. DeMarco 2009). Hence, for the production of soluble therapeutic proteins in *E. coli*, secretion into the periplasm constitutes the preferred route.

The oxidative environment of the periplasm allows disulfide bond formation and thus facilitates proper folding of disulfide bond-containing recombinant proteins (Huang et al. 2012). Protein targeting towards the periplasm offers further advantages. As the periplasm contains only 4 % of the whole cell protein content (Nossal & Heppel 1966) the target protein is effectively concentrated and can thus be more easily purified. The number of proteases in the periplasm is lower than in the cytoplasm (Swamy & Goldberg 1982) indicating less likely protein degradation. Furthermore, upon translocation the signal peptide required for secretion is cleaved which generates an authentic N-terminus of secreted target proteins (Talmadge & Gilbert 1982).

Table 1-1: Periplasmic folding modulators. The periplasmic folding modulators can be divided into generic chaperons, specialized chaperons, peptidyl-prolyl isomerases (PPIases) and proteins involved in disulfide bond formation. The periplasmic folding modulators and their preferred substrates are listed. The table was copied from a previously published review article (François Baneyx & Mujacic 2004).

Classification	**Protein**	**Substrates**
Generic chaperones	Skp (OmpH)	Outer membrane proteins and misfolded periplasmic proteins
	FkpA	Broad substrate range
Specialized chaperones	SurA	Outer membrane proteins
	LolA	Outer membrane lipoproteins
	PapD (and its family)	Proteins involved in P pili biosynthesis
	FimC	Proteins involved in type 1 pili biosynthesis
PPIases	SurA	Outer membrane β-barrel proteins
	PpiD	Outer membrane β-barrel proteins
	FkpA	Broad substrate range
	PpiA (RotA)	Unknown
Proteins involved in disulfide bond formation	DsbA	Reduced cell-envelope proteins
	DsbB	Reduced DsbA
	DsbC	Proteins with nonnative disulfides
	DsbG	Proteins with nonnative disulfides
	DsbD	Oxidized DsbC, DsbG and CcmG
	DsbE (CcmG)	Cytochrome c biogenesis
	CcmH	Cytochrome c biogenesis

Another advantage of the periplasm is the native periplasmic folding machinery assisting for example in correct protein folding, secretion and insertion into the membrane. The periplasmic folding modulators (Table 1-1) can be divided into generic chaperons, specialized chaperons, peptidyl-prolyl isomerases (PPIases) and proteins involved in disulfide bond formation (François Baneyx & Mujacic 2004). Thiol-disulfide oxidoreductases such as the Disulfide bond (Dsb) proteins catalyse disulfide bond formation and isomerization in the periplasm (Hiniker & Bardwell 2003; Kadokura et al. 2004). PPIases catalyse the isomerization of peptidyl-prolyl bonds and can be grouped into three distinct families of cyclopholins (e.g. PpiA), FK506 binding proteins (e.g. FkpA) and parvulins (e.g. PpiD and SurA) (Pliyev & Gurvits 1999). In addition, generic and specialized chaperones preventing non-productive folding reactions were identified in the periplasm. For example, the generic chaperone Skp catalyses the correct folding of proteins and their insertion into the outer membrane (Schäfer et al. 1999). For secretion into the periplasm, proteins have to be transported across the inner membrane. In most cases this export into the *E. coli* periplasm occurs via the type II secretion mechanisms.

1.4.2. Protein Secretion into the Periplasm

As previously reviewed, proteins are secreted into the periplasm via three different pathways including the SecB-dependent, the signal recognition particle (SRP) or the twin-arginine translocation (TAT) pathway (Mergulhao et al. 2005). An overview on the secretion pathways and periplasmic folding mechanisms in *E. coli* can be found in Figure 1-4. Independent of the used pathway, proteins which should be secreted contain N-terminal signal sequences. These sequences are approximately 20 amino acids in length and consist of a basic region at the N terminus, followed by a hydrophobic region and a region with polar amino acids. Upon translocation through the membrane, the signal sequence of the preprotein is cleaved by proteases (e.g. Lep or LspA protease) (Snyder et al. 2010).

The vast majority of preproteins in *E. coli* are secreted via the SecB-dependent pathway in an unfolded state (François Baneyx & Mujacic 2004; Mergulhao et al. 2005). Preproteins which are targeted to the SecB-dependent pathway contain N-terminal signal sequences with a positively charged amino terminus and a hydrophobic core. On the SecB-dependent pathway preproteins which emerge from the ribosome are initially bound by trigger factor (TF). TF prevents co-translational folding and binding to SRP components (Mergulhao et al. 2005). During translation TF dissociates and the preprotein is recognized by DnaK or SecB (François Baneyx & Mujacic 2004). SecB is a specialized chaperone, which keeps presecretion proteins in an unfolded, translocation-competent state (Mergulhao et al. 2005). Preproteins can also be maintained in an unfolded conformation by assistance of the generic chaperone DnaK (François Baneyx & Mujacic 2004). SecB targets the preprotein to the ATP-dependent motor protein SecA which is bound in the inner membrane (A. J. M. Driessen & Nouwen 2008). SecA binds simultaneously to the signal sequence of the preprotein and to the SecYEG

translocon. Upon binding of ATP to SecA, SecB is released from the membrane. Subsequently the preprotein is released from SecA into the SecYEG translocon (A. J. Driessen et al. 1998). The SecYEG channel consists of the three integral membrane proteins SecY, SecE and SecG and assists in translocating proteins through the inner membrane (A. J. M. Driessen & Nouwen 2008). The energy for protein translocation through the membrane is provided by ATP hydrolysis and proton-motive force (PMF) (Snyder et al. 2010).

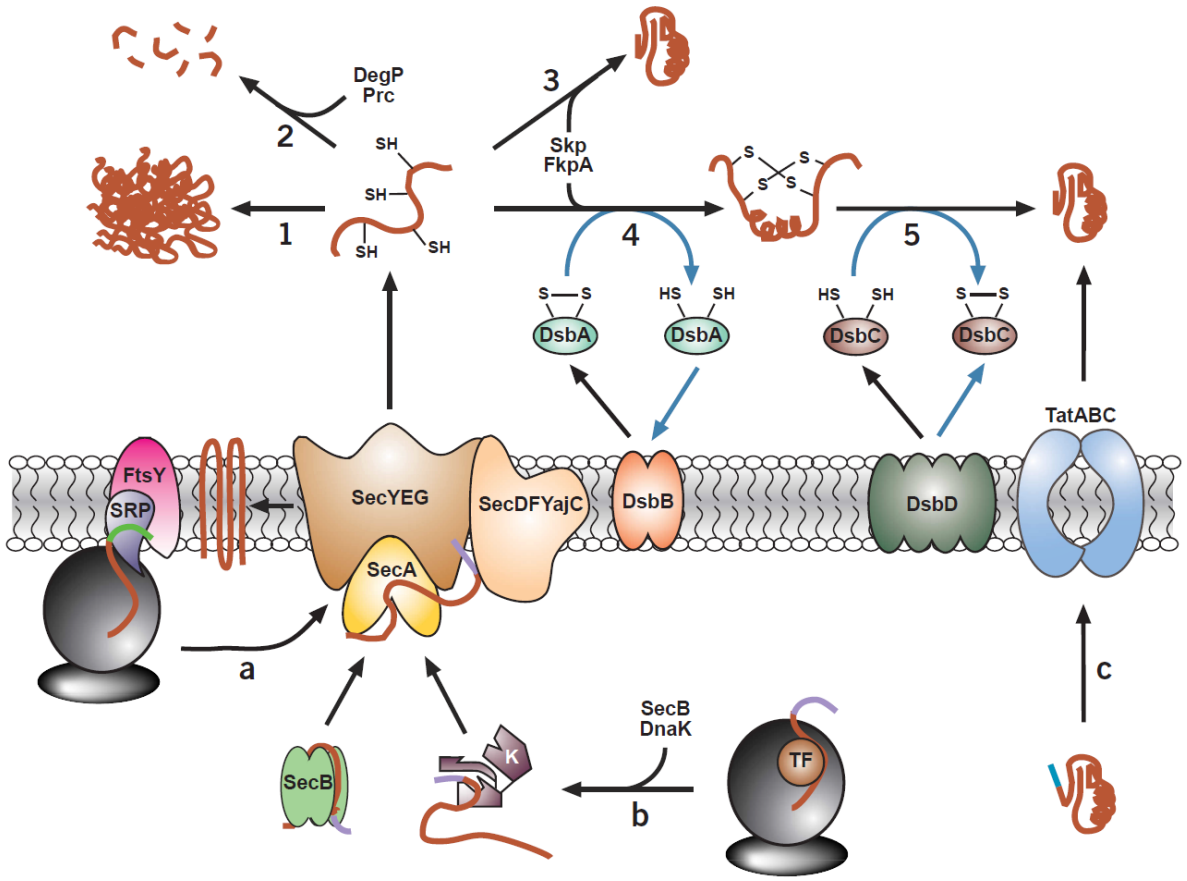

Figure 1-4: Secretion pathways and periplasmic folding mechanisms in *E. coli*. The secretion of proteins into the *E. coli* periplasm is accomplished via one of three different pathways of type II secretion mechanisms. **(a)** Signal recognition particle (SRP) pathway: Preproteins containing an N-terminal signal sequence with a highly nonpolar core (green) are recognized and bound by SRP cotranslationally. The SRP-ribosome complex associates with the FtsY receptor, which assist in translocating the nascent polypeptide chain via the SecYEG translocon cotranslationally. **(b)** SecB-dependent pathway: The vast majority of preproteins contain less hydrophobic signal sequences (lavender) and undergo SecB-dependent secretion into the periplasm. Trigger factor (TF) binds to the signal sequence of the preprotein and prevents cotranslational folding. After dissociation of TF the preprotein is transferred the SecB or DnaK, which keep the presecretion protein in an unfolded conformation. The preprotein is than targeted to the membrane-bound SecA protein. Under ATP hydrolysis and utilization of the proton-motive force (PMF) the preprotein is exported through the SecYEG translocon. **(c)** Twin-arginine translocation (TAT) pathway: Preproteins which contain two consecutive arginine residues in their signal sequence (cyan) are transported via the TAT pathway in a folded state. The signal sequence is bound by TatB and TatC causing TatA to form a channel in the membrane. After successful secretion into the periplasm and cleavage of the signal sequence, unfolded or partially folded proteins may aggregate due to incorrect folding **(1)**, undergo protease-mediated proteolysis **(2)**, or attain their native conformation with potential assistance of periplasmic folding modulators such as Skp or FkpA **(3)**. Disulfide bond formation and isomerization of periplasmic proteins is catalyzed by DsbA **(4)** and DsbC **(5)**. After reaction DsbA and DsbC are reactivated by the transmembrane proteins DsbB and DsbD, respectively. This figure was copied from a previously published review article (François Baneyx & Mujacic 2004).

In *E. coli* the SRP pathway is primarily used for the targeting of inner membrane proteins (Economou 1999). Preproteins are translocated by the SRP pathway cotranslationally (Mergulhao et al. 2005). These preproteins contain N-terminal signal sequences with a highly hydrophobic core and lacking the binding site of TF (Patzelt et al. 2001). SRP recognizes and binds to the hydrophobic signal sequences of the preproteins as they emerge from the ribosome which results in a pause of translation. Then the SRP-ribosome complex associates with the FtsY, a specific receptor on the membrane (Snyder et al. 2010). Due to the GTPase activity of FtsY (Nagai et al. 2003) the nascent polypeptide chain is translocated cotranslationally via the SecYEG channel.

Preproteins which are folded or partially folded in the cytoplasm cannot be transported by the SecYEG translocon. In *E. coli* such proteins are transported by the TAT pathway and contain signal sequences with two consecutive arginine residues. Substrates of the TAT pathway are in most cases cofactor-binding proteins which are folded in the cytoplasm prior to export (Bogsch et al. 1998). The TAT pathway comprises the four integral membrane proteins TatA, TatB, TatC and TatE. In review articles published in 2004 and 2005 it was stated that knowledge about the specific mechanisms of the TAT pathway has been missing (François Baneyx & Mujacic 2004; Mergulhao et al. 2005). However, it is known that the signal sequence on the presecretory protein is bound by TatB and TatC. Then TatA is activated and forms a channel in the membrane (Snyder et al. 2010). Protein secretion via the TAT pathway is ATP-independent (Yahr & Wickner 2001) and the energy for translocation is obtained by PMF (DeLeeuw et al. 2002).

All three secretion pathways have successfully been used for the production of soluble recombinant proteins and examples can be found in some review articles (Mergulhao et al. 2005; Huang et al. 2012). It has been reviewed that the SecB-dependent pathway is most commonly used for soluble periplasmic production of recombinant target proteins (François Baneyx & Mujacic 2004; Mergulhao et al. 2005; Kolaj et al. 2009). However, the inability to transport folded proteins constitutes a drawback of the SecB-dependent pathway. Since SecB-dependent transport occurs largely posttranslational, the secretion of proteins which are quickly folded in the cytoplasm may not be possible. If the secretory protein folds too quickly in the cytoplasm the SRP-dependent pathway could be used since this pathway enables cotranslational translocation into the periplasm (Mergulhao et al. 2005). The TAT pathway is the secretion route of choice, if folded or partially folded proteins should be secreted. However, since the TAT pathway requires excessive energy for high level secretory protein production (DeLisa et al. 2004) it may be less efficient than the SecB pathway. Furthermore, proper folding of some recombinant proteins (e.g. disulfide-bond containing proteins) may not be possible in the cytoplasm which could preclude the export of such proteins by the TAT pathway. However, some biopharmaceuticals including human growth hormone, interferon α2b and antibody fragments have been efficiently exported by the Tat pathway in the absence of formed disulfide bonds (Alanen et al. 2015). In conclusion, each of the three secretion pathways has its advantages and drawbacks. The efficiency of protein

secretion depends on the protein synthesis rate, the used host strain and the secretory protein. Hence, a trial-and-error approach is required to optimize secretion of target proteins into the periplasm (Huang et al. 2012).

1.4.3. Approaches to Bypass Potential Bottlenecks for Production of Recombinant Proteins in the *Escherichia coli* Periplasm

Soluble Periplasmic Protein Production May be Connected to Some Limitations. It was previously reviewed that the efficiency of the soluble production of active recombinant proteins in *E. coli* relies on the availability of molecular factors such as foldases, chaperones or membrane proteins (A. DeMarco 2013). This indicates that the final yield of a target protein depends on the limiting step in the overall production process. Hence, it appears necessary to identify the molecular elements which may become limiting in a soluble production process. Periplasmic production in *E. coli* is often limited due to an overload of the secretion apparatus (Mergulhao et al. 2005; A. DeMarco 2013). It was shown that the carrier capacity of the Sec-translocon is easily saturated (Schlegel et al. 2013). The TAT pathway represents an alternative secretion route which can be used for periplasmic protein production. However, rapid saturation was also demonstrated for the TAT pathway (DeLisa et al. 2004). An overload of the secretion apparatus can result in accumulation of the unfolded target protein in the cytoplasm. As a consequence the overproduced proteins may aggregate. Cytoplasmic aggregation could have a toxic effect on cells by impairing correct cell growth and promoting cell lysis (A. DeMarco 2013). Limiting availability of components of the periplasmic folding machinery might represent another bottleneck of soluble protein production. As previously reviewed high-level secretory protein production can overload the periplasmic folding machinery resulting in undesired aggregation of the product in the periplasm (Huang et al. 2012). As a consequence the soluble yield of the periplasmic target protein remains low.

The Fine-Tuning of Synthesis Rates Can Improve Soluble Periplasmic Protein Production. Soluble periplasmic product yields can be improved by optimizing the synthesis rate of the target protein. Figure 1-5 illustrates how the synthesis rate of a target protein determines the folding rate and thus the soluble product yield. A decrease in the proteins synthesis rate might be a potential solution to prevent protein aggregation caused by saturation of the secretion apparatus and/or the periplasmic folding machinery. If fewer polypeptides are synthesized per cell, more correctly folded proteins can be obtained as the cell machinery might work more effectively (A. DeMarco 2013). Hence, a reduction in synthesis rate could decrease the metabolic burden of the production host and improve the folding quality of the target protein (Hoffmann & Rinas 2004).

One possibility to decrease the synthesis rate and improve soluble protein production is to reduce the incubation temperature (Schein & Noteborn 1988; Vasina & F. Baneyx 1997; Vera

et al. 2007). Recombinant protein production performed between 15 - 25 °C was reviewed to result in lower protein aggregation and higher soluble yields (Rosano & Ceccarelli 2014).

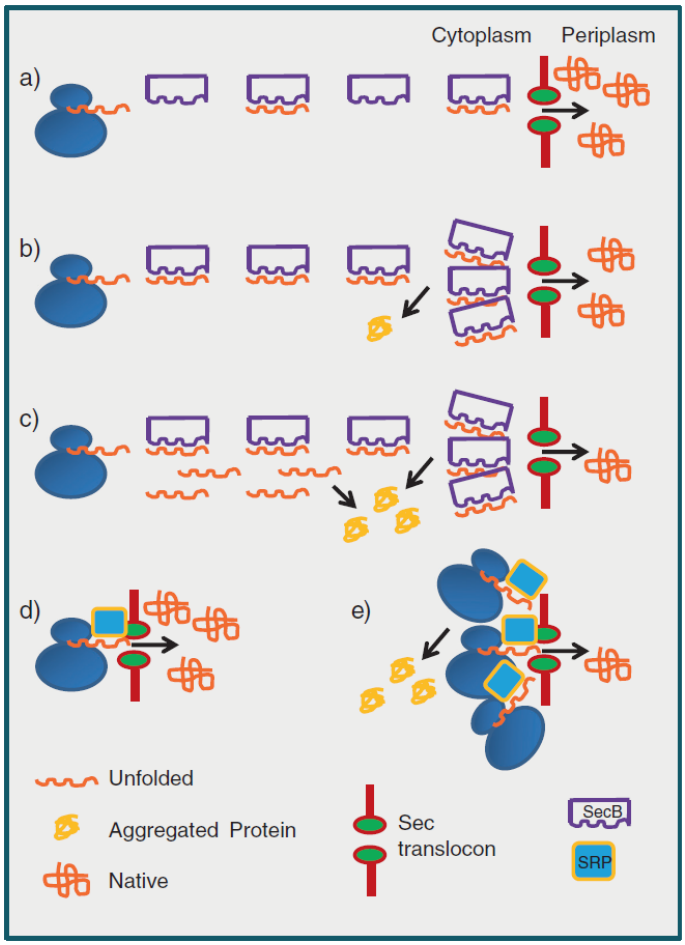

Figure 1-5: The concentration of correctly folded target proteins in the periplasm is determined by their synthesis rate. The efficiency of a soluble protein production process in *E. coli* is dependent on the availability of essential molecular elements involved in the secretion and folding process. High-level production of secreted proteins can lead to an overload of the periplasmic folding machinery and/or the secretion apparatus. **(a)**: Using an optimal synthesis rate, recombinant proteins can be successfully exported across the inner membrane by the Sec translocon and sufficient amounts of folding modulators are available for correct folding in the periplasm. At higher expression rates recombinant proteins are prone to aggregate in the cytoplasm because of an overload of the Sec translocon **(b)** or limitations in SecB availability **(c)** leading to a decrease in periplasmic protein yield. The co-translational SRP pathway could overcome the SecB limitation **(d)** but shares the same secretion apparatus with the SecB-dependent pathway. Hence, overloading of the Sec translocon would still lead to protein aggregation in the cytoplasm and lower periplasmic protein yields **(e)**. This figure was copied from a previously published review article (A. DeMarco 2013).

Regulation of the numbers of target gene expression cassettes inside the *E. coli* cell is another possibility to adjust the synthesis rate of the target protein. The use of plasmid-based expression cassettes is widely spread and their application and optimization is discussed in several review articles (Samuelson 2011; Huang et al. 2012; Overton 2014; Rosano & Ceccarelli 2014). Plasmid copy number (PCN) control within a cell is primarily regulated by the origin of replication (*ori*) (DelSolar & Espinosa 2000). It is critical to choose the optimal PCN. Low numbers of target gene expression cassettes can result in low protein

productivity. On the other hand, high PCN can lead to the desired high productivity of the target protein but may also impose increased metabolic burdens on the host cells (Huang et al. 2012; Overton 2014). It is known that the metabolic burden increases with rising gene expression rates and a higher PCN (Samuelson 2011). Hence, the presence of high copy number plasmids can lead to reduced cell growth as a large proportion of cellular resources is required for the production and maintenance of the plasmids (Huang et al. 2012). Furthermore, high copy number plasmids possess a higher segregational instability, in particular under non-selective conditions (Friehs 2004). The metabolic burden affiliated with high copy number plasmids can also result in plasmid rejection and plasmid loss and thereby lead to the overgrowth of plasmid-free cells (Striedner et al. 2010). The overgrowth of plasmid-free cells may then result in a loss of protein productivity (Huang et al. 2012). The metabolic burden for the host cells can be minimized by using low-copy number plasmids which are affiliated with 40 or less plasmid copies per cell. Examples of widely used "low-copy" *oris* include pMB1, oriV, p15A or pSC101 (Samuelson 2011). To further minimize the metabolic burden for the host cell, plasmid-free chromosomal expression systems can be used instead of plasmid-based systems (A. DeMarco 2013). A previous study showed that chromosomal integration of multiple gene copies constitute a suitable approach to generate strains which can be used in industrial production processes (Chen et al. 2008). Advantages of chromosome-based expression systems compared to plasmid-based systems include low basal expression levels and high system stability and robustness. Plasmid-free expression systems facilitate simple upstream processing and high flexibility in process design. Furthermore, genomic integration of the gene of interest has the benefit of flexible expression rate control. By inducer titration the expression level of the target gene can be tuned as desired. On the other hand, complex cloning procedures are one drawback of plasmid-free expression systems (Striedner et al. 2010). In conclusion, the balance between low PCN for decreased metabolic burden and high PCN for high recombinant protein productivity has to be determined individually for each target process (Overton 2014).

The choice of a suitable promoter system is another way to optimize synthesis rates for soluble protein production attempts. Multiple inducible promoters such as *lac*, *tac*, *trc*, T7, pL, pR, *Pho*A and p*lux* (see Table 1-2) have previously been successfully used to produce different recombinant proteins as summarized in several review articles (Overton 2014; Huang et al. 2012; Lebendiker & Danieli 2014; Rosano & Ceccarelli 2014). An ideal promoter should provide a sufficient transcription rate of the target gene and be tightly regulated to avoid leaky expression. Leaky expression should be avoided as it can constitute a metabolic burden for cells (Mairhofer et al. 2013). Further desired characteristics of a promoter system include a simple and cost-effective induction method which should be independent of the media components (Huang et al. 2012). In addition, tuneable promoters are often used since they enable the adjustment of the target gene's expression level by inducer titration. Hence, the transcription rate of the gene of interest can be adjusted by varying inducer concentrations e.g. IPTG (Winograd et al. 1993).

Table 1-2: Promoters commonly used for recombinant protein production. Promoter type, induction strategy and key features are indicated. The table was copied from a review article (Huang et al. 2012).

Promoter	**Induction strategy**	**Key features**
lac	IPTG	Relative low-level expression, titratable, leaky
tac, *trc*	IPTG	High-level expression, titratable, leaky
T7	IPTG	Very high-level expression, titratable, leaky
Phage *λ* pR, pL	Temperature shift	High-level expression, tight control
PhoA	Phosphate depletion	High-level expression, tight control, media limitation
p*lux*	Homoserine lactone	High-level expression, tight control, inexpensive inducer

Another possibility to tune transcription rates is to modify the strength of the promoter. Promoter strength is defined as the binding affinity of RNA polymerase (RNAP) holoenzyme to the promoter DNA sequence (Brewster et al. 2012). Prior to start of transcription, the σ-factor of RNAP holoenzyme associates with two conserved sequences in the promoter region, termed "promoter consensus sequences" (Harley & Reynolds 1987). The promoter consensus sequence recognized by the σ^{70}-factor, the primary *E. coli* σ-factor, is characterized by two stretches of six nucleotides located at 10 (-10 box) and 35 (-35 box) nucleotides upstream of the transcription start site (+1) (see Figure 1-6). In σ^{70}-controlled promoters the -35 and -10 box are separated by a 17 bp non-conserved nucleotide sequence, called the spacer (Snyder et al. 2010). Nucleotide changes in the consensus sequences usually result in reduced promoter strength (Voskuil et al. 1995; Dombroski et al. 1992). Hence, mutations in the -35 box, spacer sequence or -10 box may change the binding frequency of RNAP and can be used to tune transcription rates and gene expression levels (DeMey et al. 2007; Davis et al. 2010; Brewster et al. 2012; Anderson 2006).

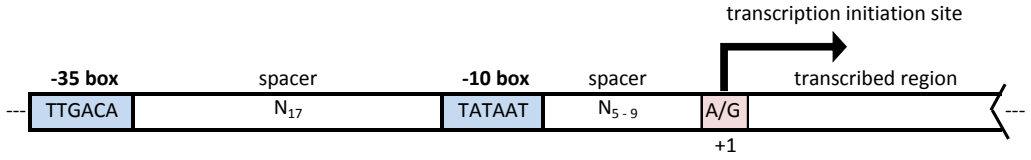

Figure 1-6: Schematic structure of a typical sigma^{70}-controlled bacterial promoter. The transcription initiation site (+1) is indicated by an arrow. -35 and -10 consensus sequences are coloured and referred to as -35 and -10 box, respectively. A/G: RNA synthesis typically starts with an A or a G nucleotide. N: Any nucleotide, index indicates number of nucleotides.

In conclusion, there is no promoter which is suitable for the production of all recombinant proteins (Overton 2014). Hence, the choice of the promoter system depends on the target protein and the production process. The synthesis rate of the target protein can be optimized by varying inducer concentrations or modifying the promoter strength.

Translation rate adjustment constitutes another option for fine-tuning of the target protein's synthesis rate. The use of high translation rates in periplasmic production processes may overload the secretion apparatus and thus result in cytoplasmic aggregation and low soluble product yields. This was also shown in a previous report since the soluble product yield increased with decreasing strength of the ribosomal binding site (RBS) (Samuelson 2011). It was shown that for enhanced secretory protein production the translation level should be optimized rather than maximized (Simmons & Yansura 1996). Technologies are available to design synthetic RBS leading to different translation initiation rates (Salis et al. 2009). Such technologies enable the fine-tuning of translation and the rational control in recombinant protein expression.

In summary, a plethora of possibilities to fine-tune synthesis rates for improving soluble periplasmic protein production is available. The method of choice of biological parts or combinations thereof depends on the recombinant target protein and the applied production procedure. Currently, no predictive tool for optimal expression cassette design is available and thus a trial-and-error approach is required.

Increasing the Cellular Level of Selected Molecular Elements May Also Enhance Soluble Periplasmic Protein Yields. As stated above, limitations in the availability of molecular components of the periplasmic folding machinery and/or the secretion apparatus might constitute bottlenecks for soluble periplasmic protein production. As previously reviewed, overproduction of molecular elements of the secretion apparatus may enhance the translocation of secretory proteins (Mergulhao et al. 2005). For example, limitations of the SecB-dependent secretion pathway were successfully counteracted by SecB overproduction. This approach resulted in improved soluble periplasmic protein yields in previous studies (Chou et al. 1999). Also the efficiency of protein secretion via the TAT pathway could be optimized by co-expression of the *tatABC* operon. The overexpression of *tatA/B/C* led to a 20-fold increase in the level of soluble GFP in a previous study (Barrett et al. 2003).

Likewise, increased levels of molecular elements of the folding machinery (e.g. periplasmic folding modulators) could improve soluble production of periplasmic proteins in *E. coli*. It was previously reviewed that the overproduction of the thiol-disulfide oxidoreductases DsbA and DsbC increased the functional yields of several recombinant proteins (Kolaj et al. 2009; François Baneyx & Mujacic 2004; A. DeMarco 2009). Also the co-production of Thioredoxin (Trx) was shown to increase the yield of a recombinant protein 3-4-fold (García-Ortega et al. 2000). Co-production experiments with the PPIases FkpA and SurA yielded also promising results. SurA co-production improved folding of aggregation-prone proteins in the periplasm (Missiakas et al. 1996). FkpA overproduction enhanced production of several scFv fragments up to 10-fold (Bothmann & A. Plückthun 2000) and was shown to reduce aggregation and periplasmic IB formation of recombinant proteins (Arié et al. 2001). Co-production of the periplasmic chaperone Skp resulted in improved antibody fragment production and delayed cell lysis in a previous study (Hayhurst & Harris 1999). Improved production of active scFv (Bothmann & A. Plückthun 1998) and Fab fragments (Lin et al. 2008) was also demonstrated

in *skp* co-expression experiments. To improve the folding of recombinant proteins in the *E. coli* periplasm, several periplasmic folding modulator genes can be co-expressed simultaneously. The co-expression plasmid pTUM4 (Figure 1-7) bears the four folding modulator genes *dsbA*, *dsbC*, *fkpA* and *surA* under the control of constitutive promoters (Schlapschy et al. 2006). Application of pTUM4 had a positive influence on cell viability, increased soluble periplasmic protein yield and induced efficient disulfide bond formation of a human plasma retinol-binding protein (RBP) and the human dendritic cell membrane receptor DC-SIGN in previous studies (Schlapschy et al. 2006). The presence of the co-expression plasmid pTUM4 could also raise the yield of a soluble, functional Fab fragment by a factor > 100 (Friedrich et al. 2010).

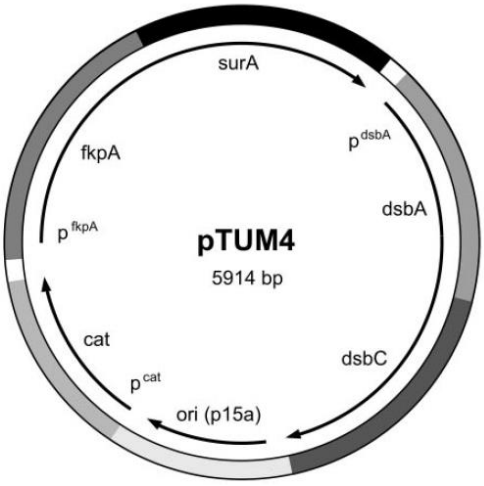

Figure 1-7: Schematic representation of the co-expression plasmid pTUM4. The 5914 bp plasmid pTUM4 carries a p15A origin of replication (*ori*) and the chloramphenicol resistance gene (*cat*) under control of its own constitutive promoter (p^{cat}). The plasmid harbours two artificial dicistronic operons, the first with the genes *dsbA* and *dsbC* under control of the constitutive *dsbA* promoter (p^{dsbA}). The second dicistronic operon includes the genes *fkpA* and *surA* controlled by the constitutive *fkpA* promoter (p^{fkpA}). The figure was copied from a previously published article (Schlapschy et al. 2006).

In conclusion, several studies showed that the overproduction of molecular components of the periplasmic folding machinery and/or the secretion apparatus had a positive impact on soluble periplasmic protein production (see above). A review article published in 2009 summarizes co-production strategies which can be used to overcome potential bottlenecks during recombinant protein production (Kolaj et al. 2009). It was stated in some other review articles that the folding modulator gene co-expression needs to be optimized for each recombinant target protein (Martínez-Alonso et al. 2010; Overton 2014). Hence, the success of increased levels of folding modulators cannot be sufficiently predicted on a rational basis. A trial-and-error approach is required to identify suitable folding modulators and their levels which can improve the soluble yields of a recombinant target protein in a certain production process. Thus, efficient tools are required to screen different folding modulators and levels to overcome potential folding bottlenecks.

1.5. Aim and Objectives

The soluble production of disulfide-bond containing proteins, such as antibody fragments, in the periplasm of *E. coli* constitutes a reasonable alternative to inclusion body processes, as cumbersome protein refolding procedures can be avoided. Soluble production of the model protein FabZ was attempted by targeting both monomers of this antibody fragment into the oxidative environment of the *E. coli* periplasm. However, soluble production attempts in a previous part of this project resulted in periplasmic aggregation and low soluble FabZ yields (Buettner 2016). It was assumed that aggregation of FabZ was caused by an overload of the periplasmic folding machinery. Thus, it was expected that increased levels of periplasmic folding modulators might enhance soluble target protein production in the periplasm. Numerous previous studies have reported positive influences of co-synthesis of periplasmic folding modulators on soluble recombinant protein production. However, the success of co-synthesis seems to be strongly depend on the target protein and further external parameters. To improve the soluble periplasmic production of a protein of interest by folding modulator co-synthesis, a trial-and-error approach is required to find the suitable folding modulator and its appropriate production level. Hence, the aim of this work was to establish a co-expression system which enables a quick screening for appropriate folding modulator types and levels in case of different target proteins and processes.

The co-expression system was supposed to be based on the periplasmic folding modulator genes of the thiol-disulfide oxidoreductases DsbA and DsbC, the PPIases FkpA, PpiD and SurA and the generic chaperone Skp. In this work constitutive promoters should be used for the control of folding modulator gene expression, since previous T7 promoter-based co-expression systems interfered with target gene expression (Schuller 2015; Buettner 2016). An appropriate promoter evaluation procedure using GFP as reported protein was supposed to be developed to determine the strength of constitutive promoters. Promoters of different strength should be selected to enable production of different folding modulator levels.

In the second part of this project, the new co-expression system was supposed to be evaluated using FabZ as a model protein. As stated above, periplasmic production of FabZ resulted in aggregation and thus should be improved by folding modulator co-production. *E. coli* BL21(DE3) cells bearing a genome-integrated FabZ expression cassette were supposed to be used as FabZ production strain. These were transformed with the newly created folding modulator gene co-expression plasmids. Resulting plasmid strains should be analysed concerning their FabZ production in shake flask and fed-batch fermentation experiments. By doing so, it should be examined if the newly established co-expression system can enhance soluble target protein production in different production scales. If the co-expression system appears suitable to improve periplasmic FabZ production, the system was supposed to be tested concerning soluble production of other target proteins.

2. Materials and Methods

2.1. Materials

Technical equipment and software used during this work is listed in Table 2-1.

Table 2-1: Technical equipment and software used in this work. Model and/or type of technical equipment and the manufacturer are presented. Equipment is arranged in alphabetical order.

Equipment	**Model / Type**	**Company**
Auto Plate Washer	Elx405	BioTek® Instruments
Autoclave	Systec-D65 68L	Systec
Autoclave	FVA3/A1	Fedegari
Centrifuge	5810R	Eppendorf
Combi-Spin	FVL-2400N	peQ-Lab
Electrophoresis Cell	Sub-Cell® GT	Bio-Rad
Electrophoresis Power Supply	PowerPac™ Basic	Bio-Rad
ELISA Software	Gen5	BioTek® Instruments
Fermenter	6.9 L Computer-Controlled Stirred-Tank BIOSTAT®Cplus Bioreactor	Sartorius Stedium Biotech
Fluorescence Microplate Reader	Safire$^{2™}$	Tecan Group
Gel Imaging System	Gel Doc™ EZ Imager	Bio-Rad
Gel Imaging System Software	Quantity One 4.6.1	Bio-Rad
Incubation Shaker	Multitron II	HT Infors
Incubator	BD 23	Binder
Laminar Flow Safety Cabinet	HERAsafe®	Kendro Laboratory Products
Micro Volume Spectrophotometer	NanoDrop ND-1000	peQ-Lab
Microcentrifuge	5415R	Eppendorf
Microplate Reader	PowerWave HT	BioTek® Instruments
Microwave	Innowave	Siemens
NanoDrop Software	ND-1000 V3.3.0	NanoDrop Technologies
Pipetboy	Accu-jet® Pro	Brand

Equipment	Model / Type	Company
Pipettes	Single Channel, Research Plus (0.1 - 2.5 µL, 0.5 - 10 µL, 2 - 20 µL, 20 - 200 µL, 100 - 1000 µL) Multi Channel, Research Plus (10 - 100 µL, 50 - 300 µL, 100 - 1000 µL)	Eppendorf
Scales	PR5002 and PM460 Delta Range	Mettler Toledo
SDS-Gel Imaging System	Gel-Doc™ EZ Imager	Bio-Rad
SDS-PAGE Electrophoresis Cell	Criterion™	Bio-Rad
SDS-PAGE Power Supply	Electrophoresis Power Supply EPS601	Amersham Biosciences
SDS-PAGE Software	Image Lab 5.0	Bio-Rad
Software Fluorescence Microplate Reader	Magellan V7.1	Tecan Group
Thermocycler	PTC-200 Peltier thermal cycler	MJ Research
Thermomixer (1.5 + 2.0 mL)	Comfort	Eppendorf
UV/VIS Spectrophotometer	Genesys 10S	Thermo Scientific
Vortex Mixer	Genie 2	Scientific Industries

Table 2-2 lists media and buffers used for basic molecular biology methods, shake flask experiments and protein analytics during this work.

Table 2-2: Media and buffers used in this work. The composition and/or supplier of solutions as well as their use in this work are shown. Media and buffers are arranged in alphabetical order.

Solution	Composition / Supplier	Use
Ampicillin Stock Solution	50 mg/mL Ampicillin Sodium salt	Selection of pJET1.2/blunt-bearing strains
Chloramphenicol Stock Solution	25 mg/mL Chloramphenicol	Selection of pTUM4-bearing strains
IPTG Stock Solution	238.3 g/L IPTG (1 M)	Induction of product formation
Kanamycin Stock Solution	50 mg/mL Kanamycin sulfate	Selection of FabZ production strain *E. coli* BL21(DE3) Tn7::<*FabZ*>(ompA kan^R pt7)
NEBuffer 2, NEBuffer 3, CutSmart™ Buffer	New England BioLabs	Buffer for restriction digests
NuPAGE® LDS Sample Buffer (4x)	Life Technologies	Sample Loading Buffer for SDS-PAGE

Solution	Composition / Supplier	Use
OD Buffer	20.7 g/L $Na_2HPO_4 \cdot 12H_2O$ 5.7 g/L KH_2PO_4 11.6 g/L NaCl	Dilution buffer for OD measurement
PBS Buffer with 0.15 % (v/v) Tween 20	100 mL/L 10x PBS (purchased from Cell Signaling) 1.5 mL/L Tween 20	ELISA Wash Buffer
Rapid Ligation Buffer (2x)	Promega	Buffer for ligation
S-LB Agar (low salt)	5 g/L Bacto Yeast 5 g/L NaCl 10 g/L Soy peptone 15 g/L Bacto Agar	Strain construction, plating of colonies
S-LB Medium (low salt)	5 g/L Bacto Yeast 5 g/L NaCl 10 g/L Soy peptone	Basic cloning techniques, overnight cultures, preparation of cryo cultures
Sodium Carbonate Buffer (0.1 mM)	8.4 g/L $NaHCO_3$ (0.1 mM) pH adjustment to 9.5 with 0.1 mM Na_2CO_3 solution	ELISA Coating Buffer
Stock Solution of Tris-acetate-EDTA (TAE) (50x)	242 g/L Tris 57.2 g/L Glacial acetic acid 18.6 g/L EDTA	Buffer for Agarose Gel Electrophoresis
Streptomycin Stock Solution	50 mg/mL Streptomycin sulfate	Selection of plasmid-bearing strains
T4 DNA Ligation Buffer (10x)	New England BioLabs	Buffer for phosphorylation of oligonucleotides
T7 Preculture Medium	See confidential supplement for medium composition	Used for pre-culture cultivation in shake flask experiments
T7 Shake Flask Medium	See confidential supplement for medium composition	Used for main culture cultivation in shake flask experiments
TBS 1 % Casein Blocker (1x)	20 mM Tris 500 mM NaCl 1 % (w/v) casein pH 7.4	ELISA Blocking Buffer
TBS (10x) with 0.1 % (v/v) Tween20	5.6 g/L Tris base 24.0 g/L Tris-HCl 88.0 g/L NaCl 1.0 mL/L Tween 20	ELISA Sample Diluent Buffer

Kits and consumables used during this work are presented in Table 2-3.

Table 2-3: Kits and consumables used in this work. Type, manufacturer and the use of different kits and consumables are indicated. Kits and consumables are arranged in alphabetical order.

Kit / Consumable	**Type / Cat. No.**	**Company**	**Use**
Bug Buster® Protein Extraction Reagent	- / 70584-4	Novagen	Extraction reagent for cell wall disruption of *E. coli*
CloneJET PCR Cloning Kit	- / K1231	Thermo Scientific	Cloning of blunt-end DNA fragments in pJET1.2/blunt
Costar® 96-Well Plates, UV - Transparent, Flat Bottom	- / 3635	Sigma-Aldrich	Microtiter plate for fluorescence measurement
Costar® Stripette® Serological Pipettes	2, 5, 10, 25, 50 mL / CLS4488	Sigma-Aldrich	Steril or non-steril pipetting of solutions
Criterion™ TGX Stain-Free™ Precast Gel	12 + 2 well comb / 567-8083	Bio-Rad	Stain-free gel for SDS-PAGE analysis
Cryo Tube Vials	Nunc, 1.8 mL / -	Thermo Scientific	Aliquoting and storage of cryo cultures
Lysonase™ Solution	- / 71230	Novagen	Extraction reagent for cell wall disruption of *E. coli*
MinElute™ PCR Purification Kit	- / 1026476	Qiagen	Purification of small DNA fragments (70 bp to 4 kb)
NUNC™ Microwell™ 96-Well Microplates	- / -	Thermo Scientific	Preparative microtiter plates for ELISA
Polypropylene Centrifuge Tubes (15 mL)	SuperClear™ / 21008-216	VWR	Centrifugation / Reaction tubes
Polypropylene Tubes (50 mL)	Cellstar® / 227261	Greiner	Centrifugation / Reaction tubes
Polystyrene Clear Flat Bottom 96-Well ELISA Microplate	Microlon® / 655061	Greiner	Microtiter plate used as ELISA measurement plate
QIAprep® Spin MiniPrep Kit	- / 27106	Qiagen	Purification of plasmid DNA
QIAquick® Gel Extraction Kit	- / 28706	Qiagen	Purification of DNA fragments after AGE
QIAquick® PCR Purification Kit	- / 28106	Qiagen	Purification of PCR products
Safe-Lock Tubes	0.5, 1.5, 2.0 mL / -	Eppendorf	Centrifugation / Reaction tubes
Sterile Disposable Filter Units	Nalgene™ CN 0.2 µm / xxx-0020	Thermo Scientific	Sterile filtration of media components
Syringe Filter Unit	0.22 µm Millex-GV / SLGV033RS	Merck Millipore	Filtration of supernatant samples

In Table 2-4 enzymes for molecular biology methods and antibodies for ELISA analysis used during this work are listed.

Table 2-4: Enzymes and antibodies used in this work. Supplier and use of enzymes and antibodies are indicated. Enzymes and antibodies are arranged in alphabetical order.

Enzyme / Antibody	**Company**	**Use**
*BamH*I	New England BioLabs	Restriction digest
Mouse anti-human IgG antibody, Ab7497	Abcam	Coating antibody for ELISA
*EcoR*I - HF	New England BioLabs	Restriction digest
*Hind*III	New England BioLabs	Restriction digest
*Kpn*I - HF	New England BioLabs	Restriction digest
*Nde*I	New England BioLabs	Restriction digest
HRP-conjugated anti-human IgG (H+L) (monkey adsorbed), AP003CUS01	The Binding Site	Secondary antibody for ELISA
*Sal*I - HF	New England BioLabs	Restriction digest
*Sph*I - HF	New England BioLabs	Restriction digest
T4 DNA Ligase	Promega	Ligation reaction
T4 Polynucleotide Kinase	New England BioLabs	Phosphorylation of oligonucleotides
*Xho*I	New England BioLabs	Restriction digest

2.2. Strain Construction

2.2.1. Bacterial Strains and Competent Cells

***Escherichia coli* DH5α** (Genotype: F^- ϕ80*lac*ZΔM15 Δ(*lac*ZYA-*arg*F)U169 *rec*A1 *end*A1 *hsd*R17(r_k^-, m_k^+) *pho*A *sup*E44 *thi*-1 *gyr*A96 *rel*A1 λ^- (Invitrogen 2006)) Subcloning Efficiency™ DH5α™ chemically competent cells (Invitrogen, Life Technologies, Cat. No.: 18265-017) were used for routine cloning applications and stored at -80 °C until further use.

***Eschrichia coli* BL21(DE3)** (Genotype: F^- *omp*T *hsd*SB(rB^-, mB^-) *gal dcm* (DE3)) cells (Novagen, Cat. No.: 69450) were used for protein expression in shake flask experiments and fermentations. *E. coli* BL21(DE3) cells contain the T7 RNA polymerase gene linked to the IPTG-inducible promoter and can therefore be used with expression plasmids containing the T7 promoter. Chemically competent *E. coli* BL21(DE3) cells were prepared in a previous part of this project (Schuller 2015) and stored at -80 °C until further use.

***Escherichia coli* BL21(DE3) Tn7::<*FabZ*>(ompA kan^R pt7)** was constructed in a previous part of this project (Buettner 2016). The dicistronic FabZ gene expression cassette was integrated into the genome of BL21(DE3) cells by homologous recombination (Datta et al. 2006; Sharan et al. 2009). The genome-integrated FabZ expression cassette harbors the genes for the light chain (LC) and heavy chain (HC) part of the Fab fragment as well as a kanamycin resistance gene downstream of the FabZ-coding sequence. To enable translocation into the periplasm, the coding sequences for both Fab monomer parts were genetically fused to the outer membrane protein A (OmpA) signal peptide coding sequence. Transcription of both, LC and HC is under the control of the T7 promoter which leads to the generation of one single mRNA. Translation of the LC and HC genes is independently controlled by separate ribosomal binding sites (RBS). The integration was performed prior to this part of the project (Buettner 2016) targeting the *attTn7* site of the genome of *E. coli* BL21(DE3). Chemically competent *E. coli* BL21(DE3) Tn7::<*FabZ*>(ompA kan^R pt7) cells were previously prepared (Schuller 2015) and stored at -80 °C until further usage in this project.

2.2.2. Creation of Plasmid Constructs

Restriction Digest, Separation and Purification of DNA Molecules: Restriction endonuclease (REN) digests of DNA were performed employing restriction enzymes and buffers from New England BioLabs.

Table 2-5: Pipetting scheme of preparative and analytical REN digests. Individual components were mixed in 1.5 mL reaction tubes and sterile RO-water was added to complete to total volume. Applied volume of DNA samples depended on initial DNA concentration. The appropriate combination of enzymes and buffer (NEBuffer 2, NEBuffer 3 or CutSmart™ buffer) was selected according to the manufacturer's instruction (New England BioLabs). 10x BSA (New England BioLabs) was only used in combination with either NEBuffer 2 or NEBuffer 3. AGE: Agarose gel electrophoresis. REN: Restriction endonuclease.

Components	Preparative REN digest	Analytical REN digest
Total volume	50 µL	20 µL
DNA amount	100 to 2000 ng	200 ng
Volume enzyme 1	0.5 µL	0.2 µL
Volume enzyme 2	0.5 µL	0.2 µL
Buffer volume	5 µL	2 µL
Volume 10x BSA (if required)	5 µL	2 µL
Addition of 6x Purple Loading Dye before AGE	10 µL	4 µL

Restriction digest were pipetted according to Table 2-5 and incubated for 1 to 2 h at 37 °C in a Thermomixer. Subsequently 6x Purple Loading Dye (New England BioLabs) was added and the reaction solutions were loaded on 1.0 - 1.5 % agarose gels. The concentration of the agarose gel was selected depending on the size of the DNA fragments to be separated. The required amount of agarose (Agarose NEEO Ultra-Qualität, Roth) was dissolved in 1x Tris-acetate-EDTA (TAE). Three to four drops of 0.025 % ethidium bromide aqueous solution (Roth) per 200 mL of dissolved gel were added as staining reagent. DNA molecules were separated by gel electrophoresis. The applied voltage was adjusted depending on the agarose concentration, size of the gel and the molecular weight of the DNA molecules. After separation, DNA molecules of choice were excised from the agarose gel under UV light and purified using the QIAquick® Gel Extraction Kit (Qiagen) according to the manufacturer's instruction. For purification of DNA fragments with less than 200 bp in size, MinElute™ Spin Columns (Qiagen) were applied.

Ligation and Transformation: For ligation of DNA molecules 0.5 µL T4 DNA Ligase (Promega) and 5 µL 2x Rapid Ligation Buffer (Promega) were used in a total volume of 10 µL. Combinations of 3.5 to 4 µL of insert and 0.5 to 1 µL of vector backbone were applied to obtain at least a 3-fold molar excess of insert over backbone. The ligation reaction was performed at 25 °C for 45 min. For heat-shock transformation, chemically competent *E. coli* DH5α cells (Invitrogen, Life Technologies) were thawed on ice and mixed with 5 µL of the ligation reaction. Afterwards, the suspension was incubated on ice for 10 min, at 42 °C for exactly 45 sec in a Thermomixer and on ice for another 2 min. 900 µL of S-LB medium were added prior to incubating the cell suspension at 37 °C and 600 rpm in a Thermomixer for approximately 50 min. Subsequently, the cell suspension was sedimented by centrifugation at 3220 x g for 30 sec and 700 µL of the supernatant were discarded. Sedimented cells were resuspended in the residual 200 µL and plated on S-LB plates containing an appropriate antibiotic. Transformed plates were incubated in inverted position at 37 °C over night (o/n).

Plasmid DNA Purification and Sequence Confirmation: Bacterial colonies grown on plates after o/n incubation were used to inoculate 5 mL S-LB medium supplemented with an appropriate antibiotic in 15 mL centrifuge tubes employing sterile inoculation loops. After incubation at 37 °C and 250 rpm o/n cells were sedimented by centrifugation at 3220 x g and room temperature (RT) for 10 min. Plasmids were purified using the QIAprep® Spin MiniPrep Kit (Qiagen) according to the manufacturer's instruction. Expected plasmid composition was verified by an analytical REN digest followed by an agarose gel electrophoresis (AGE) as described above. Enzymes in analytical REN digest were selected to enable clearly evaluable band patterns. Plasmid preparations which showed the expected band pattern were subjected to sequencing. Sequencing was focused on the areas of the plasmid which were genetically modified due to insertions, substitutions or removal of DNA sequences. Plasmid-containing solutions (V = 20 µL, c = 40 ng/µL) and corresponding sequencing primers (V = 20 µL, c = 10 µM) were prepared for Sanger sequencing conducted by GATC Biotech (Cologne, Germany).

Insertion of Insulated Promoter Modules in pJET1.2/blunt: Construction of genetic modules, consisting of cloning sites, an insulated promoter and a RBS, was performed using 182 bp double-stranded GeneArt® Strings™ DNA Fragments (Invitrogen). These genetic modules were further termed "insulated promoter modules". Upon delivery of freeze-dried DNA fragments, these were dissolved using the appropriate amount of sterile RO-H_2O. Resuspended DNA fragments were incubated at RT for at least 1 h and subsequently stored at -20 °C. Blunt-end DNA fragments were directly inserted into pJET1.2/blunt (Figure 2-1) using the CloneJET PCR Cloning Kit (Thermo Scientific) according to the manufacturer's instruction.

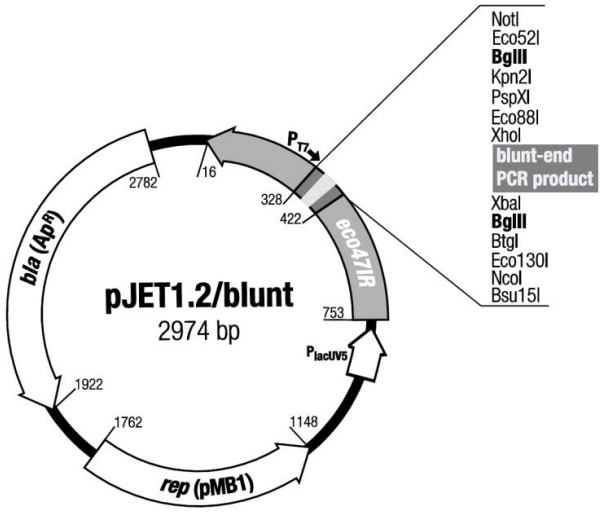

Figure 2-1: Vector map of pJET1.2/blunt. Insulated promoter modules obtained as 182 bp double-stranded GeneArt® Strings™ DNA Fragments (Invitrogen) were inserted into pJET1.2/blunt. The vector map was obtained from the user guide of the CloneJET PCR Cloning Kit (Thermo Scientific).

Plasmid DNA purification and sequence determination of resulting pJET-plasmids were performed as described above. pJET-plasmids containing insulated promoter modules were used for preparative REN digests in order to insert the respective DNA Fragment into vector backbones of choice. 2000 ng of pJET-plasmids carrying insulated promoter modules were cut with *Nde*I and *Sal*I - HF. Subsequently, insulated promoter modules were ligated with a likewise cut basic vector of choice.

Preparation of "Second Generation" Promoter Module Plasmids: Promoter modules which lack the insulation sequence and bear a weak ribosomal binding site (RBS), further termed "Second Generation" promoter modules, were constructed using single-stranded oligonucleotides (Sigma Aldrich). Complementary oligonucleotides were designed with the objective to resemble a double-stranded REN-cut-like (*Nde*I and *Sal*I) DNA molecule after annealing. Double-stranded oligonucleotides were then inserted into a vector backbone of choice cut with *Nde*I and *Sal*I as schematically illustrated in Figure 2-2. Oligonucleotides purchased by Sigma were centrifuged prior to opening and then supplemented with an

appropriate amount of RO-H_2O to yield a concentration of 100 µM. After incubation at RT for at least 1 h oligonucleotides were stored at -20 °C until further usage.

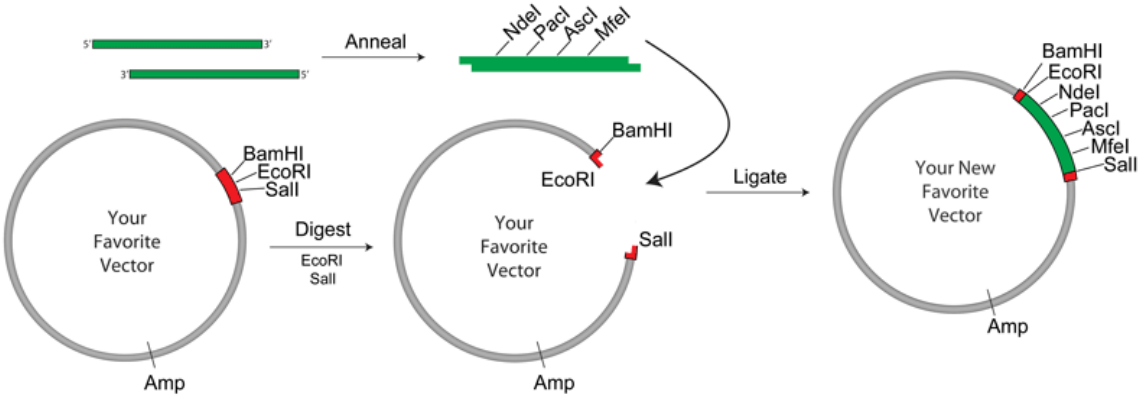

Figure 2-2: Schematic illustration of oligonucleotide cloning. Oligonucleotides were designed to have *Nde*I and *Sal*I - cut-like sticky ends after annealing. Double-stranded oligonucleotides were then ligated into an *Nde*I and *Sal*I - cut vector backbone of choice. The scheme was copied from Addgene's publically available website (Addgene 2014).

Phosphorylation and hybridization reactions of oligonucleotides were conducted in a PTC-200 Peltier thermal cycler (MJ Research) by applying the temperature profiles shown in Table 2-6.

Table 2-6: Phosphorylation and hybridization of oligonucleotides. Single-stranded oligonucleotides were phosphorylated by mixing the indicated components and incubating the solution in a PTC-200 Peltier thermal cycler (MJ Research). For phosphorylation the following temperature profile was applied: 37 °C for 30 min, 65 °C for 20 min and finally cooling down to 10 °C. For hybridization, complementary oligonucleotides were combined and the following temperature profile was applied: 95 °C for 3 min, 72 °C for 1 min, 50 °C for 1 min and finally cooling down to 10 °C.

Reaction	**Components**	**Volume**	**Temperature profile in thermal cycler**
Phosphorylation	Single-stranded oligonucleotide (100 µM)	3 µL	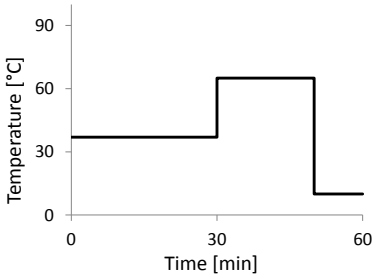
	10x T4 DNA Ligation Buffer (New England BioLabs)	5 µL	
	T4 Polynucleotide Kinase (New England BioLabs)	1 µL	
	Sterile RO-H_2O	41 µL	
Hybridization	For hybridization complementary forward and revers oligonucleotides were mixed together by combining the corresponding solutions obtained after phosphorylation	50 µL of complementary oligonucleotide solutions after phosphorylation	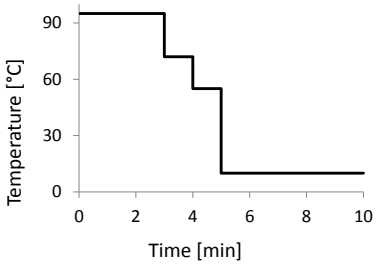

The resulting double-stranded DNA fragments encoding the Second Generation promoter modules (C1 - C9) were purified using the QIAquick® PCR Purification Kit (Qiagen) according to the manufacturer's instruction. The ligation reaction of the purified double-stranded oligonucleotides with the desired vector backbone cut with *Nde*I and *Sal*I was performed as described above except for applying only 2 µL of insert solution. Transformation, plasmid purification and sequencing of resulting plasmids were conducted as described above.

Plasmid Constructs Created in this Work: All plasmid constructs created in this work are summarized in Table 2-7.

Table 2-7: Plasmid constructs created in this work. MCS: Multiple cloning site; Second Generation promoter module: Promoter modules which lack the insulation sequence and bear a different ribosomal binding site (RBS). *gfp.1*: gene encoding a GFP mutant with 99 % DNA sequence similarity to GFPmut3b (Cormack et al. 1996). In a previous part of this project (Buettner 2016) the recognition sequence for *Nde*I was removed by a single base substitution and *gfp.1* was obtained. The proteins of GFP.1 and GFPmut3b share a 100 % identical amino acid sequence. [a] Plasmid pBI4iST7.7-gfp.1 was previously generated (Schuller 2015). [b] Plasmids carrying the gene for ampicillin resistance. Remaining plasmids carry the gene for streptomycin resistance. Fm: folding modulator gene *dsbA*, *dsbC*, *fkpA*, *ppiD*, *skp* or *surA.* Plasmids are arranged according to date of creation.

Plasmid	**Gene in MCS**	**Features**
pBI4iST7.7-gfp.1 [a]	*gfp.1*	Native T7 promoter, T7 terminator, *cer* element present, *lacI*/*lacO* absent
pJET1.2/blunt-C_n [b] (C_n = insulated promoter module Ci, Cii, Ciii, Civ, Cv, Cvi, Cviii, Cix)	none	GeneArt® DNA Fragments of insulated promoter modules inserted in pJET1.2/blunt
pBI4iSCi.2-gfp.1 pBI4iSCii.2-gfp.1 pBI4iSCiii.2-gfp.1	*gfp.1*	Insulated promoter module, T7 terminator, *cer* element present
pBI4iST7.9-gfp.1	*gfp.1*	Native T7 promoter, tZenit terminator, *cer* element present, *lacI*/*lacO* absent
pBI4iSCi.4-gfp.1 pBI4iSCii.4-gfp.1 pBI4iSCiii.4-gfp.1	*gfp.1*	Insulated promoter module, tZenit terminator, *cer* element present
pBI4iST7.10-gfp.1	*gfp.1*	Native T7 promoter, tZenit terminator, w/o *cer* element, *lacI*/*lacO* absent
pBI4iSCi.3-gfp.1 pBI4iSCii.3-gfp.1 pBI4iSCiii.3-gfp.1 pBI4iSCviii.3-gfp.1	*gfp.1*	Insulated promoter module, tZenit terminator, w/o *cer* element
pBI4iSCi.3 pBI4iSCiii.3	none	Insulated promoter module, tZenit terminator, w/o *cer* element
pBI4iSCi.3-fm	*dsbA, dsbC, fkpA, ppiD, skp, surA*	Insulated promoter module, tZenit terminator, w/o *cer* element

Plasmid	Gene in MCS	Features
pBI4iSC$_m$.3-gfp.1 (C_m = Second Generation promoter module C1, C2, C3, C4, C5, C8, C9)	*gfp.1*	Second Generation promoter module, tZenit terminator, w/o *cer* element
pBI4iSC1.3 pBI4iSC2.3 pBI4iSC3.3 pBI4iSC8.3 pBI4iSC9.3	none	Second Generation promoter module, tZenit terminator, w/o *cer* element
pBI4iSC2.3-fm	*dsbA, dsbC, fkpA, ppiD, skp, surA*	Second Generation promoter module, tZenit terminator, w/o *cer* element
pBI4iSC3.3-fm	*dsbA, skp*	Second Generation promoter module, tZenit terminator, w/o *cer* element
pBI4iSC8.3-fm	*dsbA, dsbC, fkpA, ppiD, skp, surA*	Second Generation promoter module, tZenit terminator, w/o *cer* element
pBI4iSC9.3-fm	*dsbA, skp*	Second Generation promoter module, tZenit terminator, w/o *cer* element
pBI4iSCiii.11-gfp.1	*gfp.1*	Insulated promoter module with new RBS from Second Generation promoter module, tZenit terminator, w/o *cer* element
pBI4iSC3.12-gfp.1	*gfp.1*	Second Generation promoter module with old RBS from Insulated promoter module, tZenit terminator, w/o *cer* element

2.2.3. Preparation of Cryo Cultures

Cryo cultures were prepared prior to shake flask experiments and. All strains created in this work and stored as cryo cultures are illustrated in Table 2-8. Host strains were transformed with 10 ng of the respective plasmid DNA in accordance with the transformation method described in 2.2.2. On the following day cells from a single colony of the transformed plates were transferred to a 50 mL reaction tube containing 15 mL S-LB medium supplemented with 50 µg/mL streptomycin. Cells were grown at 37 °C and 250 rpm until an OD_{550} of 0.2 - 0.5 was reached. Subsequently 2.7 mL autoclaved 87 % glycerol were added. After mixing the solution by inverting, aliquots of 1.5 mL were transferred to Nunc 1.8 mL Cryo tubes (Thermo Scientific) and stored at -80 °C until further use.

Table 2-8: Strains created in this work. Basic bacterial strains transformed with the indicated plasmids are shown. In addition, the area of application of indicated strains is stated. Cryo cultures of all strains were prepared in accordance with the method described in 2.2.3 and stored at -80 °C until further usage in shake flask experiments or fermentations. fm = folding modulator genes *dsbA*, *dsbC*, *fkpA*, *ppiD*, *skp* and *surA*. Plasmids are arranged according to date of creation.

Basic Strain / Area of application	**Plasmids used for transformation**
E. coli BL21(DE3)	pBI4iST7.7-gfp.1
Used in promoter tests for promoter module strength determination	pBI4iSCi.3 pBI4iSC8.3
	pBI4iSC$_x$.3-gfp.1 (C_x = Ci, Cii, Ciii, Cviii)
	pBI4iSC$_y$.3-gfp.1 (C_y = C1, C2, C3, C4, C5, C8, C9)
	pBI4iSCiii.11-gfp.1 pBI4iSC3.12-gfp.1
E. coli BL21(DE3) Tn7::<FabZ>(ompA kanR pt7)	pBI4iSC$_z$.3 (C_z = Ci, C2, C3, C8, C9)
Used in FabZ co-production experiments	pBI4iSCi.3-fm pBI4iSC8.3-fm pBI4iSC2.3-fm

2.3. Shake Flask Experiments

2.3.1. Basic Setup for Shake Flask Experiments

Strains listed in Table 2-8 were analysed in shake flask experiments for their GFP or FabZ production. Pre-cultures were prepared in 50 mL reaction tubes (Greiner). 30 mL T7 Pre-culture Medium were supplemented with an appropriate antibiotics. For all plasmid strains listed in Table 2-8 the T7 Pre-culture Medium was supplemented with 50 µg/mL streptomycin. 30 µg/mL kanamycin were added to the T7 Pre-culture Medium in case of the plasmid-free FabZ production strain. The pre-culture medium was inoculated with 50 µL of the respective cryo culture which was thawed at RT for 30 min prior to use. Cells were incubated o/n at 37 °C and 250 rpm. For main culture cultivation 1000 mL unbaffled Erlenmeyer flasks containing 200 mL of T7 Shake Flask Medium supplemented with the appropriate antibiotics were used. Main cultures were inoculated to an OD_{550} of 0.2 and the required pre-culture volume was calculated according to equation 2.3.1.1. The calculated volume of a pre-culture was transferred to a 50 mL reaction tube under aseptic conditions.

$$\frac{OD_{main\ culture\ start} \cdot Volume_{main\ culture}}{OD_{pre-culture\ end} - OD_{main\ culture\ start}} = Volume_{pre-culture} \qquad (2.3.1.1)$$

Subsequently, cells were sedimented by centrifugation at 3220 x g and RT for 10 min. Sedimented cells were resuspended using 5 mL sterile 0.9 % (v/v) NaCl solution and used to inoculate the T7 Shake Flask Medium. Cells were incubated at 37 °C and 300 rpm until an OD_{550} of 0.8 ± 0.25 was reached. Subsequently, main culture Erlenmeyer flasks were transferred to a second shaker incubator, which was set to 25 °C. Incubation at 25 °C and 300 rpm was carried out for a minimum of 30 min. Recombinant protein production of the FabZ production strains (BL21(DE3) Tn7::<FabZ>(ompA kanR pt7)) was induced by addition of 1 mM IPTG at an OD_{550} of 1.0 ± 0.2. In order to simulate FabZ production conditions, IPTG was also added in production experiments which employed *E. coli* BL21(DE3) basic strains. Depending on the aim of the experiment incubation at 25 °C and 300 rpm was conducted for 12 (FabZ production experiments, see 2.3.3), 24 (promoter tests, see 2.3.2) or 48 h (plasmid stability tests, see 2.3.4). Sampling was done aseptically at respective time points by transferring cell suspensions corresponding to a volume of 5 mL/OD_{550} to 15 mL centrifuge tubes. Subsequently, cell suspension samples were centrifuged at 3220 x g and 4 °C for 10 min. The centrifugation supernatant was decanted and filtrated by 0.22 µm Millex-GV syringe filter units (Merck Millipore). Both, sedimented cell and filtrated supernatant samples were stored at -20 °C until further use.

2.3.2. Determination of Promoter Module Strength

The basic setup for shake flask experiments was used to evaluate the strength of different constitutive "promoter modules", comprising the respective σ^{70} promoter sequence and RBS, in a procedure henceforth be referred to as "promoter test". The general procedure of the shake flask experiment is described in 2.3.1 while this chapter is focused on the conduction of the promoter test. Thus, strains, media and antibiotics, duration of experiment and sampling time points used specifically for the promoter test are mentioned. GFP-producing *E. coli* BL21(DE3) strains listed in Table 2-8 were subjected to the promoter test in 1000 mL unbaffled Erlenmeyer flasks with 200 mL of T7 Shake Flask Medium supplemented with 50 µg/mL streptomycin. To simulate the conditions of FabZ production experiments, 1 mM IPTG was added at an OD_{550} of 1.0 ± 0.2. The production phase at 25 °C and 300 rpm was conducted for 24 h. Cell suspension samples corresponding to a volume of 5 mL/OD_{550} were taken at four to five different time points. In each promoter test sampling was done directly before (T0) and 24 h after (EoF) addition of 1 mM IPTG. Two or three further samples were taken between T0 and EoF time points. Specific sampling time points are shown in the Results and Discussion chapter. Samples were prepared as described in 2.3.1 with the exception of completely removing and discarding the supernatant after centrifugation. Sedimented cell samples were stored at -20 °C until further use.

2.3.3. FabZ Production Experiments

The influence of three cellular levels of six folding modulators (DsbA, DsbC, FkpA, PpiD, Skp and SurA) on soluble periplasmic production of the model protein FabZ was tested using the basic setup for shake flask experiments. The general procedure of the shake flask experiment is mentioned in 2.3.1 while this chapter is focused on the conduction of FabZ production experiments. Thus, strains, media and antibiotics, duration of experiment and sampling time points used specifically in FabZ production experiments are mentioned. *E. coli* BL21(DE3) Tn7::<FabZ>(ompA kanR pt7) cells transformed with plasmids listed in Table 2-8 were examined in FabZ production experiments. Main culture incubation was performed in 1000 mL unbaffled Erlenmeyer flasks with 200 mL of T7 Shake Flask Medium supplemented with 30 µg/mL kanamycin. The production phase at 25 °C and 300 rpm was conducted for 12 h. Sampling occurred directly before induction (T0) and 12 h after addition of 1 mM IPTG (EoF). Cell suspensions samples corresponding to volumes of 5 mL/OD_{550} were taken. Supernatant and sedimented cell samples were prepared as described in 2.3.1 and stored at -20 °C until further use.

2.3.4. Evaluation of Plasmid Stability

Plasmid pBI4iSCiii.3-gfp.1, representative for a plasmid w/o *cer* element, was tested concerning its plasmid stability. Plasmid stability was tested using the basic setup for shake flask experiments. The general procedure of the shake flask experiment is mentioned in 2.3.1 while this chapter is focused on plasmid stability experiments. Thus, strains, media and antibiotics, duration of experiment and sampling time points used specifically in plasmid stability experiments are mentioned. Main culture incubation was performed in 1000 mL unbaffled Erlenmeyer flasks with 200 mL of T7 Shake Flask Medium without adding any antibiotics. Despite constitutive expression of *gfp.1*, 1 mM IPTG was added at an OD_{550} of 1.0 ± 0.2 in order to simulate cultivation conditions of FabZ production experiments. Incubation at 25 °C and 300 rpm was conducted for 48 h. A 1 mL cell suspension sample was taken aseptically 24 and 48 h after addition of IPTG. Cell suspension samples were diluted up to 10^8-fold in sterile 0.9 % (v/v) NaCl solution. 100 µL of 10^{-6}, 10^{-7} and 10^{-8} dilutions were plated on non-selective S-LB agar plates which were incubated o/n at 37 °C. Single colonies were picked and transferred to a non-selective agar plate and in parallel to an S-LB agar plate containing 50 µg/mL streptomycin (see Figure 2-3). The plates were incubated o/n at 37 °C and the resulting colonies were counted. Numbers of colonies of the non-selective S-LB agar plates were compared to colony numbers of the S-LB agar plate containing 50 µg/mL streptomycin. Plasmid stability was calculated by dividing colony count of the streptomycin plate by colony count of the non-selective plate. In addition results were verified by evaluating the number of GFP - producing and thus fluorescing colonies on both plates.

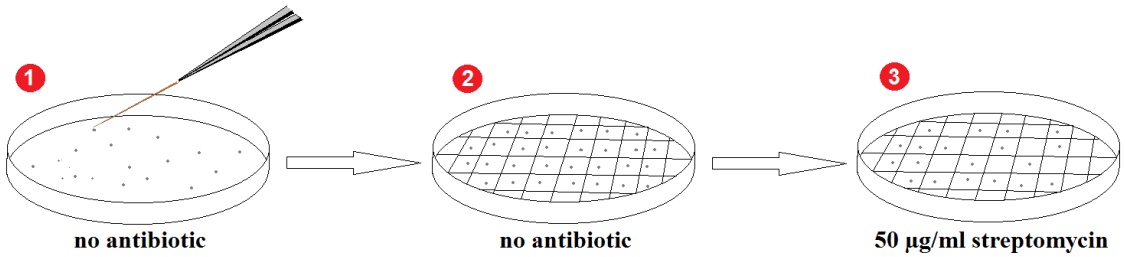

Figure 2-3: Illustration of plasmid stability analysis. Plasmid stability of the *cer* element lacking strain BL21(DE3)(pBI4iSCiii.3-gfp.1) was tested using the basic setup for shake flask experiments (2.3.1). Cells were incubated at 25 °C and 300 rpm and cell suspension samples were taken 24 and 48 h after addition of 1 mM IPTG. 100 µL of appropriate dilutions (10^{-6}, 10^{-7} and 10^{-8}) of cell suspension samples were plated on non-selective ager plates (1) and incubated o/n at 37 °C. Single colonies were transferred to a non-selective ager plate (2) and in parallel to an S-LB agar plate containing 50 µg/mL streptomycin (3). After o/n incubation at 37 °C, colony numbers of plate 2 and 3 were determined. Plasmid stability was calculated by dividing colony numbers on plate 3 by colony numbers on plate 2. The scheme was copied from a diploma thesis which was prepared previously in this project (Schuller 2015).

2.4. Fed-batch Fermentation Experiments

E. coli BL21(DE3) Tn7::<FabZ>(ompA kanR pt7) cells transformed with plasmids listed in Table 2-8 were analysed concerning their FabZ productivity in fed-batch fermentations. Fed-batch fermentations were carried out in a 6.9 L computer-controlled stirred-tank BIOSTAT® Cplus bioreactor (Sartorius Stedium Biotech). The pH was maintained at 6.8 ± 0.2 by the addition of 25 % ammonia solution and 3 M phosphoric acid, respectively. The dissolved oxygen (DO) level was adjusted to ≥20 % and an over pressure of 1000 mbar was applied. The DO was stabilized by stirrer speed adjustment (400 to 1200 rpm) and aeration variation (total aeration rate: 5 L/min, air flow: 2.5 - 5 L/min, oxygen flow: 0 - 2.5 L/min). Chemically defined growth medium (for composition see Confidential Supplemental Information) was supplemented with 1 mL/L polypropylenglycol (2000 g/mol, Wacker-Chemie) in order to supress foaming. If required additional polypropylenglycol (PPG 2000) was added during the fermentation course. For pre-cultures 1000 mL unbaffled Erlenmeyer flask were used. 300 mL of T7 Pre-culture Medium supplemented with 50 µg/mL streptomycin was inoculated with 100 µL of a cryo culture which was thawed on RT for 30 min prior to usage. Cells were incubated at 33.5 °C and 250 rpm until reaching an OD_{550} of approximately 2. Based on the pre-culture's OD_{550} value, an inoculation volume equivalent to 35 mL of a solution with an OD_{550} value of 2.0 was used to start the fed-batch culture. To start the batch phase of fermentation, the respective volume of a pre-culture suspension was added with a sterile syringe to the fermenter containing 2500 mL sterilized Batch Medium (for composition see Confidential Supplemental Information). Temperature was kept constant at 37 °C during the whole fermentation. Batch phase was completed upon appearance of a pronounced pO_2 peak. Subsequent to batch phase an exponential feeding profile was started by addition of

increasing amounts of Glucose Feed solution (calculated growth rate: $\mu = 0.177/h$) (for composition see Confidential Supplemental Information). In case of occurring glucose accumulation (> 0.5 g/L), feed rates were adapted manually. After 12 h of exponential feeding, a constant feed rate was employed for another 15 h maintaining the final feed rate of the exponential feed phase. FabZ production was induced 14 h after starting the exponential feed phase by addition of 0.894 g IPTG, resulting in an average concentration of 1 mM. After the addition of the inducer IPTG, cells were cultivated for another 13 h. During the protein production phase, OD_{550}, dry cell weight (DCW) and glucose concentration were determined on regular basis. Sampling occurred prior to induction (T0) and 3.25 (T1), 6.5 (T2), 9.75 (T3) and 13 h (EoF) after induction. Cell suspension samples corresponding to a volume of 10 mL/OD_{550} were taken and subsequently centrifuged at 3220 x g and 4 °C for 10 min. Centrifugation supernatant derived from DCW - measurement was filtrated using 0.22 µm Millex-GV syringe filter units (Merck Millipore) and applied as supernatant samples for protein analysis. Both, sedimented cell and filtrated supernatant samples were stored at -20 °C until further use. Fed-batch fermentations were conducted in the course of a PhD thesis. Detailed description of the process can be found therein (Buettner 2016).

2.5. Protein Analytics

2.5.1. GFP Fluorescence Measurement

Intracellular GFP which was produced in shake flask experiments as described in 2.3.2 was used to determine the promoter module-mediated expression level, henceforth termed “promoter module strength” (Figure 2-4). Frozen samples of sedimented cells containing intracellular GFP were thawed at RT for 15 min. Subsequently samples were resuspended in 5 mL OD buffer resulting in a cell suspension with an OD_{550} of 1.0. 200 µL of the cell suspension were transferred to a 96-well flat bottom transparent UV-plate (Costar®, Sigma-Aldrich). Each sample was applied in all eight wells of one column. Fluorescence of the samples was measured using a Safire^{2}™ fluorescence microplate reader (Tecan Group) applying the following parameters:

- Excitation wavelength: 475 nm
- Emission wavelength: 512 nm
- Excitation and emission bandwidth: 20.0 nm
- Gain: 200
- Number of reads: 10
- Flashmode: High sensitivity
- Integration time: 500 µs
- Lag time: 60 µs
- Z-Position (Manual): 12400 µm
- Shake duration (Orbital Low): 30 s
- Shake settle time: 10 s

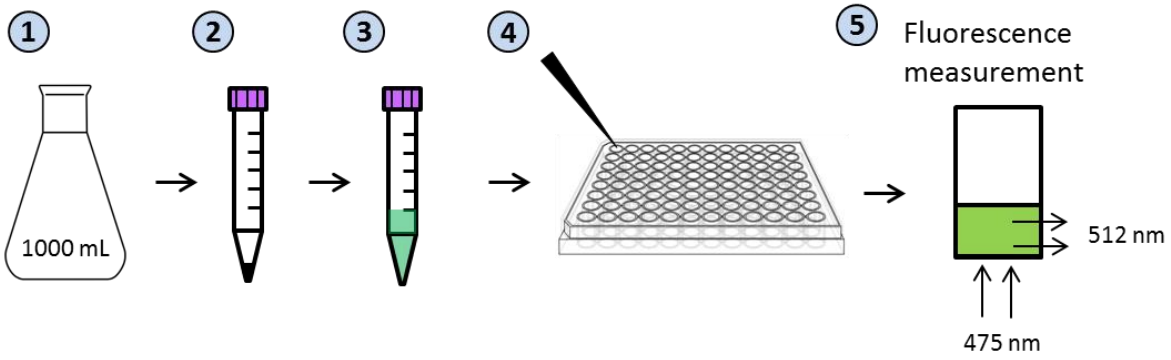

Figure 2-4: Schematic overview of the promoter test procedure. Plasmid-bearing *E. coli* BL21(DE3) strains listed in Table 2-8 were subjected to promoter tests as described in 2.3.2. Cells were cultivated in 1000 mL unbaffled Erlenmeyer flasks in 200 mL of T7 Shake Flask Medium supplemented with 50 µg/mL streptomycin (1). Cell suspension samples corresponding to a volume of 5 mL/OD_{550} were taken aseptically and transferred to 15 mL centrifuge tubes. Samples were centrifuged at 3220 x g and 4 °C for 10 min. The resulting supernatant was discarded and sedimented cell samples were stored at -20 °C (2). Cell pellets were thawed at RT for 15 min and resuspended in 5 mL OD buffer (3) resulting in a suspension with an OD_{550} value of approximately 1.0. 200 µL of each sample were transferred to all eight wells of one column of a 96-well flat bottom transparent UV-plate (Costar®, Sigma-Aldrich) (4). Fluorescence of the samples was measured using a Safire^{2}™ fluorescence microplate reader at an excitation wavelength of 475 nm and an emission wavelength of 512 nm (5). Resulting fluorescence was displayed in relative fluorescence units (RFU) using the software Magellan V7.1 (Tecan Group).

Fluorescence of GFP-bearing cell suspension samples was measured at an excitation wavelength of 475 nm and an emission wavelength of 512 nm. The measured $fluorescence_{Exc.475/Em.512}$ was displayed in relative fluorescence units (RFU) using the software Magellan V7.1 (Tecan Group). Mean value and standard deviation of each fluorescence value was calculated and used as basis for determination of the Coefficient of Variation (CoV). By measuring the $fluorescence_{Exc.475/Em.512}$ of GFP-producer strains over time, the time course of intracellular GFP level and hence GFP synthesis rate can be determined. Measured RFU values comprise intracellular GFP levels and the low level of background autofluorescence of *E. coli* BL21(DE3) cells. Hence, fluorescence of non-GFP-producing strains such as BL21(DE3)(pBI4iSCi.3), BL21(DE3)(pBI4iSC8.3) and BL21(DE3)(pBI1ST7.2) was considered autofluorescence and subtracted from fluorescence of all GFP-producing strains. Resulting GFP fluorescence values were used for relative promoter strength calculation. Depending on the experimental setup GFP fluorescence of one GFP-bearing cell suspension sample was selected and set to 100 %. Relative promoter module strength was determined by dividing the GFP fluorescence of a respective strain by the 100 % set point value. More details on the promoter test procedure including sampling time points, selection of 100 % reference and calculation of relative promoter strength can be found in the Results and Discussion chapter.

2.5.2. Enzyme-Linked Immunosorbent Assay

Soluble FabZ produced in shake flask experiments as described in 2.3.3 and fed-batch fermentations (2.4) was analysed by sandwich enzyme-linked immunosorbent assay (ELISA) (Figure 2-5).

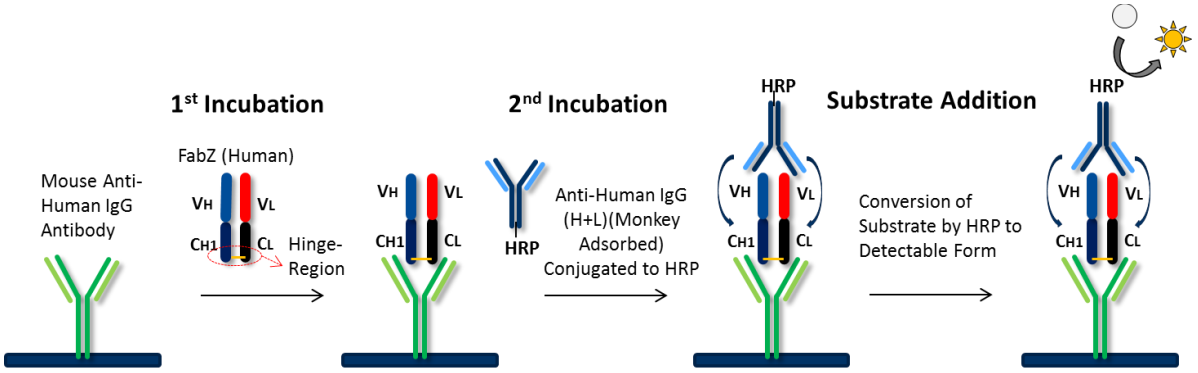

Figure 2-5: Principle of sandwich ELISA used for FabZ analysis. Polystyrene clear flat bottom 96 Well ELISA Microplates (Microlon®, Greiner) were used as microtiter measurement plate and filled with 100 µL of a 4000-fold dilution of the mouse anti-human IgG coating antibody (Ab7497, Abcam). After blocking with 200 µL 1x TBS 1 % Casein Blocker, 100 µL of FabZ containing sample and reference solutions were added to the microtiter measurement plate. The coating antibody aims at the hinge-region of properly folded antibodies and specifically captures FabZ LC/HC heterodimers (Einhorn 2013). 100 µL of a 4000-fold dilution of HRP-conjugated anti human IgG (H+L) (monkey adsorbed) immunoglobulins (AP003CUS01, The Binding Site) were added to the wells as secondary antibody. The secondary antibody interacts with various epitopes of human IgG immunoglobulins and is conjugated to horse reddish peroxidase (HRP). The enzyme HRP catalyses a colour reaction upon addition of 100 µL of the Substrate Solution (TMB One Component Microwell Substrate, SouthernBiotech). The substrate reaction is stopped by the addition of 100 µL Stopping Solution (1 M HCl) and absorbance at 620 and 450 nm was measured using a microplate reader (PowerWave HT, BioTek® Instruments). This figure was obtained from an unpublished presentation of a master thesis (Einhorn 2013) and slightly modified within this diploma thesis.

Sample Preparation: Frozen samples of sedimented cells obtained from sampling in FabZ production experiments were thawed at RT for 15 to 30 min. Cell samples from shake flask and fermentation experiments were resuspended in 250 µL and 500 µL BugBuster® Protein Extraction Reagent (Novagen) containing 2 µL/mL Lysonase™ solution (Novagen), respectively. Cells were disrupted by incubating the BugBuster® suspensions for 15 min and 1400 rpm at RT in a Thermomixer. The supernatant obtained after centrifugation at 16100 x g at RT for 15 min represents the soluble intracellular protein fraction (WC-sol) which was subjected to ELISA analysis. Frozen filtrated supernatant samples (Sup) of FabZ production experiments were thawed at RT prior to ELISA analysis. Appropriate dilutions of both WC-sol and Sup fractions were prepared by dilution with Sample Diluent Buffer (Table 2-9). Solutions of 25, 10, 7.5, 5, 3.75, 2.5 and 1 ng/mL reference protein were prepared by diluting the standard solution containing 5.91 mg/mL purified FabZ with Sample Diluent Buffer. The FabZ standard solution was produced and purified in a previous part of the project (Buettner 2016). Sample Diluent Buffer was used as blank for determination of the calculated standard curve.

Table 2-9: Dilutions of samples subjected to ELISA analysis. Soluble intracellular protein fraction was obtained after disrupting sedimented cells with BugBuster® Protein Extraction Reagent (Novagen) containing 2 µL/mL Lysonase™ solution (Novagen). Upon cell lysis the samples were centrifuged and the resulting supernatants were subjected to ELISA analysis (WC-sol). Supernatant samples (Sup) were obtained by filtration (0.22 µm Millex-GV syringe filter units) of the culture supernatant from FabZ production experiments and represent the soluble extracellular protein fractions. Dilutions of WC-sol and Sup samples from shake flask experiments and fed-batch fermentations used for ELISA analysis are indicated.

Production Experiment	Sample Type	Dilutions
Shake flask experiment	WC-sol	250-, 1500- and 4500-fold
	Sup	100-, 1000- and 5000-fold
Fed-batch fermentation	WC-sol	500-, 2000- and 3000-fold
	Sup	1000-, 10000- and 20000-fold

Plate Preparation: Polystyrene clear flat bottom 96-well ELISA Microplates (Microlon®, Greiner) were used as microtiter measurement plates for ELISA analysis. Each well of the microtiter measurement plate was filled with 100 µL of a 4000-fold dilution of the coating antibody (mouse anti-human IgG antibody, Ab7497, Abcam) in Coating Buffer, sealed using Parafilm M® (Bemis) and stored o/n at 4 °C. The next day the microtiter measurement plate was subjected to the "Washing Procedure" in which wells were first emptied by aspiration and then washed three times with 250 µL of Wash Buffer using an auto plate washer Elx405 (BioTek® Instruments). At the end of the Washing Procedure the plate was tapped onto paper towels to remove remaining solution droplets. Subsequently, 200 µL of Blocking Solution were added to each well of the microtiter measurement plate. After incubation at RT on a shaker station (450 rpm) for 1 h the microtiter measurement plate was again subjected to the Washing Procedure. 150 µL of each sample and each reference solution was loaded into a NUNC™ Microwell™ 96-Well Microplate (Thermo Scientific). From this plate, 100 µL of the reference samples, blank and the three dilutions of the samples were transferred to the microtiter measurement plate in triplicates (see Figure 2-6).

<>	1	2	3	4	5	6	7	8	9	10	11	12
A	Ref 25	Ref 10	Ref 7.5	Ref 5	Ref 3.75	Ref 2.5	Ref 1	Ref 0	S06 Dil1	S06 Dil2	S06 Dil2	S06 Dil2
B	Ref 25	Ref 10	Ref 7.5	Ref 5	Ref 3.75	Ref 2.5	Ref 1	Ref 0	S06 Dil1	S06 Dil3	S06 Dil3	S06 Dil3
C	Ref 25	Ref 10	Ref 7.5	Ref 5	Ref 3.75	Ref 2.5	Ref 1	Ref 0	S06 Dil1	S07 Dil1	S07 Dil1	S07 Dil1
D	S01 Dil1	S01 Dil1	S01 Dil1	S01 Dil2	S01 Dil2	S01 Dil2	S01 Dil3	S01 Dil3	S01 Dil3	S07 Dil2	S07 Dil2	S07 Dil2
E	S02 Dil1	S02 Dil1	S02 Dil1	S02 Dil2	S02 Dil2	S02 Dil2	S02 Dil3	S02 Dil3	S02 Dil3	S07 Dil3	S07 Dil3	S07 Dil3
F	S03 Dil1	S03 Dil1	S03 Dil1	S03 Dil2	S03 Dil2	S03 Dil2	S03 Dil3	S03 Dil3	S03 Dil3	S08 Dil1	S08 Dil1	S08 Dil1
G	S04 Dil1	S04 Dil1	S04 Dil1	S04 Dil2	S04 Dil2	S04 Dil2	S04 Dil3	S04 Dil3	S04 Dil3	S08 Dil2	S08 Dil2	S08 Dil2
H	S05 Dil1	S05 Dil1	S05 Dil1	S05 Dil2	S05 Dil2	S05 Dil2	S05 Dil3	S05 Dil3	S05 Dil3	S08 Dil3	S08 Dil3	S08 Dil3

Figure 2-6: Layout of 96 well microtiter measurement plate used for ELISA analysis. 100 µL of reference protein, blank and three dilutions of each sample were added in triplicates to a polystyrene, clear flat bottom 96-well ELISA Microplates (Microlon®, Greiner). Ref 0 - Ref 25: reference solutions obtained upon dilution of standard solution containing 5.91 mg/mL purified FabZ with Sample Diluent Buffer. Numbers 1 - 25 indicate FabZ concentration in ng/mL, whereby Ref 0 refers to the blank solution (Sample Diluent Buffer). S01 - S08: Samples 1 - 8 diluted with Sample Diluent Buffer according to scheme shown in Table 2-9 resulting in three different dilutions abbreviated as Dil 1, Dil2 and Dil 3.

After incubation at RT on a shaker station (450 rpm) for 1 h the microtiter measurement plate was again subjected to the Washing Procedure. Afterwards, 100 µL of secondary antibody solution (4000-fold dilution of HRP-conjugated anti human IgG (H+L) (monkey adsorbed) immunoglobulins (AP003CUS01, The Binding Site) in Blocking Solution) were added in each well. After incubation at RT on a shaker station (450 rpm) for 1 h the microtiter measurement plate was once more subjected to the Washing Procedure. 100 µL of Substrate Solution (TMB One Component Microwell Substrate, SouthernBiotech) were added in each well and the plate was incubated for exactly 10 min at RT in the dark. The substrate reaction was stopped by the addition of 100 µL Stopping Solution (1 M HCl) into each well.

Measurement and Data Analysis: Within 30 min after stopping the substrate reaction the absorbance at 620 and 450 nm was measured using a microplate reader (PowerWave HT, BioTek® Instruments). For product concentration calculations ΔOD values were determined by subtracting the OD_{620} values from the OD_{450} values. A standard curve was established using the eight concentrations of reference protein and their respective ΔOD values. The standard curve was evaluated using the Coefficient of Determination with an acceptance criterion of $R^2 \geq 0.99$. The soluble FabZ concentration in the wells of the microtiter measurement plate was calculated based on measured ΔOD values using the determined standard curve equation. Soluble FabZ concentration in mg/L of WC-sol and Sup samples was obtained by determining the mean value of all nine calculated FabZ concentrations for the triplicates of the three dilutions of a sample. ΔOD values outside the range of the standard curve were excluded from mean value calculations. In addition, single outliers of ΔOD values within a triplicate measurement of one dilution were removed prior to mean value calculations. Furthermore, three FabZ concentrations of one dilution of a sample were excluded from mean value calculations if the respective FabZ concentrations were identified as outliers compared to the calculated FabZ concentration of the other two dilutions of the same sample. The calculated mean values of soluble FabZ concentration of WC-sol and Sup solutions were summarized to obtain the total soluble FabZ concentration in mg/L of a sample.

2.5.3. Sodium Dodecyl Sulfate Polyacrylamide Gel Electrophoresis

Sodium dodecyl sulfate polyacrylamide gel electrophoresis (SDS-PAGE) was used to analyse the whole cell protein content of FabZ production strains. Frozen samples of sedimented cells obtained in shake flask experiments as described in 2.3.3 were thawed at RT for a minimum of 15 min and subjected to SDS-PAGE analysis. Cells were resuspended in 250 µL BugBuster® Protein Extraction Reagent containing 2 µL/mL Lysonase™ solution (Novagen). Subsequently, cells were disrupted by incubation for 15 min and 1400 rpm at RT in a Thermomixer. 9 parts 4x NuPAGE® LDS Sample Buffer (Novex®) were mixed with 1 part β-mercaptoethanol (Sigma-Aldrich). The obtained solution was diluted twofold using MilliQ®-

water (Merck Millipore) to prepare 2x LDS buffer. The 2x LDS buffer was mixed with equal parts of MilliQ®-water to obtain 1x LDS buffer. Subsequently, samples were diluted threefold with 2x LDS buffer and incubated at 80 °C and 450 rpm for 5 min. Reference solutions containing 0.2, 0.8 and 1.4 µg FabZ were prepared by diluting a standard solution, containing 5.91 mg/mL FabZ, with 1x LDS buffer. The FabZ standard solution was prepared in a previous part of the project (Buettner 2016). Reference protein solutions were also denaturated at 80 °C and 450 rpm for 5 min. Before loading onto the gel, the samples and reference solutions were allowed to cool down to RT. Subsequently, 10 µL of sample solutions and 5 µL of MW standard (Precision Plus (Unstained), BioRad) and reference protein solutions were loaded onto a Criterion™ TGX Stain-Free™ Precast gel (12 + 2 well comb, Bio-Rad). Protein separations were carried out using 1x TGS buffer and applying a voltage of 200 V for approximately 35 min. Gel images were acquired using the gel-Doc™ EZ Imager (Bio-Rad) and analysed using the Image Lab 5.0 software. Image tools were applied and lanes and bands were determined using the Image Lab 5.0 software. Protein quantity was determined using a standard curve calculated from the reference protein samples by linear regression. Only curves having a Coefficient of Determination $R^2 \geq 0.99$ were used for protein quantification.

3. Results and Discussion

3.1. Establishing a Co-Expression System to Enable Screening of Different Periplasmic Folding Modulators and Levels

3.1.1. Developing an Appropriate GFP Fluorescence Measurement Method

In this work a co-expression system based on constitutive promoters and six periplasmic folding modulators (DsbA, DsbC, FkpA, PpiD, Skp and SurA) was established. This co-expression system should enable to quickly screen for appropriate folding modulators which could enhance the soluble periplasmic production of different target proteins. In this study the influence of co-expression of folding modulator genes on soluble production of the antibody binding fragment FabZ was examined. In order to determine the activity of the constitutive promoter modules, which were used for the control of folding modulator gene expression, an assay based on fluorescence measurement of the green fluorescence protein (GFP) was used. Therefore the constitutive promoter modules were cloned into expression vectors to control production of GFP. *E. coli* BL21(DE3) cells were subsequently transformed with the respective promoter probing vectors. The activity of the promoter module was determined by measuring the fluorescence of intracellular GFP which was produced in shake flask experiments by the corresponding GFP-producing cells. Relative fluorescence units (RFU) of cell samples resuspended in OD buffer were measured in a Safire^{2}™ fluorescence microplate reader. Fluctuating RFU values obtained for one and the same cell suspension sample were determined in initial measurement attempts (data not shown). It was assumed that the position of a cell suspension sample on the measurement plate exerted a significant influence on the resulting RFU value. Hence, the fluorescence measurement method was evaluated and optimized, prior to promoter module strength determination.

During the evaluation it was examined, if the factors “plate”, “row” and “column” exert an influence on the measured RFU values. Cell samples of the plasmid strain BL21(DE3) pBI4iSC3.3-gfp.1 in which GFP production is controlled by the C3 promoter module were used for this evaluation. BL21(DE3) pBI4iSC3.3-gfp.1 cells were grown in shake flask experiments as described in 2.3.2. A cell suspension sample was taken 24 h after addition of IPTG. After centrifugation of the cell suspension sample the supernatant was discarded. Sedimented cells were resuspended in OD buffer resulting in a cell suspension with an OD_{550} of 1.0. Two identical 96-well flat bottom transparent UV-plates (Costar®, Sigma-Aldrich) were used for the fluorescence measurement. Two hundred µL of the cell suspension were transferred to each well of both plates. Fluorescence of GFP was measured at an excitation wavelength of 475 nm and an emission wavelength of 512 nm and represented in RFU. A detailed measurement protocol and the parameters of fluorescence measurement are

documented in Chapter 2.5.1. Results of the fluorescence measurement are presented as a heat map in Figure 3-1. To statistically evaluate the data the analysis of variance (ANOVA) method was used. Three different factors, "row" A - H, "column" 1 - 12 and "plate" 1 - 2, were defined to determine the influence of the sample position on the measured RFU values. A significance level of 5 % (α = 0.05) was chosen for the ANOVA analysis. The corresponding F_{crit} values were obtained from a publicly accessible F-distribution table. Results of ANOVA analysis are summarized in Table 3.1.

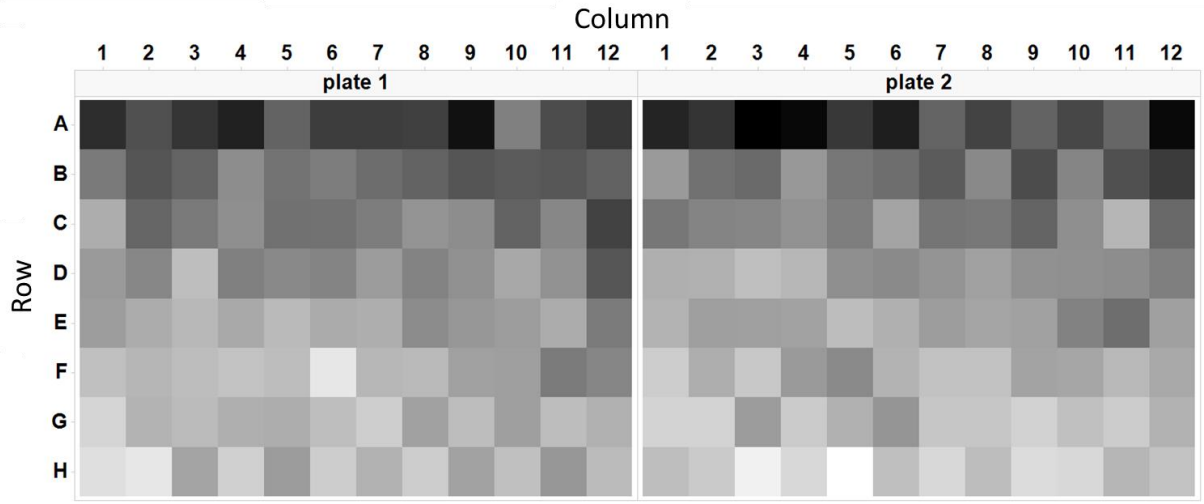

Figure 3-1: Influence of plate position on measured RFU value displayed as heat map. It was examined how the position of a GFP-bearing cell sample on the measurement plate influenced the measured RFU values. Cells of the plasmid strain BL21(DE3) pBI4iSC3.3-gfp.1 were subjected to shake flask experiments as described in 2.3.2. Cell suspension samples were taken 24 h after addition of IPTG. The samples were centrifuged and the supernatant was discarded. Sedimented cell samples were resupended in OD buffer resulting in a cell suspension with an OD_{550} of 1.0. 200 µL of the cell suspension were applied to each well of two identical 96-well flat bottom transparent UV-plates. Relative fluorescence units (RFU) of the sample were determined by measuring the fluorescence of the intracellular GFP content at an excitation wavelength of 475 nm and an emission wavelength of 512 nm. RFU values of each well of the two plates is displayed in the heat map. Colour intensity corresponds to the measured RFU value. Black: Maximal RFU value (13708). White: Minimal RFU value (7995).

Table 3-1: Statistical evaluation of the influence of the plate position on measured RFU value by analysis of variation (ANOVA) method. Factors "row", "plate" and "column" were examined concerning whether they exert a statistically significant influence on measured RFU values. The calculated p-value and F_{Stat} value at a significance level of 5 % (α = 0.05) for the factors "row", "plate" and "column" are indicated. The corresponding F_{crit} values were obtained from an F-distribution table.

Factors	**p-value**	**F_{Stat}**	**F_{crit}**
Row	4.89×10^{-54}	84.36	2.01
Plate	4.74×10^{-1}	0.55	3.84
Column	8.66×10^{-1}	0.52	1.79

The heat map (Figure 3-1) shows obvious differences in colour intensities between different rows. A colouring trend across the plates or between columns can visually not be stated. These results indicate that the position between rows seemed to exert a significant influence on the measured RFU values, but the different columns or plates do not. The variance in colour intensities and hence RFU values appeared to be particularly high between the first three rows. ANOVA analysis revealed p-values higher than the significance level of 5 % for the factors "plate" and "column". In addition, the F_{stat} value of these factors was smaller than the corresponding F_{crit} values. These results indicate that the factors "plate" and "column" do not exert a statistically significant influence on the fluorescence measurement and the resulting RFU values. On the other hand a highly significant p-value far below the significance level was obtained for the analysis of the factor "row". In addition, the F_{stat} value of the factor "row" was higher than the corresponding F_{crit} value. This indicates that a statistically significant influence on the measured RFU value is exerted by the row in which a sample is positioned. Thus, influence of plate and column on a RFU value of a sample is negligible while the row position of a sample is highly relevant. Since there is no influence by the used plate itself, samples measured on different plates can directly be compared. To compensate the variance of RFU values measured in different rows for the later experiments, samples were applied in every well of an entire column. The mean value of this eightfold measurement was determined and used for further calculations.

3.1.2. A Genetic Module Containing a Weak Insulated Promoter and an Improved Vector Backbone Appear Suitable for Creation of Co-Expression Plasmids

Insulated Promoter Modules for the Co-Expression System Were Created. A co-expression system based on the folding modulator genes *dsbA*, *dsbC*, *fkpA*, *ppiD*, *skp* and *surA* was created and applied in FabZ production experiments previously in this project (Schuller 2015; Buettner 2016). In this previous part of the project the native T7 promoter and three T7 promoter mutants of various strength (3, 20 and 61 % in comparison to the native T7 promoter) were used to control the transcription rate of the folding modulator genes. Severe drawbacks of the T7 promoter-based co-expression system were observed as interference between folding modulator gene and FabZ gene expression was demonstrated. Additional regulatory elements of the T7 co-expression system (*lacI* and *lacO*) introduced by the T7 expression cassette of the co-expression plasmid were identified as probable root cause for interference with the genomically integrated T7 system driving FabZ gene expression (see Figure 3-2) (Buettner 2016). Because of the interference phenomenon the DNA sequences of the regulatory elements *lacI* and *lacO* were removed from the folding modulator gene co-expression plasmids. The application of the modified co-expression system using the T7 promoter mutant of 3 % relative strength led to improved soluble FabZ yields in shake flask experiments for the periplasmic folding modulators DsbA, FkpA, PpiD,

Skp and SurA. However, these promising results could not be reproduced in 5 L fed-batch fermentation experiments (Buettner 2016).

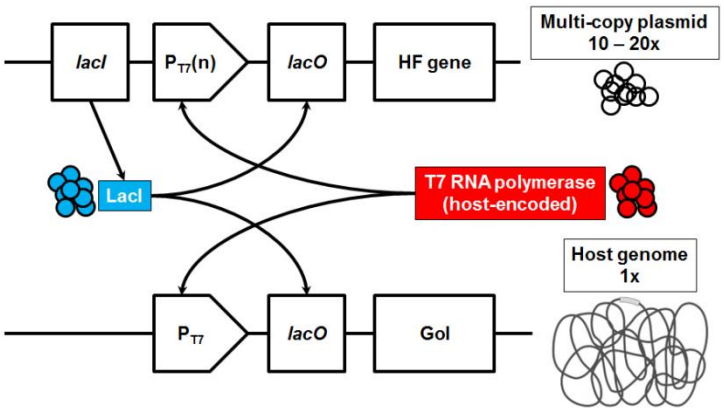

Figure 3-2: Potential interference between FabZ- and folding modulator gene co-expression within an *E. coli* cell. Arrows indicate interactions between target DNA sequences and proteins. LacI: *lac* repressor protein. *lacI*: gene encoding *lac* repressor protein. P_{T7}(n): native T7 promoter or T7 promoter mutant of 3, 20 or 61 % respective relative strength compared to native T7 promoter. *lacO*: *lac* repressor binding site. HF gene: DNA sequence encoding a folding modulator gene (*dsbA*, *dsbC*, *fkpA*, *ppiD*, *skp* or *surA*). GoI: Gene of interest (here: FabZ gene). The figure was copied from a PhD thesis prepared in the course of this project (Buettner 2016).

In contrast to inducible T7 promoters, constitutive promoters could be an alternative for controlling the synthesis rate of folding modulators on co-expression plasmids. Folding modulator gene transcription controlled by constitutive promoters should not interfere with FabZ gene transcription as observed for the T7 co-expression system. Furthermore, the application of constitutive promoters would permanently up-regulate expression of a respective folding modulator and should not be influenced by the induction time point of FabZ gene expression. Hence, sufficient amounts of the respective folding modulator would be present from the beginning of the recombinant FabZ production. Increased levels of folding modulators should enable proper FabZ folding in the periplasm directly after the induction of FabZ gene expression by IPTG. In addition, cells would be adapted to the metabolic burden affiliated with a permanently up-regulated folding modulator gene co-expression. Constitutive promoters have already been successfully applied in co-expression attempts for production of several recombinant proteins in the periplasmic space (Schlapschy et al. 2006; Friedrich et al. 2010). As stated in several review articles, the folding modulator co-production needs to be optimized for each recombinant target protein (Martínez-Alonso et al. 2010; Overton 2014). To improve the soluble periplasmic production of a protein of interest by folding modulator co-synthesis, a trial-and-error approach is required. Thus, in the course of this work a co-expression system based on constitutive promoters of various strengths was supposed to be established to enable screening for different folding modulators and levels. The influence of the co-expression system on soluble target protein production should then be analysed using the antibody fragment FabZ. To design a co-expression system which meet these demands, constitutive promoter sequences covering a broad range of promoter strength were selected.

Sequence information of six different constitutive promoters (-35 box, 17 bp spacer, -10 box, 6 bp spacer and transcription initiation site +1), was obtained from the publicly accessible "Anderson collection" (Anderson 2006). The -35 and -10 consensus sequences of the constitutive promoters are referred to as -35 and -10 box, respectively. Constitutive promoters from the "Anderson collection" are based on the consensus sequence of a typical σ^{70} promoter (see Figure 1-6) (Snyder et al. 2010). Hence, transcription from constitutive promoters from the "Anderson collection" is initiated by the *E. coli* σ^{70} RNA polymerase (RNAP) holoenzyme. RNAP holoenzyme is formed upon association of the RNAP core enzyme with a specific transcription initiation factor, termed sigma (σ) factor (Burgess et al. 1969). The σ-factor provides the binding specificity of RNAP holoenzyme to specific promoter DNA sequences (Snyder et al. 2010). Several different types of σ-factors are known, whereby σ^{70} is the primary or "housekeeping" σ-factor in *E. coli* (Gross et al. 1998). The σ^{70} factor is responsible for the transcription of most genes expressed in exponential growth phase (Gross et al. 1998). The majority of other sigma factors are required for a certain physiological role, e.g. σ^{38} for stress/starvation response, σ^{28} for flagellum synthesis, σ^{32} for heat shock response and σ^{54} for nitrogen limitation (Wösten 1998). The activity of promoters from the "Anderson collection" is exclusively dependent on the availability of σ^{70} and thus transcription should be active under most growth conditions. Differences in strength of the promoters from the "Anderson collection" are associated with 1-5 base substitutions in the -35 and/or -10 consensus sequence and/or in the 17 bp spacer in between (Anderson 2006). The activity of different constitutive promoters from the Anderson collection has previously been shown (Davis et al. 2010; Kelly et al. 2009). To extend the strength range of the constitutive promoters, three further promoter sequences were obtained from another constitutive promoter library (Davis et al. 2010). These promoter sequences are based on the *E. coli* rrnB P1, which is a strong σ^{70} -dependent promoter (Davis et al. 2010). Differences in the promoter strengths of "Davis promoters" are exclusively affiliated with base substitutions in the -10 consensus sequence.

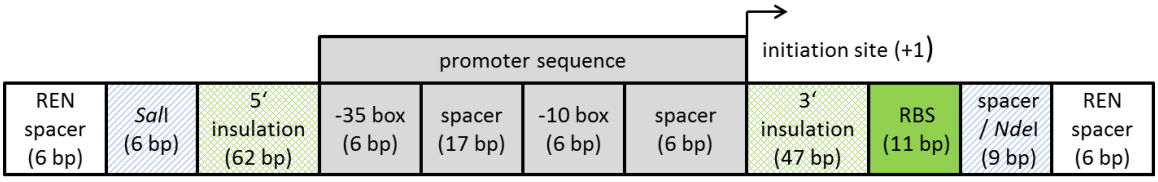

Figure 3-3: Schematic representation of insulated promoter modules. All elements of insulated promoter modules (Ci - Cix) and their respective sequence length are shown. Insulated promoter modules were ordered as double-stranded GeneArt® Strings™ DNA fragments (Invitrogen). REN spacers: 6 bp random sequences needed for proper endonuclease restriction. *Sal*I: Recognition sequence for *Sal*I. 5' insulation: Insulation sequence upstream of the promoter sequences. Promoter sequence: Comprises -35 box, 17 bp spacer, -10 box and a spacer sequence between core promoter and transcription initiation site (indicated by an arrow). Insulated promoter modules differ from each other in 1-5 base positions in their promoter sequences. 3' insulation: Insulation sequence downstream of promoter sequence. RBS: Ribosomal binding site. Spacer / *Nde*I: 3 bp spacer between RBS and *Nde*I recognition site resulting in optimal 6 bp spacing between RBS and ATG starcodon. The *Nde*I recognition sequence includes the start ATG of the gene of interest.

The activity of promoters often varies with the genetic environment or the gene which is transcribed (Alper et al. 2005; Kelly et al. 2009; Jensen & Hammer 1998; Hammer et al. 2006). An up to 300-fold enhancement of promoter activity due to improved binding of the α subunit of RNAP can for example be caused by A/T-rich promoter sequences. Such sequences are known as UP elements and located approximately 60 bp upstream of the transcription initiation site (Ross et al. 2001; Estrem et al. 1999). In order to decouple promoter strength from the native genetic context, adjoining upstream and downstream sequences were added to all core promoter sequences. This sequences, termed 3' and 5' "insulation sequences", were copied from a previously published study (Davis et al. 2010) and slightly modified within this work. To provide similar transcription rates of different folding modulator genes, 5' and 3' insulation sequences (62 and 47 bp, respectively) were added to the nine selected core promoter sequences. Usually this sequence range up and downstream of the core promoter includes the majority of elements affecting promoter strength, such as transcription factor-binding sites (Mendoza-Vargas et al. 2009). The protein coding sequence is not affected by the insulation sequences as the RBS and the startcodon are located downstream of the 3' insulation sequence. A RBS module (11 bp + 3 bp spacer) was added downstream the 144 bp long sequences of the nine different insulated, constitutive promoters. For cloning, recognition sequences for *Sal*I (6 bp + 6 bp REN spacer) and *Nde*I (6 bp + 6 bp REN spacer) were added to the 5' and 3' end of the promoter modules. The ATG startcodon is included in the *Nde*I recognition sequence. REN spacers were added in order to enable proper restriction endonuclease (REN) cleavage of *Sal*I and *Nde*I. Finally, nine different genetic modules of 182 bp length (uncut) containing insulated promoters of different strength were obtained (Figure 3-3). These genetic modules will be termed "insulated promoter modules". The insulated promoter modules will be denoted with the Roman numerals Ci - Cix. Sequence details of the used insulated promoter modules are shown in the Confidential Supplemental Information in Table A-1. Upon restriction digest with *Sal*I and *Nde*I insulated promoter modules were supposed to be inserted into a GFP-bearing vector backbone for promoter activity analysis.

Plasmid Modifications Were Necessary to Enable Cloning of Insulated Promoter Modules. Relative insulated promoter module mediated expression levels, here referred to as "promoter strength", was measured by analysing the intracellular GFP levels. These measurements were performed in a similar manner as shown in previous studies (DeMey et al. 2007; Kelly et al. 2009; Davis et al. 2010). After promoter strength determination, constitutive promoter modules of different strength should be applied in the co-expression system to control the expression of the folding modulator genes. Initially it was attempted to insert the insulated promoter modules into a basic vector bearing a *gfp* gene, to obtain the respective promoter probing vectors used for the promoter test. Plasmid pBI4iST7.7-gfp.1 was initially used as basic vector for the insertion of the insulated promoter modules. The backbone of this vector was part of a co-expression system used previously in this project (Buettner 2016). The T7 promoter module present in pBI4iST7.7-gfp.1 should be replaced by the insulated promoter modules. However, replacement of the T7 promoter module of the

basic vector with the insulated promoter modules did not work properly. By removing and substituting modules like the terminator or the *cer* element, the vector backbone of pBI4iST7.7-gfp.1 was made more suitable for the intended insertion of the promoter modules. An overview of the finally generated promoter probing vectors is displayed in Table 3-2.

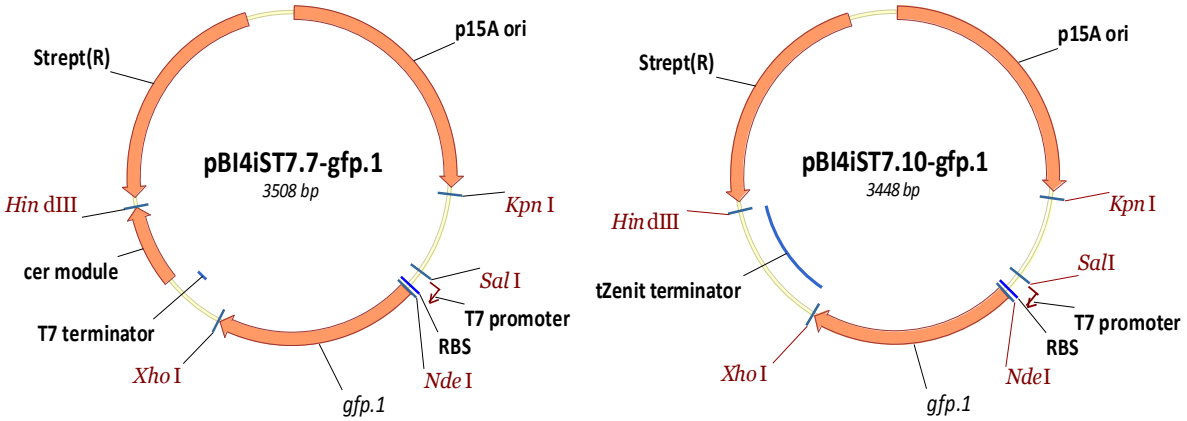

Figure 3-4: Plasmid maps of basic vectors used for the creation of promoter probing vectors. Both basic vectors pBI4iST7.7-gfp.1 and pBI4iST7.10-gfp.1 bear a streptomycin resistance gene cassette (Strept(R)), a p15A replicon (p15A *ori*) and the *gfp.1* gene under transcriptional control of the native T7 promoter. The *gfp.1* gene varies in a single silent point mutation from the gene encoding GFPmut3b (Cormack et al. 1996). In a previous part of this project (Schuller 2015) a single point mutation occurred in the DNA sequence of the p15A *ori.* pBI4iST7.7-gfp.1: Plasmid containing T7 terminator and *cer* module initially used as basic vector for creation of promoter probing vectors. Vector pBI4iST7.7-gfp.1 was itself used in a promoter test to determine the T7 promoter-mediated GFP synthesis rate. pBI4iST7.10-gfp.1: Plasmid, in which the T7 terminator was substituted with the tZenit terminator and *cer* module was removed. Later pBI4iST7.10-gfp.1 was used as new basic vector for creation of promoter probing vectors. Insulated promoter modules Ci - Cix were attempted to be inserted between *Sal*I and *Nde*I REN recognition sites to replace the T7 promoter. REN recognition sequences used during this work are indicated.

The basic vector pBI4iST7.7-gfp.1 (Figure 3-4) contains the native T7 promoter and T7 terminator controlling transcription of *gfp.1*, a streptomycin resistance cassette, the *cer* element and a p15A origin of replication (*ori*) (Selzer et al. 1983). In a previous part of this project (Schuller 2015) a single point mutation occurred within the DNA sequence of the p15A *ori*. Henceforth, the mutated p15A *ori* was abbreviated “4i” (instead of “4”) in the name of the plasmid. The *gfp.1* gene used in this work has a single base substitution compared to the gene encoding GFPmut3b (Cormack et al. 1996). In a previous part of this project (Buettner 2016) the *Nde*I recognition sequence within the coding sequence of GFPmut3b was removed by a single base substitution leading to the here used *gfp.1* gene. The proteins of GFP.1 and GFPmut3b share a 100 % identical amino acid sequence. It should be noted that the basic vector pBI4iST7.7-gfp.1 itself was used as promoter probing vector to determine the T7 promoter-mediated GFP synthesis rate.

It was attempted to replace the T7 promoter module of the basic vector by the insulated promoter modules Ci - Cix. DNA fragment Cvii failed to be synthesized by Invitrogen.

Therefore, construction of promoter probing vectors was conducted only with the remaining eight insulated promoter modules. Successful creation of promoter probing vectors was achieved with insulated promoter modules Ci, Cii and Ciii, yielding plasmids pBI4iSCi.2-gfp.1, pBI4iSCii.2-gfp.1 and pBI4iSCiii.2-gfp.1. Even after repeated attempts, insertion of all other insulated promoter modules into pBI4iST7.7-gfp.1 failed. Only a small number of positive *E. coli* clones was obtained for the plasmids pBI4iSCii.2-gfp.1 and pBI4iSCiii.2-gfp.1 after transformation of chemically competent *E. coli* DH5α cells (Invitrogen) with the respective ligation reactions. The limited number of resulting colonies indicated a potentially negative effect of the respective plasmids on cell growth. Furthermore, strains carrying the promoter probing vectors pBI4iSCii.2-gfp.1 and pBI4iSCiii.2-gfp.1 required 24 - 48 h until reaching the desired visually detectable turbidity in S-LB overnight cultures at 37 °C and 250 rpm. The transformation and growth phenomena mentioned above were not observed in case of plasmid pBI4iSCi.2-gfp.1, which was expected to bear the weakest constitutive insulated promoter module Ci.

If RNAP transcription is not properly terminated at the respective termination sequence, transcription of DNA sequences continues downstream of the respective terminator. Such events are defined as transcriptional read-through events and can led to up-regulation of gene expression of other plasmid encoded elements and thus increase the cell's metabolic burden (Mairhofer et al. 2013). Read-through events can thereby also interfere with the regulatory elements of a plasmid, e.g. *cer* module or control elements for plasmid copy number (Mairhofer et al. 2014). Termination efficiency (TE) of the native T7 terminator was previously shown to be limited (Macdonald et al. 1994; R. Sousa et al. 1992; Telesnitsky & Chamberlin 1989). Furthermore, read-through events associated with the use of the native T7 terminator were observed (Mairhofer et al. 2014). It was also shown that the TE of the T7 terminator is noticeably lower if the native *E. coli* RNAP is used instead of the T7 RNAP (Giacomelli & Depetris 2012). Hence, transcriptional read through events caused by a leaky T7 terminator were identified as potentially problematic in the creation of promoter probing vectors using insulated promoter modules. The tZenit terminator with a TE of 98.5 % (Witwer 2010) would be a more efficient transcription terminator variant. The tZenit terminator comprises the native T7 terminator, the T1 termination signal of the *rrnB* gene and the artificial T7UUCG terminator (Witwer 2010). Thus, to reduce the probability of read-through events and the associated increased metabolic burden for the cell, the T7 terminator was substituted with the tZenit terminator. Thereby, the basic vector pBI4iST7.9-gfp.1 was obtained. Subsequently, the eight remaining insulated promoter modules were used to replace the T7 promoter module of this basic vector. Also here, only the insertion of insulated promoter modules Ci, Cii and Ciii was successful and promoter probing vectors pBI4iSCi.4-gfp.1, pBI4iSCii.4-gfp.1 and pBI4iSCiii.4-gfp.1 were generated. However, insertion of the other five insulated promoter modules failed also when using the tZenit containing plasmid. The results led to the hypothesis that either the TE of the tZenit terminator is not that high as stated or the read-through events are not the root cause of the observed cloning issues.

Table 3-2: Overview on the creation of promoter probing vectors. The three basic vectors used for generation of promoter probing vectors are shown. Genetic features which were modified in order to improve the used vector backbone are indicated. It was attempted to replace the T7 promoter module of the basic vectors with the insulated promoter modules Ci - Cix. Successfully inserted promoter modules and the resulting promoter probing vectors are shown. Observed improvements of the plasmid creation procedure are stated.

Basic vector	**Genetic features**	**Successfully inserted promoter modules**	**Obtained promoter probing vectors**	**Improvements in plasmid creation procedure**
pBI4iST7.7-gfp.1	T7 terminator *cer* element	Ci Cii Ciii	pBI4iSCi.2-gfp.1 pBI4iSCii.2-gfp.1 pBI4iSCiii.2-gfp.1	-
pBI4iST7.9-gfp.1	tZenit terminator *cer* element	Ci Cii Ciii	pBI4iSCi.4-gfp.1 pBI4iSCii.4-gfp.1 pBI4iSCiii.4-gfp.1	None
pBI4iST7.10-gfp.1	tZenit terminator	Ci Cii Ciii Cviii	pBI4iSCi.3-gfp.1 pBI4iSCii.3-gfp.1 pBI4iSCiii.3-gfp.1 pBI4iSCviii.3-gfp.1	More colonies after transformation. Improved growth behavior in liquid cultures.

Since the application of the tZenit terminator did not lead to the intended improvement, it was assumed that the TE of the tZenit terminator might not be as high as quoted. The *cer* element on pBI4iST7.9-gfp.1 is the next genetic element downstream the *gfp.1* gene and its control might be influenced by an insufficient transcription termination. It was shown that read through events can lead to long transcripts of noncoding RNA structures which may interfere with the plasmid replication mechanism (Mairhofer et al. 2013). Further, it was assumed that read-through events of the *cer* element might have an additional negative impact on the plasmid maintenance. Thus, the *cer* element was removed from vector pBI4iST7.9-gfp.1 yielding the new basic vector pBI4iST7.10-gfp.1 (see Figure 3-4). Based on this plasmid it was attempted to replace the T7 promoter module with each one of the eight insulated promoter modules. Again insertion of promoter modules Ci, Cii and Ciii in the new basic vector pBI4iST7.10-gfp.1 was successful. In addition, promoter module Cviii could be successfully inserted. Thus, promoter probing vectors pBI4iSC$_x$.3-gfp.1 (C$_x$ = Ci, Cii, Ciii, Cviii) were generated. Creation of promoter probing vectors bearing all other insulated promoter modules failed. Hence, only 4 out of 8 insulated promoter modules were successfully inserted in the basic vector pBI4iST7.10-gfp.1. More colonies were obtained after transforming ligation reactions based on pBI4iST7.10-gfp.1 into *E. coli* DH5α cells, compared to cells transformed with ligation reactions based on pBI4iST7.9-gfp.1. In addition, the cells transformed with the four promoter probing vectors originating from pBI4iST7.10-gfp.1 showed an improved growth behaviour in liquid cultures.

In conclusion, the maintenance of promoter probing vectors based on pBI4iST7.10-gfp.1 seemed to exert a reduced negative influence on *E. coli* DH5α cells. However, the modifications within the promoter probing vector backbone (removal of the the *cer* element and substitution of the T7 terminator with the tZenit terminator) did not reveal such a beneficial effect as expected. Obviously, the issues during the plasmid creation procedure and cell growth refer to a too excessive GFP synthesis. The constitutive expression of *gfp.1* at high levels could constitute an increased metabolic burden for cells and hence negatively impact cell growth. Due to its improved behaviour during the plasmid creation procedure, the backbone of pBI4iST7.10-gfp.1 was used for the creation of promoter probing vectors and later on for the generation of folding modulator gene co-expression vectors. Promoter probing vectors pBI4iSC$_x$.3-gfp.1 (C$_x$ = Ci, Cii, Ciii, Cviii) were used to transform *E. coli* BL21(DE3) cells which also were used later on for the expression of the antibody binding fragment FabZ. Cryo cultures of the respective cells were prepared and employed in shake flask experiments to examine plasmid stability and GFP synthesis rate.

The Basic Plasmid Showed Sufficient Stability during Shake Flask Experiments. It is commonly known that plasmid-based protein production and even the presence of a plasmid as such poses a metabolic burden for cells (Bentley et al. 1990). The metabolic burden increases with rising gene expression rates and higher copy numbers of the plasmid (Samuelson 2011). In particular under non-selective conditions, as present during technical fermentation procedures, high-copy number plasmids possess a higher segregational instability (Friehs 2004). High metabolic burden can result in plasmid loss and thereby lead to overgrowth of plasmid-free cells (Striedner et al. 2010). Previously it was shown that a specific DNA sequence on plasmids, called *cer* element, could improve stability of plasmids bearing a ColE1 replicon (Summers & Sherratt 1988). In this work the *cer* element was removed from the basic vector to facilitate insertion of the insulated promoter modules (see above). In order to analyse stability of the promoter probing vectors based on the *cer* element-deficient backbone of pBI4iST7.10-gfp.1, *E. coli* BL21(DE3)(pBI4iSCiii.3-gfp.1) cells were subjected to plasmid stability tests. The metabolic burden of this strain was assumed to be quite high due to the presence of the obviously strong Ciii promoter module which controls *gfp.1* expression.

The plasmid stability test of strain *E. coli* BL21(DE3)(pBI4iSCiii.3-gfp.1) was performed in accordance with the method described in 2.3.4. Main culture incubation was performed in 1000 mL unbaffled Erlenmeyer flasks with 200 mL of T7 Shake Flask Medium without antibiotics. Despite constitutive expression of *gfp.1*, 1 mM IPTG was added when the culture reached an OD_{550} of 1.0 ± 0.2 in order to simulate the intended cultivation conditions during the FabZ production experiments. Incubation at 25 °C and 300 rpm was conducted for 48 h. An aseptical sample of 1 mL cell suspension was taken 24 and 48 h after addition of IPTG. Sampling time points were chosen to cover the intended time frames of shake flask and fermentation experiments. 100 µL of appropriate dilutions (10^{-6}, 10^{-7} and 10^{-8}) of the cell suspension were plated on non-selective S-LB agar plates. Agar plates were incubated o/n at

37 °C. Single colonies were transferred to new non-selective ager plates and in parallel to S-LB agar plates containing 50 µg/mL streptomycin. After o/n incubation at 37 °C, colonies on non-selective and streptomycin agar plates were counted. Plasmid stability was calculated by dividing the number of colonies grown on the streptomycin plates by the number of colonies grown on the non-selective plates (see Chapter 2.3.4, Figure 2-3).

The number of colonies on non-selective and streptomycin plates was identical at both time points (24 and 48 h) (Table 3-3). Hence, a plasmid stability of 100 % was determined for the *cer* module-deficient promoter probing vector pBI4iSCiii.3-gfp.1. All colonies (< 50 per plate) on all plates showed noticeable fluorescence when exposed to UV light indicating presence of GFP and, thus, presence of the expression plasmid. Therefore, only a small number of colonies (32) were used for the plasmid stability test.

Table 3-3: Results of the plasmid stability test. Plasmid stability of the *cer* element-deficient plasmid pBI4iSCiii.3-gfp.1 in *E. coli* BL21(DE3) cells was determined. The plasmid stability test was performed in accordance with the method described in 2.3.4 in 200 mL of T7 Shake Flask Medium w/o antibiotics. Samples were taken 24 and 48 h after addition of 1 mM IPTG. Appropriate dilutions of the cell suspension samples were plated on non-selective S-LB agar plates. Upon o/n incubation at 37 °C single colonies were transferred to new non-selective ager plates and in parallel to an S-LB agar plates containing 50 µg/mL streptomycin. After o/n incubation at 37 °C, resulting colonies on non-selective and streptomycin agar plates were counted and plasmid stability was calculated.

Sampling time	Colonies on non-selective plate	Colonies on streptomycin plate	Calculated plasmid stability
24 h	32	32	100 %
48 h	32	32	100 %

Despite an assumed high metabolic load and the absence of the stabilizing *cer* element, the culture of BL21(DE3)(pBI4iSCiii.3-gfp.1) cells was found to be constituted to 100 % of plasmid-bearing cells even after 48 h. Previous experiments in the context of this project revealed a comparable plasmid stability of 100 % of cells harbouring p15A replicon-bearing plasmids with but also w/o *cer* element when cultivated at 25 °C for 60 h under non-selective conditions (Schuller 2015). Based on these results plasmids originating from pBI4iST7.10-gfp.1 were considered to be stable during experimets lasting up to 48 h after induction of recombinant gene expression. Subsequently, *E. coli* plasmid strains BL21(DE3) (pBI4iSC$_x$.3-gfp.1) (C$_x$ = Ci, Cii, Ciii or Cviii) were subjected to the promoter test procedure. By measuring intracellular GFP levels, the strength of the insulated promoter modules Ci, Cii, Ciii and Cviii should be determined.

Insulated Promoter Module Ci Appeared Appropriate for Folding Modulator Gene Co-Expression. Previous studies showed that co-production of optimal chaperone combinations and appropriate expression levels were specific for each target protein (A. DeMarco & V. DeMarco 2004). As recently reviewed, increasing levels of folding modulators had in some cases positive effects and in other cases negative effects on soluble protein production, whereby the determined effect was strongly dependent on the target protein (Overton 2014). Hence, the co-expression system in terms of folding modulator and its synthesis rate has to be optimized for each recombinant target protein. Previous studies in the course of this project showed that low expression levels of folding modulator genes had a presumably more positive effect on soluble periplasmic FabZ yields compared to high expression levels (Buettner 2016). Hence, in this work a set of rather weak constitutive promoters of various strength should be identified to obtain a functional expression system for folding modulator co-production. Therefore, the expression levels of *gfp.1* controlled by the insulated promoter modules of the promoter probing vectors pBI4iSC$_x$.3-gfp.1 (C$_x$ = Ci, Cii, Ciii or Cviii) were analysed.

To determine the strength of insulated promoter modules BL21(DE3) cells were transformed with one of the pBI4iSC$_x$.3-gfp.1 (C$_x$ = Ci, Cii, Ciii and Cviii) plasmids. The resulting plasmid strains were subjected to a promoter test as described in 2.3.2. Main cultures were performed in 1000 mL unbaffled Erlenmeyer flasks with 200 mL of T7 Shake Flask Medium supplemented with 50 µg/mL streptomycin. Incubation was done at 25 °C under shaking. Cell suspension samples corresponding to a volume of 5 mL/OD$_{550}$ were taken directly before and 1, 3 and 24 h after addition of 1 mM IPTG at an OD$_{550}$ of 1.0 ± 0.2. The applied BL21(DE3) plasmid strains harbor a *gfp.1* gene under transcriptional control of the constitutive promoter modules. The addition of IPTG only induces the production of the host's T7 RNAP. It is not expected that the induction of T7 RNAP has an effect on the examined system based on constitutive promoters. However, IPTG was added in order to simulate the conditions of the subsequent FabZ production experiments. Fluorescence of cell samples resuspended in OD buffer was measured using a Safire2™ fluorescence microplate reader (Tecan Group). For fluorescence measurement an excitation wavelength of 475 nm and an emission wavelength of 512 nm was applied (see 2.5.1).

Figure 3-5 displays the measured fluorescence$_{Exc.475/Em.512}$ of strains subjected to the promoter test in dependence of the sampling time. Measured RFU values comprise intracellular GFP levels and the low level of background autofluorescence of *E. coli* BL21(DE3) cells. RFU values determined for samples of the negative control strain BL21(DE3)(pBI1ST7.2) were comparable to fluorescence$_{Exc.475/Em.512}$ measured w/o sample (data not shown). Thus, BL21(DE3) cells do not exhibit a noticeable autofluorescence and do not interfere with the GFP measurement. RFU values determined by fluorescence$_{Exc.475/Em.512}$ measurement therefore indirectly describe the intracellular GFP levels.

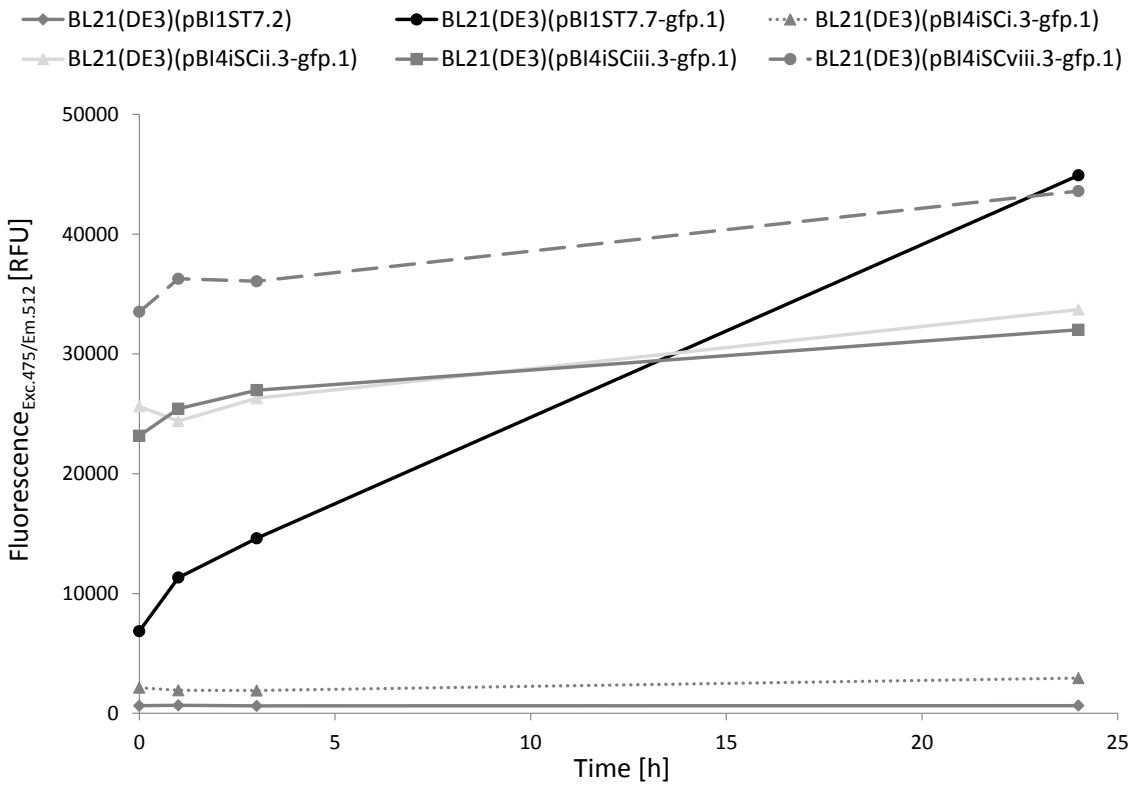

Figure 3-5: Activity of constitutive insulated and selected reference promoter modules. GFP production controlled by insulated and reference promoter modules is represented as relative fluorescence and plotted over time after addition of IPTG. Plasmid strains BL21(DE3)(pBI4iSC$_x$.3-gfp.1) (C$_x$ = Ci, Cii, Ciii and Cviii) and reference strains BL21(DE3)(pBI4iST7.7-gfp.1) and BL21(DE3)(pBI1ST7.2) were cultivated in 1000 mL shake flask containing 200 mL of T7 Shake Flask Medium supplemented with 50 µg/mL streptomycin (see 2.3.2). Cultures were incubated at 25 °C and 300 rpm. BL21(DE3)(pBI1ST7.2): non-GFP-producer strain used as negative control. BL21(DE3)(pBI4iST7.7-gfp.1): strain bearing the native T7 promoter which controls *gfp.1* expression used as high productive reference strain. Cell samples corresponding to 5 mL / OD_{550} were taken directly before and 1, 4, 19 and 24 h after addition of 1 mM IPTG at OD_{550} of 1.0 ± 0.2. Cell samples were resuspended in 5 mL OD buffer. 200 µL of these cell suspensions were subjected to fluorescence measurements (according to 2.5.1) using a Safire^{2}™ fluorescence microplate reader at an excitation wavelength of 475 nm and an emission wavelength of 512 nm. Indicated RFU values correspond to the mean values of the eightfold measurement as described in 3.1.1.

Intracellular GFP level increased throughout the production phase when *gfp.1* expression was under transcriptional control of the native T7 promoter (strain BL21(DE3)(pBI4iST7.7-gfp.1)). A fluorescence$_{Exc.475/Em.512}$ value of approximately 7000 RFU was measured in the case of the cell sample taken before induction of gene expression by IPTG. This indicates significant basal expression of the T7 promoter system. Leaky expression of the genome-integrated T7 RNAP gene of *E. coli* BL21(DE3) cells controlled by a *lacUV5* promoter in the absence of the inducer IPTG is commonly known and described in the literature (Studier 1991; Pan & Malcolm 2000). An even further increased level of basal expression was expected as the used T7 promoter system was modified by removing the regulatory elements *lacI* and *lacO* which repress basal expression of the system. As expected, GFP synthesis driven by the constitutive promoter modules Ci, Cii, Ciii and Cviii was rather constant over time after addition of IPTG. However, a slight increase in intracellular GFP

levels over time was determined for the *gfp.1* expression controlled by the constitutive promoter modules. A previous study showed that the formation of the GFP chromophore is temperature dependent and shows stronger fluorescence when produced at 25 °C compared to 37 °C (DeMey et al. 2007). Hence, the slightly increasing RFU values of $fluorescence_{Exc.475/Em.512}$ measurement of cell samples during the first hours after IPTG addition could be explained by a temperature effect. The promoter test was started at 37 °C and temperature was reduced to 25 °C after addition of IPTG. This might explain the slightly increasing GFP fluorescence values. RFU values of cells from strain BL21(DE3)(pBI4iSCi.3-gfp.1) were quite low, but still 3.5-fold higher compared to RFU values determined for the GFP-lacking negative control. Thus, a significant activity of insulated promoter module Ci could be shown in shake flask experiments. The other analysed insulated promoter modules facilitated rather high-level production of GFP

To determine the relative promoter module strength based on the measured RFU values, the background fluorescence of the non-GFP-producing strain BL21(DE3)(pBI1ST7.2) was initially subtracted from fluorescence of all GFP-producing strains. In a previous parts of this project (Schuller 2015) T7 promoter variants were generated and used to control the expression of folding modulator genes on co-expression plasmids. Their relative promoter strength was evaluated compared to the native T7 promoter module. Therefore, also here the native T7 promoter module controlling GFP production in strain BL21(DE3)(pBI4iST7.7-gfp.1) was used as reference to determine the relative strength of constitutive promoter modules. Since the induced GFP production of the T7 system can not directly be compared to a constitutive production system, the GFP fluorescence of the sample obtained after 24 h of production (approximately 44000 RFU) was selected as 100 % set point. Approximately 24 h after IPTG addition intracellular GFP levels of plasmid strain BL21(DE3)(pBI4iST7.7-gfp.1) reached its peak before decreasing again (data not shown). Relative strength of constitutive promoter modules was determined by dividing the GFP fluorescence measured 24 h after IPTG addition by the 100 % set point value. Relative promoter strengths of 97, 75, 71 and 5 % were determined for the insulated promoter modules Cviii, Cii, Ciii and Ci, respectively (see Figure 3-6).

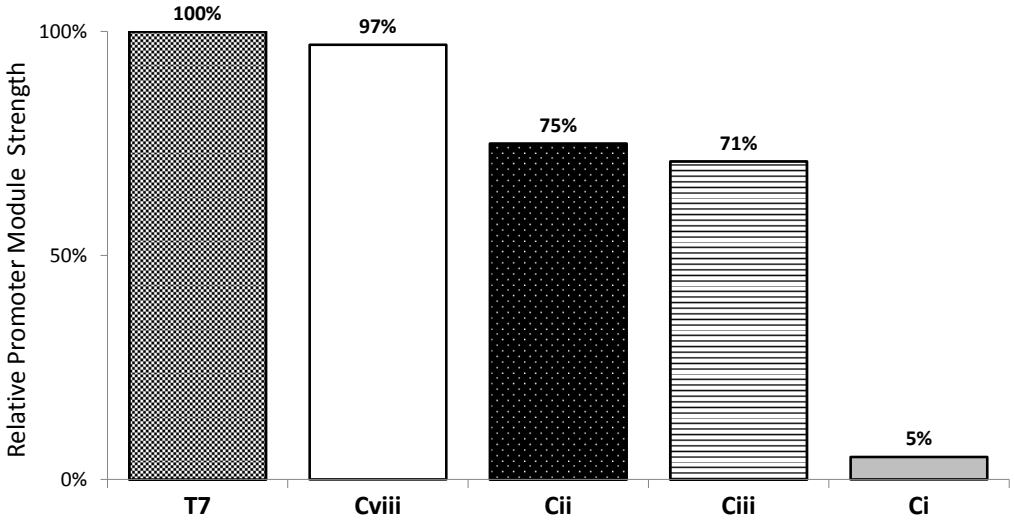

Figure 3-6: Relative strength of insulated promoter modules compared to the native T7 promoter module. The respective promoter module can be found on the x-axis and the relative promoter strength in % is shown on the y-axis. To determine the strength of insulated promoter modules the strains BL21(DE3)(pBI4iSC$_x$.3-gfp.1) (C$_x$ = Ci, Cii, Ciii and Cviii), BL21(DE3)(pBI4iST7.7-gfp.1) (100 % reference) and BL21(DE3)(pBI1ST7.2) (negative control) were subjected to a promoter test (2.3.2). Fluorescence of intracellular GFP was measured at an excitation wavelength of 475 nm and an emission wavelength of 512 nm (2.5.1). Resulting RFU values were corrected by subtraction of the background fluorescence of cell samples from the negative control BL21(DE3)(pBI1ST7.2). Relative strength of insulated promoter modules was calculated by referring their GFP fluorescence determined 24 h after IPTG addition to the GFP fluorescence of strain BL21(DE3)(pBI4iST7.7-gfp.1) at the same time point. Relative strength of insulated promoter modules is indicated on top of bars.

Expression levels of *gfp.1* controlled by the modules Cii, Ciii and Cviii ranged from 71 to 97 %. These values compared to the native T7 promoter system are obviously very high for a constitutive system. Cloning of folding modulator genes downstream of modules Cii, Ciii and Cviii failed repeatedly. Hence, folding modulator co-expression plasmids based on Cii, Ciii and Cviii promoter could not be created. Based on the experiences made during construction of the promoter probing vectors, it apparently seemed as if constitutive expression of folding modulator genes at this high level had a severe negative effect on cell vitality. Module Ci was the only weak insulated promoter module (5 %) in comparison to the fully induced native T7 promoter module. Creation of co-expression plasmids based on the Ci promoter module worked properly. Hence, the insulated promoter module Ci with 5 % relative strength compared to fully induced T7 promoter after 24 h could be a valuable tool for folding modulator gene co-expression.

3.1.3. Removal of Insulation and Modification of RBS Yields Constitutive Promoter Modules of Appropriate Strength for the Co-Expression System

Reduced Strength of Second Generation Promoter Modules Was Revealed in a Promoter Test. As stated above, creation of folding modulator gene co-expression plasmids based on promoter modules Cvii, Cii and Ciii failed. Obviously, the relative strength of 97 (Cviii), 75 (Cii) and 71 % (Ciii) compared to the fully induced T7 promoter module was too high for successful creation of folding modulator gene co-expression plasmids. To obtain promoter modules of reduced strength, molecular modifications were introduced into the insulated promoter modules. The RBS and the 3'- and 5' insulation sequences can on the one hand significantly affect expression rates and on the other hand they can easily be modified. Thus, the insulation sequences of insulated promoter modules were removed and the RBS was substituted by a potentially weaker one. The sequence of the alternative RBS was copied from a previously published work (Davis et al. 2010). According to previous analysis the new RBS constitutes a translation initiation signal of medium strength (Warsaw 2010). The use of a weaker RBS could not just contribute to reductions in translation but also in expression rates.

Constitutive promoter modules lacking the insulation sequence and bearing the weak RBS are termed "Second Generation" promoter modules. A schematic composition of these modules is illustrated in Figure 3-7. Second Generation promoter modules are indicated by Arabic numerals (C1 - C9) in a way, that they correspond to their insulated promoter module counterparts (indicated by Roman numerals Ci - Cix). This means, that the promoter sequence including -35 box, 17 bp spacer, -10 box and the spacer downstream of the core promoter are identical in both promoter variants (e.g. Ci and C1). To design the Second Generation promoter modules, the 5' and 3' insulation sequences were removed. In exchange for the insulation sequences a 6 bp and 8 bp spacer was added upstream and downstream of the promoter sequences, respectively. Those spacer sequences were designed according to a previous publication (Davis et al. 2010). As minor modification two basepairs were removed from the 5' spacer in order to eliminate an *Xba*I recognition sequence. Sequence details of the Second Generation promoter modules are shown in the Confidential Supplemental Information in Table A-2. Second Generation promoter modules were constructed using single-stranded oligonucleotides (Sigma Aldrich). After annealing of complementary oligonucleotides as described in 2.2.2 double-stranded REN (*Nde*I and *Sal*I) cut-like DNA molecule were obtained.

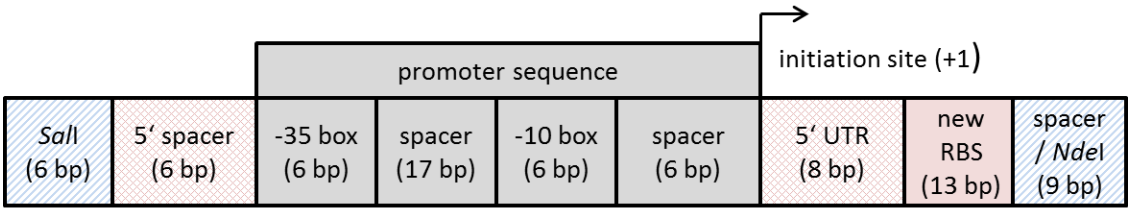

Figure 3-7: Schematic representation of Second Generation promoter modules. All relevant elements of Second Generation promoter modules C1 - C9 and their respective sequence length in bp are shown. Second Generation promoter modules were ordered as single-stranded oligonucleotides (Sigma Aldrich). After annealing of complementary oligonucleotides, double-stranded REN (*Nde*I and *Sal*I) cut-like DNA molecule were obtained and used for insertion into the basic expression vector. 5’ Spacer: Sequence between *Sal*I recognition sequence and promoter sequence obtained from a previously published work (Davis et al. 2010) and modified by removing an *Xba*I recognition sequence. Promoter sequence: Comprises -35 box, 17 bp spacer, -10 box and a spacer sequence between core promoter and transcription initiation site (indiciated by an arrow). Second Generation promoter modules differ from each other in 1-5 base positions in their promoter sequences. 5’ UTR: Untranslated region downstream of the promoter sequences comprising an 8 bp spacer copied from a previously published work (Davis et al. 2010). New RBS: A new, weak RBS copied from a previously published work (Davis et al. 2010) was used for Second Generation promoter modules. Spacer / *Nde*I: 3 bp spacer between RBS and *Nde*I recognition sequence resulting in optimal 6 bp spacing between RBS and ATG starcodon, which is part of the *Nde*I recognition sequence.

Second Generation promoter modules C1 - C9 should be used to replace the T7 promoter module of basic vector pBI4iST7.10-gfp.1. Modules C1, C2, C3, C4, C5, C8 and C9 were successfully inserted into the basic vector pBI4iST7.10-gfp.1 yielding promoter probing vectors pBI4iSC$_y$.3-gfp.1 (C$_y$ = C1, C2, C3, C4, C5, C8 and C9). Insertion of modules C6 and C7 failed after repeated cloning attempts. Strains transformed with the promoter probing vectors bearing Second Generation promoter modules C2, C3 and C8 required less time to grow in S-LB cultures at 37°C and 250 rpm compared to strains harbouring plasmids with their insulated counterparts Cii, Ciii and Cviii. Hence, growth behaviour of strains carrying plasmids with Second Generation promoter modules was enhanced. These observations suggested that the exchange of insulated by Second Generation promoter modules led to a decreased metabolic burden and thus positively influenced cell growth.

To determine the strength of the Second Generation promoter modules *E. coli* BL21(DE3) cells were transformed with promoter probing vectors pBI4iSC$_y$.3-gfp.1 (C$_y$ = C1, C2, C3, C4, C5, C8 and C9). These plasmid strains were subjected to a promoter test as described in 2.3.2. Cell samples were taken before and 1, 4, 19 and 24 h after addition of 1 mM IPTG. Fluorescence of resuspended cell samples was measured at an excitation wavelength of 475 nm and an emission wavelength of 512 nm (fluorescence$_{Exc.475/Em.512}$) (see 2.5.1). Again, non-GFP-producing strain BL21(DE3)(pBI1ST7.2) was used as negative control in the promoter test. RFU values measured for cell samples of strain BL21(DE3)(pBI4iSC1.3-gfp.1) did not differ from values generated from cells of the negative control. Apparently, promoter module C1 is not active under the tested conditions. Since the test revealed no promoter activity, module C1 was excluded from further use in folding modulator gene co-expression plasmids. Intracellular GFP levels of positive control and reference strain BL21(DE3)(pBI4iST7.7-gfp.1) increased continuously after induction of its recombinant gene

expression by IPTG. GFP production driven by Second Generation promoter modules C2, C3, C4, C5, C8 and C9 increased only slightly over time. As a possible root cause the decrease in growth and production temperature was already discussed above (see Chapter 3.1.2). Prior to relative promoter strength calculation, the fluorescence of the non-GFP-producing strain BL21(DE3)(pBI1ST7.2) was subtracted from fluorescence of all GFP-producing strains. Relative promoter strength of the Second Generation promoter modules was calculated by dividing the GFP fluorescence measured 24 h after IPTG addition by GFP fluorescence of the positive control BL21(DE3)(pBI4iST7.7-gfp.1) (for more information see also Chapter 3.1.2). Compared to the native T7 promoter 24 h after addition of IPTG relative promoter strengths of 126, 100, 33, 33, 23, 20 and 0 % were determined for the Second Generation promoter modules C5, C4, C3, C9, C2, C8 and C1, respectively (Figure 3-8).

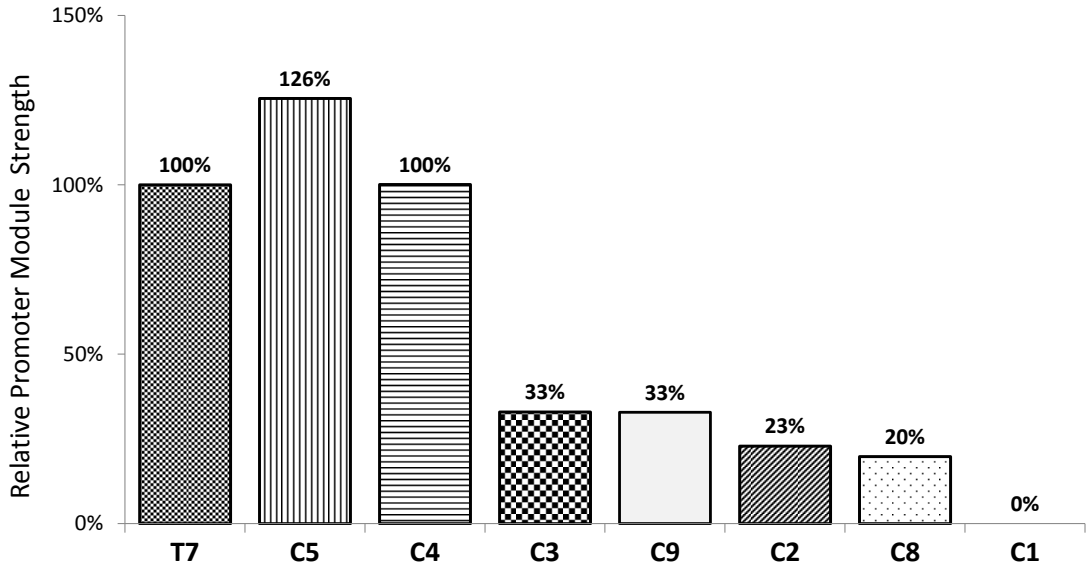

Figure 3-8: Relative strength of Second Generation promoter modules compared to the native T7 promoter module. The respective promoter module can be found on the x-axis and the relative promoter strength in % is shown on the y-axis. To determine the strength of Second Generation promoter modules the strains BL21(DE3)(pBI4iSC$_y$.3-gfp.1) (C$_y$ = C1, C2, C3, C4, C5, C8 and C9), BL21(DE3)(pBI4iST7.7-gfp.1) (100 % reference) and BL21(DE3)(pBI1ST7.2) (negative control) were subjected to a promoter test (2.3.2). Fluorescence of intracellular GFP was measured at an excitation wavelength of 475 nm and an emission wavelength of 512 nm (2.5.1). Resulting RFU values were corrected by subtraction of the background fluorescence of cell samples from the negative control. Relative strength of Second Generation promoter modules was calculated by referring their GFP fluorescence determined 24 h after IPTG addition to the GFP fluorescence of BL21(DE3)(pBI4iST7.7-gfp.1) at the same time point. Relative strength of Second Generation promoter modules is indicated on top of bars.

The promoter test revealed a reduced strength of the Second Generation promoter modules compared to their insulated counterparts. Apparently, insulation removal and RBS exchange led to the desired reduction in promoter module strength and hence *gfp.1* expression levels. As stated above, the reduced expression levels already showed a positive effect during generation of promoter probing vectors. Seven Second Generation promoter probing vectors could be created compared to only four vectors bearing insulated promoter

modules. Hence, high expression levels of *gfp.1* seemed to have been the major issue during creation of promoter probing vectors. Subsequently, the *gfp.1* gene of the promoter probing vectors was supposed to be replaced with the folding modulator genes *dsbA*, *dsbC*, *fkpA*, *ppiD*, *skp* and *surA* to obtain the respective co-expression plasmids. Second Generation promoter modules C4 and C5 were excluded from the co-expression plasmid creation procedure. Their relative promoter strengths of 126 and 100 % were evaluated to be too high for the use in folding modulator gene co-expression plasmids. In Chapter 3.1.2 it was shown that already a relative promoter strength of 71 (Ciii), 75 (Cii) and 97 % (Cviii) was too high to successfully create co-expression plasmids. Therefore, co-expression plasmids should only be based on Second Generation promoter modules C3, C9, C2 and C8 with a relative strength of 33, 33, 23 and 20 %, respectively.

Creation Attempts of Co-Expression Plasmids Based on Second Generation Promoter Modules C8 and C2 Were Successful. Relative strength of 33, 33, 23 and 20 % compared to the native T7 promoter module under full induction conditions were determined for the Second Generation promoter modules C3, C9, C2 and C8, respectively. To generate co-expression plasmids it was attempted to insert the folding modulator genes *dsbA*, *dsbC*, *fkpA*, *ppiD*, *skp* and *surA* downstream of the respective promoter module (C3, C9, C2 and C8). This was done by replacing the *gfp.1* gene in promoter probing vectors pBI4iSC2.3-gfp.1, pBI4iSC3.3-gfp.1, pBI4iSC8.3-gfp.1 and pBI4iSC9.3-gfp.1 with the folding modulator genes to obtain the respective co-expression plasmids.

Insertion of folding modulator genes downstream of the C2 and C8 promoter module worked properly. After ligation of the DNA fragments and transformation into *E. coli* cells a lot of positive colonies were obtained. This indicated that expression levels of folding modulator genes seemed to be well bearable for cells carrying co-expression plasmids based on C2 and C8 promoter modules. In contrast, attempts to insert folding modulator genes downstream of promoter modules C3 and C9 led to ambiguous results. For instance, many colonies of *E. coli* transformants were obtained during preparation of *dsbA*- and *skp*-bearing co-expression plasmids. On the other hand, no positive colonies were obtained during cloning of *dsbC*, *fkpA*, *ppiD* and *surA.* Apparently, cell growth was again negatively influenced by high constitutive overexpression of *dsbC*, *fkpA*, *ppiD* and *surA*.

In conclusion, negative impacts of constitutive folding modulator co-production on cell growth were observed during the cloning procedure of co-expression plasmids. Negative effects seemed to depend on both, expression level and folding modulator gene. Constitutive expression of all six folding modulator genes under control of promoter modules C2 and C8 had no obvious negative effect on cell growth. Thus, these promoter modules appear to be suitable for co-synthesis of folding modulators in FabZ production experiments. FabZ producing BL21(DE3)Tn7::<FabZ> cells were transformed with the folding modulator gene co-expression plasmids pBI4iSC2.3-fm and pBI4iSC8.3-fm (fm = *dsbA*, *dsbC*, *fkpA*, *ppiD*, *skp* and *surA*). Resulting plasmid strains were then analysed in FabZ production experiments.

Both Insulation and RBS Exerted An Influence on Expression Levels. Promoter test experiments revealed lower promoter strengths for Second Generation promoter modules (Figure 3-8) compared to insulated promoter modules (Figure 3-6). Table 3-4 summarizes the relative strength of insulated promoter modules Ci, Cii, Ciii and Cviii compared to their Second Generation counterparts C1, C2, C3 and C8. Apparently, a molecular modification (insulation removal or RBS exchange) of the insulated promoter modules caused the desired reduced expression levels. However, the promoter test results did not indicate which of the introduced modifications exerted the main influence on the expression level reduction.

Table 3-4: Reduction in expression levels upon molecular modifications of promoter modules. Relative strength of constitutive promoter modules compared to native T7 promoter module 24 h after addition of IPTG was determined in two promoter tests (see Figure 3-6 and Figure 3-8). Resulting relative strength of insulated promoter modules Ci, Cii, Ciii and Cviii and the respective Second Generation counterparts C1, C2, C3 and C8 are shown in the middle column. Strength of Second Generation promoter modules relative to their insulated counterpart is indicated in the right column.

Constitutive promoter module	**Relative strength to native T7 promoter module**	**Strength of Second Generation promoter modules relative to their insulated counterparts**
Ci	5 %	
C1	0 %	not applicable
Cii	75 %	
C2	23 %	31 %
Ciii	71 %	
C3	33 %	46 %
Cviii	97 %	
C8	20 %	21 %

To evaluate the influence of each individual genetic modification, further promoter modules were generated and analysed in a promoter test. The promoter sequence present in modules Ciii and C3 was used as a basis for examining the influence of insulation sequences and RBS on the expression level. This promoter sequence was selected since the creation of promoter probing vectors was successful with both, the Ciii and the C3 promoter module. In this chapter the promoter modules Ciii and C3 will be termed Ciii-RBS1 and C3-RBS2, respectively. The Roman numerals indicate presence of 5’ and 3’ insulation sequences, while Arabic numerals denote their absence. RBS1 refers to the strong RBS which was used in insulated promoter modules. RBS2 denotes the new, weak RBS which was used in Second Generation promoter modules. The first new promoter module which was created, termed Ciii-RBS2, consists of the core promoter, the original 5’ and 3’ insulation sequences and it bears the weak RBS2. The second promoter module is designated as C3-RBS1. It is based on the same core promoter used in module Ciii-RBS2, but lacks the insulation sequences and bears the old, strong RBS1. Promoter module Ciii-RBS2 was ordered as double-stranded

GeneArt® String™ DNA fragment (Invitrogen). Promoter module C3-RBS1 was ordered as single-stranded oligonucleotides (Sigma Aldrich). Promoter modules Ciii-RBS2 and C3-RBS1 were used to replace the T7 promoter module of the basic vector pBI4iST7.10-gfp.1 yielding promoter probing vectors pBI4iSCiii.11-gfp.1 and pBI4iSC3.12-gfp.1.

In the creation procedure of promoter probing vector pBI4iSC3.12-gfp.1 many colonies were obtained after the transformation step. In addition, growth of pBI4iSC3.12-gfp.1-bearing cells in S-LB cultures was normal and comparable to promoter probing vector pBI4iSC3.3-gfp.1. On the other hand, low numbers of colonies were obtained after the transformation step in the course of the generation of promoter probing vector pBI4iSCiii.11-gfp.1. In addition, strains carrying promoter probing vector pBI4iSCiii.11-gfp.1 required 24 - 48 h until reaching a visually detectable turbidity in liquid cultures. Similar growth behaviour was already observed during creation of promoter probing vectors pBI4iSCii.3-gfp.1, pBI4iSCiii.3-gfp.1 and pBI4iSCviii.3-gfp.1. Previous promoter tests (Chapter 3.1.2) revealed high intracellular GFP levels for strains carrying these promoter probing vectors. Hence, promoter module strength of Ciii-RBS2 was supposed to be in a similar range as the strength of modules Cii, Ciii or Cviii.

For determination of promoter module strength of Ciii-RBS2 and C3-RBS1 *E. coli* BL21(DE3) cells were transformed with the plasmids pBI4iSCiii.11-gfp.1 and pBI4iSC3.12-gfp.1. Resulting plasmid strains and were subjected to a promoter test as described in 2.3.2. In addition, strains BL21(DE3)(pBI4iSC3.3-gfp.1), BL21(DE3)(pBI4iSCi.3-gfp.1) and BL21(DE3)(pBI4iSC8.3) (negative control) were analysed in the same promoter test. Cell samples were prepared directly before and 24 h after addition of 1 mM IPTG. Fluorescence of the resuspended cell samples was measured at an excitation wavelength of 475 nm and an emission wavelength of 512 nm ($fluorescence_{Exc.475/Em.512}$) in accordance with the method described in 2.5.1. Background fluorescence obtained from measurements of the negative control samples was subtracted from fluorescence of GFP-producing strains. GFP fluorescence of the plasmid strain BL21(DE3)(pBI4iSCiii.3-gfp.1), carrying promoter module Ciii, was already determined in a promoter test conducted previously (see Chapter 3.1.2, Figure 3-5 and Figure 3-6). In order to enable the use of the fluorescence value previously measured for promoter module Ciii (termed Ciii-RBS1 in this chapter), results had to be normalized between both promoter tests. To do so, GFP fluorescence of plasmid strain BL21(DE3)(pBI4iSCi.3-gfp.1), which was analysed in both promoter tests, was used for normalization. The normalized fluorescence value of strain BL21(DE3)(pBI4iSCiii.3-gfp.1) 24 h after addition of IPTG was used as 100 % reference and set to 100 %. Relative promoter module strength of Ciii-RBS2, C3-RBS1 and C3-RBS2 was calculated by dividing their GFP fluorescence measured 24 h after IPTG addition by the 100 % set point value and is shown in Table 3-5.

Table 3-5: Influence of RBS and insulation on the strength of promoter modules. *E. coli* BL21(DE3) plasmid strains bearing GFP encoding promoter probing vectors with the promoter modules Ciii-RBS1, Ciii-RBS2, C3-RBS1 and C3-RBS2 were subjected to a promoter test according to 2.3.2. Fluorescence of intracellular GFP was measured at an excitation wavelength of 475 nm and an emission wavelength of 512 nm (2.5.1). Resulting RFU values were corrected by subtraction of the background fluorescence of cell samples from the negative control BL21(DE3)(pBI4iSC8.3). The normalized fluorescence value of strain BL21(DE3)(pBI4iSCiii.3-gfp.1), bearing the Ciii-RBS1 promoter module, 24 h after addition of IPTG was set to 100 %. Relative promoter module strength was calculated by referring GFP fluorescence determined 24 h after IPTG addition to the 100 % set point value. Relative strength of selected promoter modules is indicated in the right column. RBS1: strong ribosomal binding site (RBS). RBS2: weak RBS. Insulation sequences: Presence or absence of insulation sequence is indicated.

Promoter probing vector	Promoter module identifier	Insulation sequence	RBS	Promoter module strength compared to Ciii-RBS1
pBI4iSCiii.3-gfp.1	Ciii-RBS1	Yes	Strong	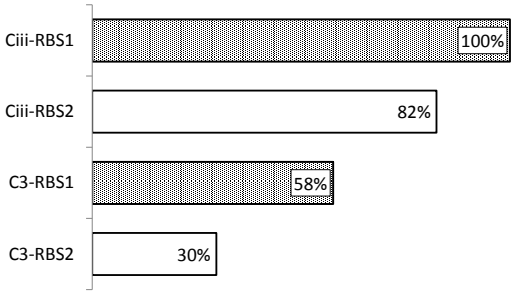
pBI4iSCiii.11-gfp.1	Ciii-RBS2	Yes	Weak	
pBI4iSC3.12-gfp.1	C3-RBS1	No	Strong	
pBI4iSC3.3-gfp.1	C3-RBS2	No	Weak	

Compared to module Ciii-RBS1 (100 %) relative promoter strengths of 82, 58 and 30 % were obtained for promoter modules Ciii-RBS2, C3-RBS1 and C3-RBS2, respectively. A decrease of approximately 18 % of intracellular GFP levels and thus fluorescence was determined when comparing strain BL21(DE3)(pBI4iSCiii.3-gfp.1) containing module Ciii-RBS1 and strain BL21(DE3)(pBI4iSCiii.11-gfp.1) containing module Ciii-RBS2. A decrease of approximately 48 % of GFP fluorescence was determined comparing BL21(DE3) strains bearing promoter probing vector pBI4iSC3.12-gfp.1 (module C3-RBS1) to strain BL21(DE3)(pBI4iSC3.3-gfp.1) (module C3-RBS2). Hence, changing the strong RBS1 to the weak RBS2 led in the first case to a 1.2-fold and in the second to a 1.9-fold reduction in promoter module strength. In the first setup (Ciii-RBS1 / Ciii-RBS2) the insulation sequence was present, while in the second setup (C3-RBS1 / C3-RBS2) the insulation sequence was absent. GFP fluorescence determined in cells of BL21(DE3)(pBI4iSC3.12-gfp.1) (C3-RBS1 module) was approximately 42 % lower than that measured for cells of the strain carrying the promoter probing vector with the Ciii-RBS1 promoter module. A decrease of approximately 64 % of GFP fluorescence was obtained when comparing GFP fluorescence of BL21(DE3)(pBI4iSCiii.11-gfp.1) cells (Ciii-RBS2 module) with cells of BL21(DE3)(pBI4iSC3.3-gfp.1) (C3-RBS2 module). Thus, removal of the insulation sequence led to a 1.7- and 2.8-fold decrease in expression. Combinations of both, the exchange of the RBS and the removal of the insulation sequences led to a 3.4-fold reduction in promoter module strength (comparing Ciii-RBS1 with C3-RBS2).

The molecular modifications including insulation removal and RBS exchange led to reductions in the *gfp.1* expression level. However, the obtained results cannot fully define which of the two genetic modifications had the main influence on expression level reduction. Obviously, a combination of insulation removal and RBS exchange is the root cause for the reduced expression level. In particular, the strong influence on expression exerted by the insulation sequences was not expected. Apparently, presence of insulation sequences resulted in increased expression levels. The 5' untranslated region (UTR) comprising the 3' insulation sequence determines the 5' end of the resulting mRNA. In a previous publication it was shown that the nucleotide sequence of the 5' UTR can influence the expression level (Roberts et al. 1979). In general, it was shown that secondary structures of the mRNA, especially in the area upstream of the translation initiation codon AUG, significantly affected translation efficiency (Iserentant & Fiers 1980; DeSmit & van Duin 1994). The 3' insulation sequence might lead to the formation of mRNA secondary structures increasing the translation initiation efficiency and thus might constitute the root cause in enhancing the expression levels.

3.2. Application of the Newly Established Co-Expression System in FabZ Production Experiments

3.2.1. Significantly Different Expression Levels Were Demonstrated for Constitutive Promoter Modules Used in the Co-Expression System

Creation of GFP encoding promoter probing vectors bearing either an insulated promoter module (Ci) or one of the two Second Generation promoter modules (C2 and C8) worked properly. During creation of the co-expression plasmids the six folding modulator genes *dsbA*, *dsbC*, *fkpA*, *ppiD*, *skp* and *surA* were successfully inserted downstream of modules Ci, C8 and C2. Successful creation of co-expression plasmids indicated sufficiently low strength of the used promoter modules. Apparently, folding modulator levels did not exert a negative effect on cell growth when expression of their respective genes was controlled by promoter modules Ci, C8 and C2. On the other hand insertion of *dsbC*, *fkpA*, *ppiD* and *surA* downstream the C3 promoter module with 33 % relative strength compared to fully induced, native T7 promoter module failed (see Chapter 3.1.3). Hence, the C3 promoter module-mediated expression level was considered as the maximal bearable folding modulator level for the cells. Therefore, the strength of promoter module C3 was defined as a new 100 % reference. It was important to bear in mind that previous assessments of constitutive promoter module strength relied on comparison with the native T7 promoter module under full induction conditions. Here a new, adapted promoter test was performed using promoter module C3 as new 100 % reference. By this test, the strength differences of promoter modules Ci, C8 and C2 should be demonstrated.

Plasmid strains BL21(DE3)(pBI4iSC$_a$.3-gfp.1) (C$_a$ = Ci, C2, C3 and C8) and the negative control BL21(DE3)(pBI4iSC8.3) (w/o *gfp.1* gene) were subjected to a promoter test as described in 2.3.2. Main culture incubation was performed in 1000 mL unbaffled Erlenmeyer flasks with 200 mL of T7 Shake Flask Medium supplemented with 50 µg/mL streptomycin. Cultivation was performed at 25 °C and 300 rpm. Cell samples were prepared directly before and 1, 4, 19 and 24 h after addition of IPTG. IPTG (1 mM) was added in order to simulate conditions of subsequent FabZ production experiments. Fluorescence of resuspended cell samples was measured using a Safire2™ fluorescence microplate reader (Tecan Group) at an excitation wavelength of 475 nm and an emission wavelength of 512 nm (fluorescence$_{Exc.475/Em.512}$) (see 2.5.1). Figure 3-9 displays the measured fluorescence$_{Exc.475/Em.512}$ in RFU of strains subjected to the promoter test in dependence of the sampling time.

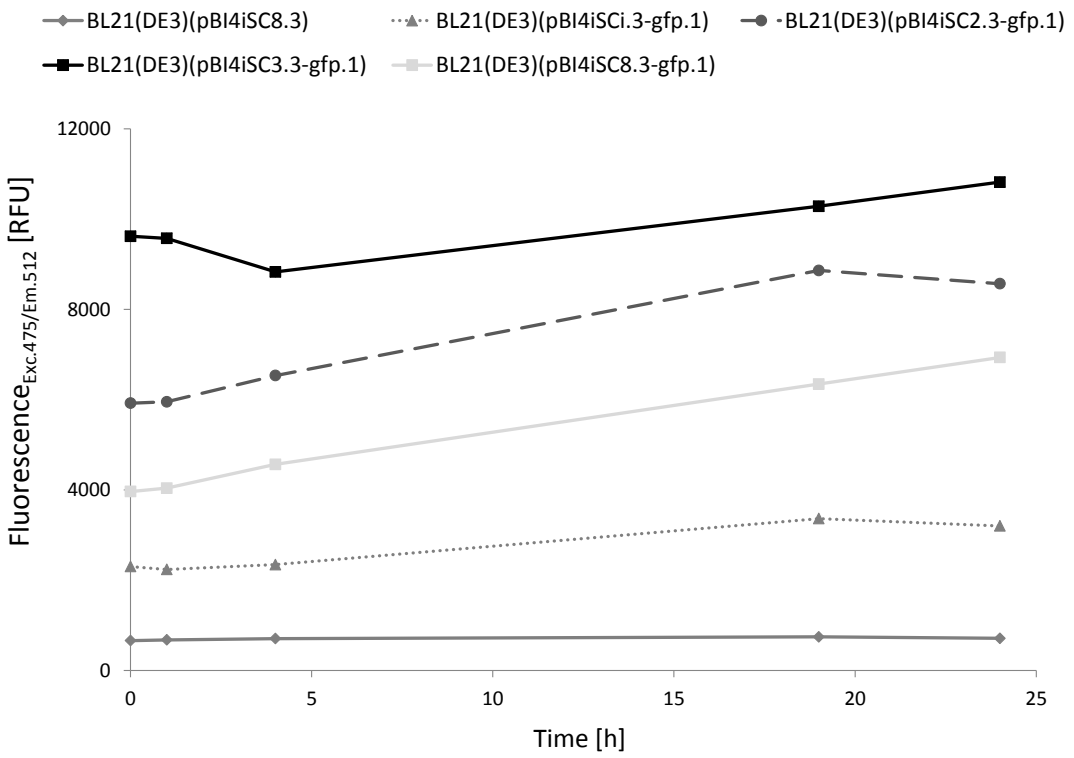

Figure 3-9: Activity of selected constitutive promoter modules. GFP production controlled by constitutive promoter modules is represented as relative fluorescence and plotted over time after addition of IPTG. Plasmid strains BL21(DE3)(pBI4iSC$_a$.3-gfp.1) (C$_a$ = Ci, C2, C3 and C8) and strain BL21(DE3)(pBI4iSC8.3) (negative control) were subjected to shake flask experiments in accordance with the method described in 2.3.2. Cell samples corresponding to a volume of 5 mL/OD$_{550}$ were taken directly before and 1, 4, 19 and 24 h after addition of IPTG. Cell samples were resuspended in 5 mL OD buffer. 200 µL of these cell suspensions were subjected to fluorescence measurements (according to 2.5.1) using a Safire^{2}™ fluorescence microplate reader at an excitation wavelength of 475 nm and an emission wavelength of 512 nm. Indicated RFU values correspond to the mean values of the eightfold measurement as described in 3.1.1.

Differences in RFU values of fluorescence$_{Exc.475/Em.512}$ measurement and hence in intracellular GFP levels were shown between promoter modules Ci, C8 and C2 for each sampling time point. Thus, different expression levels could be demonstrated for promoter modules Ci, C8 and C2. To determine the relative promoter module strength, the fluorescence values of the non-GFP-producing strain BL21(DE3)(pBI4iSC8.3) was subtracted from fluorescence values determined for the GFP-producing strains. In contrast to previous promoter test approaches, the GFP fluorescence level of plasmid strain BL21(DE3)(pBI4iSC3.3-gfp.1), employing the C3 promoter module, was used as 100 % reference. A relative promoter strength (in %) was calculated for promoter modules Ci, C8 and C2 by dividing the GFP fluorescence value of BL21(DE3) cells carrying the respective promoter probing vector by the GFP fluorescence of the 100 % reference at each sampling time point. Hence, five time-dependent relative promoter strength values were obtained. Since promoter strength appeared to be quite constant over time, the overall promoter module strength of Ci, C8 and C2 was finally determined by calculating the mean value of the five time-dependent values. Resulting mean values are presented as relative promoter module strength in Figure 3-10.

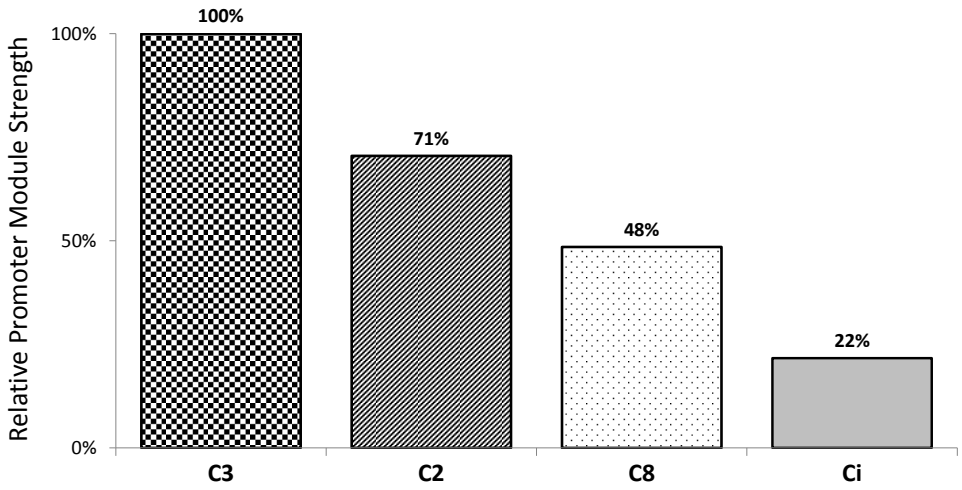

Figure 3-10: Relative strength of selected constitutive promoter modules compared to the C3 promoter module. The promoter module can be found on the x-axis and the corresponding relative promoter strength in % is shown on the y-axis. For promoter module strength determination, plasmid strains BL21(DE3)(pBI4iSC$_a$.3-gfp.1) (C$_a$ = Ci, C2, C3 and C8) and strain BL21(DE3)(pBI4iSC8.3) (negative control) were subjected to a promoter test according to 2.3.2. Fluorescence of intracellular GFP was measured at an excitation wavelength of 475 nm and an emission wavelength of 512 nm (2.5.1). Resulting RFU values were corrected by subtraction of the background fluorescence of cell samples from the negative control. GFP fluorescence of strain BL21(DE3)(pBI4iSC3.3-gfp.1), employing the C3 promoter module, was used as 100 % reference. A relative promoter strength (in %) was calculated for promoter modules Ci, C8 and C2 by dividing the GFP fluorescence of BL21(DE3) cells carrying the respective promoter probing vector by the GFP fluorescence of the 100 % reference at each of the five sampling time points. The overall promoter module strength of Ci, C8 and C2 was finally determined by calculating the mean value of the five time-dependent values. Resulting mean values are indicated on top of the bars.

Compared to the constitutive promoter module C3, relative promoter module strengths of 22, 48 and 71 % were determined for modules Ci, C8 and C2, respectively. Compared to the fully induced, native T7 promoter module 24 h after IPTG addition, relative strength of 5, 20 and 23 % were determined for promoter modules Ci, C8 and C2, respectively (see Figure 3-6 and Figure 3-8). Apparently, the relative promoter module strength of modules Ci, C8 and C2 was somewhat altered when comparing both methods. The variations in relative strength distribution can most probably be attributed to the different calculation methods. When using the C3 promoter module as 100 % reference five points of time were included in relative promoter module strength calculation. On the contrary, only one measuring point (24 h after IPTG addition) was used for the calculation of the relative promoter module strength when using the T7 promoter module as 100 % reference. This had to be done in order to consider the inherent characteristic of an inducible promoter like the T7 promoter. Maximal *gfp.1* expression levels for this inducible system were reached approximately 24 h after addition of IPTG. Thus the 24 h sampling point was used for the strength determination. To identify differences in the expression levels of the relevant constitutive promoter modules Ci, C8 and C2, the application of another constitutive promoter module as 100 % reference (here C3) seemed to be favourable. By applying this reference, significantly different expression levels of promoter modules Ci, C8 and C2, could be

demonstrated. Hence, using a co-expression system based on promoter modules Ci, C8 and C2 should provide three different synthesis rates of the respective folding modulator. Consequently, the effect of folding modulator gene co-expression at three different levels on soluble FabZ production could be analysed.

3.2.2. Positive Influence of FkpA, Skp and SurA Co-synthesis on Soluble FabZ Production in Shake Flask Experiments

The production strain *E. coli* BL21(DE3) Tn7::<FabZ>, bearing the genome-integrated FabZ expression cassette, was subjected to 5 L fed-batch fermentation experiments in a previous part of this project (Buettner 2016). In these experiments FabZ aggregates in the g/L range were observed. To determine their intracellular localization, FabZ aggregates were subjected to N-terminal sequence analysis by Edman degradation (Buettner 2016). No OmpA leader peptide sequence was detected in the analysed aggregates, indicating that aggregation of FabZ occurred in the periplasm. Apparently, translocation of FabZ across the inner membrane via the Sec translocon seemed not to be the bottleneck of secretory FabZ production. It was assumed that aggregation of FabZ could be caused by an overload of the periplasmic folding machinery. In previous review articles it was shown that the co-expression of periplasmic folding modulator genes could improve the production of several recombinant proteins (Kolaj et al. 2009; François Baneyx & Mujacic 2004; A. DeMarco 2009). Also a positive influence of folding modulator co-synthesis on periplasmic Fab fragment production was demonstrated (Levy et al. 2001; Lin et al. 2008). However, previous studies also showed that the success of single folding modulators appears to be specific for each recombinant antibody fragment (Schaefer & Andreas Plückthun 2010). In general, the folding modulator gene co-expression needs to be optimized for each recombinant target protein and requires a trial-and-error approach (Martínez-Alonso et al. 2010; Overton 2014). By now, sufficient information is lacking which folding modulators at which intracellular levels could exert a positive effect on soluble FabZ production. Hence, in this study a co-expression system was established to quickly screen for appropriate folding modulators and levels in case of FabZ and other target proteins. To enable a fine-tuned folding modulator co-production, constitutive promoter modules of different strength were analysed for their suitability to drive folding modulator gene expression. Three promoter modules (Ci, C8 and C2) causing significantly different expression levels were evaluated in a promoter test (see Chapter 3.2.1). Their relative promoter strength were determined to be 22, 48 and 71 % for Ci, C8 and C2, respectively. Subsequently, 18 co-expression plasmids were created bearing one of the six folding modulator genes (*dsbA*, *dsbC*, *fkpA*, *ppiD*, *skp* or *surA*) transcriptionally controlled by one of the three promoter modules. In addition to these 18 co-expression plasmids, three empty plasmids bearing the Ci, C8 or C2 promoter module but lacking a folding modulator gene (w/o gene) were created. These co-expression plasmids w/o gene were used as references to examine possible interferences between the basic co-expression plasmids and the target gene (FabZ) expression. The FabZ production strain without any

plasmid (w/o plasmid) was used as second reference in order to evaluate overall improvement in FabZ production. With this co-expression system, the influence of various co-synthesis levels of the thiol-disulfide oxidoreductases DsbA and DsbC, the PPIases FkpA, PpiD and SurA and the periplasmic chaperone Skp on soluble FabZ production was analysed in shake flask experiments.

E. coli BL21(DE3) Tn7::<FabZ> cells were transformed with each of the 21 co-expression and reference plasmids. Afterwards, cryo cultures of these transformants were prepared (see Table 2-8). Resulting plasmid strains were analysed concerning their soluble FabZ production behaviour in shake flask experiments as described in 2.3.3. Briefly, the respective cryo culture was thawed at RT and 50 µL of the suspension were used to inoculate 30 mL of T7 Pre-culture Medium. For the plasmid strains the T7 Pre-culture Medium was supplemented with streptomycin while the FabZ production strain w/o plasmid was cultivated with kanamycin. After o/n incubation, cell suspensions of equal cell counts were taken from the pre-cultures, sedimented by centrifugation and finally resuspended using 5 mL sterile 0.9 % (v/v) NaCl solution. Resuspended cells were used to inoculate the main culture shake flask (200 mL of T7 Shake Flask Medium) to an OD_{550} of 0.2. As all FabZ production strains harbour a genome-integrated kanamycin resistance gene, the T7 Shake Flask Medium was supplemented with kanamycin. Main cultures were incubated at 37 °C until an OD_{550} of 0.8 ± 0.25 was reached. Subsequently incubation was performed at 25 °C for at least 30 min. FabZ production was induced by addition of 1 mM IPTG at an OD_{550} of 1.0 ± 0.2. After inducer addition, cultivation at 25 °C and 300 rpm was conducted for 12 h. Sampling was performed directly before (T0) and 12 h after addition of IPTG (EoF). Sampling was done by taking cell suspensions corresponding to a volume of 5 mL/OD_{550}. Cell suspensions were subsequently sedimented by centrifugation and the resulting supernatant was decanted and filtrated. Soluble FabZ concentration of supernatant and cell samples of the EoF time points was determined by ELISA measurement (see Chapter 2.5.2). Total soluble FabZ concentration was calculated by summing up the soluble FabZ content of both fractions. In addition, OD_{550} was determined for all strains at the end of cultivation. In previous experiments total soluble FabZ concentration and OD_{550} values at EoF were determined in replicated shake flask experiments under similar cultivation conditions (Schuller 2015; Buettner 2016). The ranges between minimum and maximum values of maximum total soluble FabZ concentration and OD_{550} values were calculated based on these biological replicate measurements. The calculated range (in %) was used to estimate the positive and negative error bars for total soluble FabZ concentrations and OD_{550} values presented in this work. Figure 3-11 depicts the total soluble FabZ concentrations and OD_{550} values of shake flask experiments of FabZ production strains. To obtain an estimation of intracellular FabZ and folding modulator content of each strain, cell samples were analysed by SDS-PAGE (Figure 3-12). Table 3-6 summarizes the results of the FabZ production experiments in shake flasks.

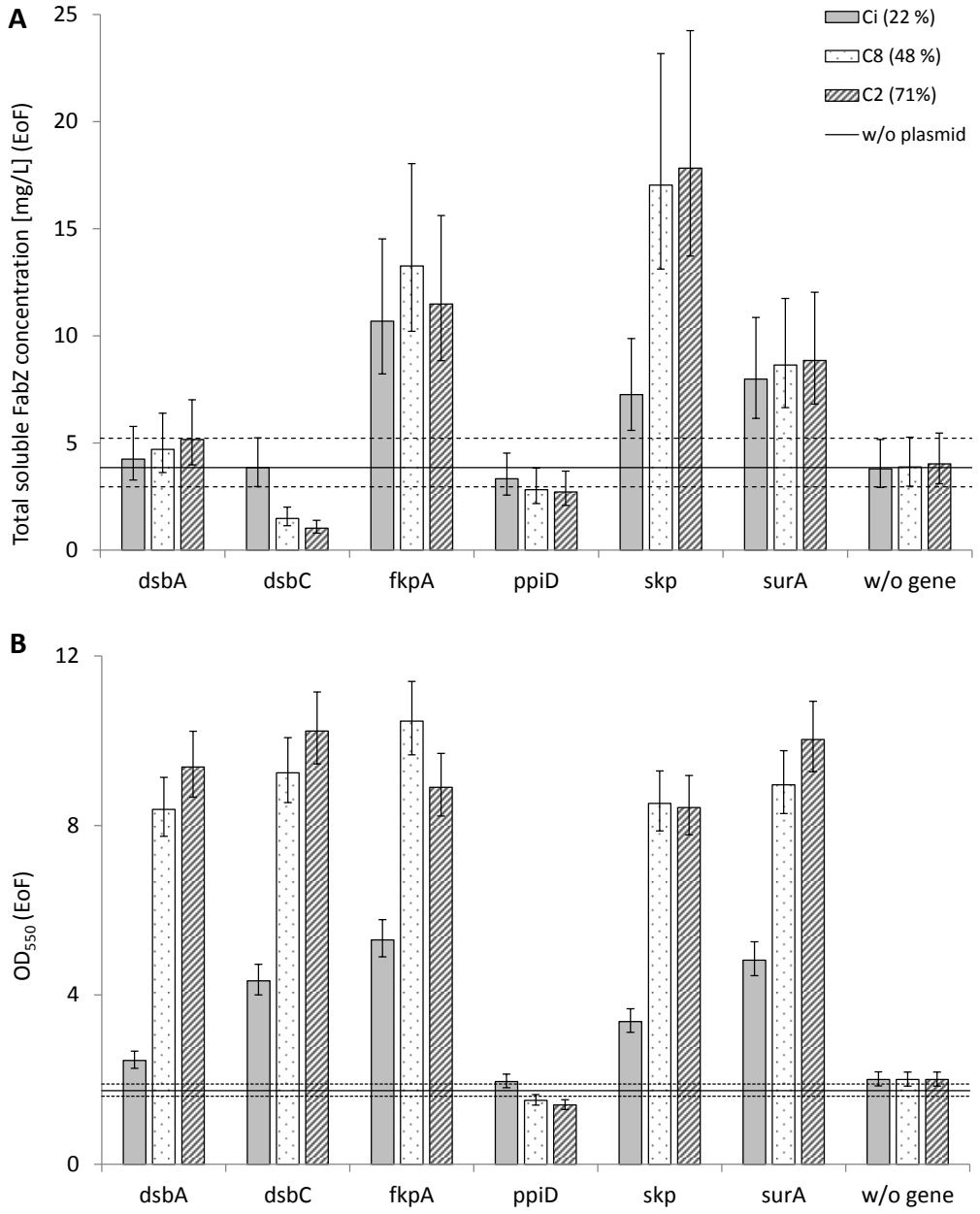

Figure 3-11: Influence of folding modulator co-synthesis on soluble periplasmic FabZ production and cell growth in shake flask experiments. A co-expression system based on three constitutive promoter modules (Ci, C8 or C2) of different strength and six periplasmic folding modulator genes (*dsbA*, *dsbC*, *fkpA*, *ppiD*, *skp* or *surA*) was established. Co-expression plasmids bear one of the folding modulator gene or do not harbour any gene (w/o gene). *E. coli* BL21(DE3) Tn7::<FabZ> cells, bearing the genome-integrated FabZ expression cassette, were transformed with each of the 21 plasmids. Resulting strains were analysed in shake flask experiments as described in 2.3.3. Cell suspension samples were taken 12 h after inducing FabZ production with 1 mM IPTG (EoF). Soluble FabZ concentration of supernatant and cell samples from EoF time points was determined by ELISA measurement. The total soluble FabZ concentration was calculated by summing up the soluble FabZ content of both analysed fractions. OD_{550} values were determined for all strains at EoF. Total soluble FabZ concentration [mg/L] (A) and OD_{550} values (B) at EoF are shown on the y-axis while the respective folding modulator gene is shown on the x-axis. Different bar designs refer to the three different expression levels of the folding modulator genes mediated by the promoter modules Ci, C8 or C2 with a relative strength of 22, 48 and 71 %, respectively. Error bars were estimated based on the range between minimum and maximum values of previously performed shake flask experiments. w/o plasmid: FabZ production strain without any plasmid. Black line: Total soluble FabZ concentration (3.9 mg/L) (A) or OD_{550} (1.7) (B) determined for the production strain w/o plasmid. Respective error bars are indicated by the dashed lines.

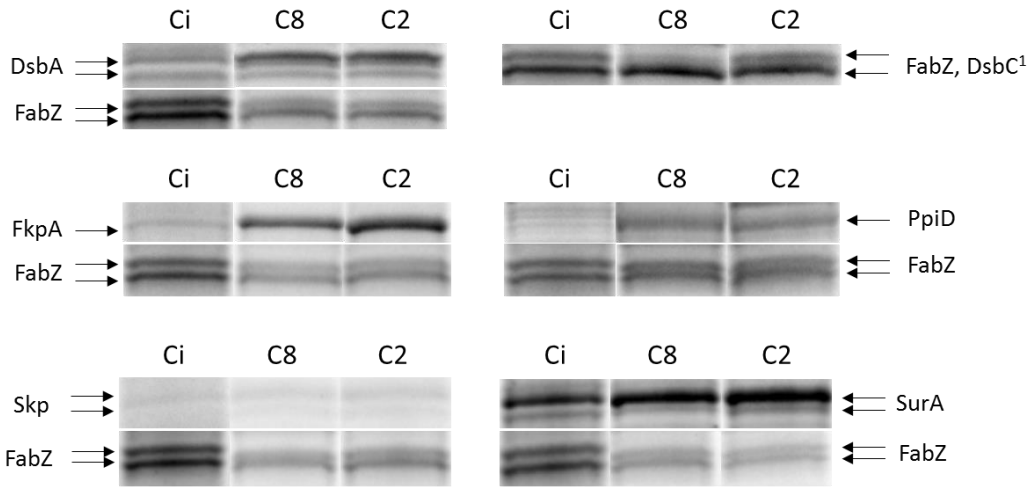

Figure 3-12: SDS-PAGE analysis to determine intracellular level of FabZ and folding modulators in dependence of the used co-expression plasmid. Cell samples obtained at the end of FabZ production experiments in shake flasks were subjected to SDS-PAGE analysis to determine intracellular levels of FabZ and folding modulators. The same samples were also used for ELSIA analysis to determine the soluble FabZ concentrations (see Figure 3-11). Cell samples were disrupted with BugBuster® Protein Extraction Reagent (Novagen). Samples were diluted three-fold with 2x LDS buffer containing the reducing reagent β-mercaptoethanol and subsequently heat denaturated. Reference protein solutions containing 0.2, ±and 1.4 µg of FabZ were prepared in 1x LDS buffer and also heat denaturated. After cooling, sample and reference solutions were loaded onto Criterion™ TGX Stain-Free™ Precast gels. Protein separation was carried out applying 1x TGS buffer and a voltage of 200 V. Gel images were acquired using a gel-Doc™ EZ Imager (Bio-Rad) and analysed using the Image Lab 5.0 software. Protein quantity was determined using a standard curve calculated by linear regression from the reference protein samples. Both FabZ monomers (LC and HC) and the folding modulators were detected and identified based on their molecular weight. Bands on the SDS-PAGE gel corresponding to FabZ LC (23 kDa), FabZ HC (23 kDa), DsbA (21 kDa), DsbC (23 kDa), FkpA (26 kDa), PpiD (68 kDa), Skp (16 kDa) and SurA (45 kDa) are indicated by an arrow. For some folding modulators two arrows are depicted, since two bands seem to represent the protein. These bands are supposed to be preprotein and mature protein of the respective folding modulator. DsbC[1]: Due to the similar molecular weights DsbC and FabZ monomers appeared at the same position on the SDS-PAGE gel. Ci, C8 and C2: Co-expression plasmids employing the constitutive promoter modules with respective relative strength of 22, 48 and 71 % to control folding modulator gene expression. Images referring to the C8 and C2 promoter modules originate from one gel, while lane images referring to promoter module Ci were obtained from a different gel.

During SDS-PAGE analysis FabZ monomers and folding modulators were identified based on their molecular weight. Two separate bands were obtained for the LC and HC of FabZ. For some folding modulators also two bands were detected on the SDS-PAGE gel. These are supposed to correspond to the preprotein containing the N-terminal leader peptide and the mature protein (after signal sequence cleavage) of the respective folding modulator. Due to similar molecular weights of DsbC and FabZ, identification of DsbC was hardly possible. Also Skp detection was difficult because of the low intensity of the corresponding bands. Based on the SDS-PAGE results, the ratio of FabZ and the respective folding modulator was determined for each plasmid strain.

Table 3-6: Total soluble FabZ concentration, OD_{550} value and intracellular ratio of FabZ to folding modulator determined in FabZ production experiments. A co-expression system based on three constitutive promoter modules of different strength and six periplasmic folding modulator genes was established. The influence of individual co-production of the six periplasmic folding modulators at three different levels on soluble FabZ production was analysed in shake flask experiments. DsbA, DsbC, FkpA, PpiD, Skp, SurA: Periplasmic folding modulators which were co-produced. w/o gene: Empty co-expression plasmid lacking a folding modulator gene. Ci, C8, C2: Promoter modules providing low (Ci), medium (C8) and high (C2) expression levels of folding modulator genes. Total soluble FabZ concentration: Sum of soluble FabZ content of supernatant and sedimented cell samples obtained by ELISA measurement (2.5.2). OD_{550}: Optical density of cell suspension samples measured at 550 nm. Intracellular ratio FabZ / FM: Intracellular FabZ and folding modulator (FM) content of cell samples was determined by SDS-PAGE analysis. Based on these results the ratio of FabZ and the respective folding modulator was determined. Asterisks: Detection of Skp via SDS-PAGE analysis was difficult and hence determination of the FabZ/FM ratio was hardly possible. EoF: End of cultivation 12 h after addition of the inducer IPTG. The basic FabZ production strain w/o plasmid was used as a reference and yielded a total soluble FabZ concentration of 3.9 mg/L and an OD_{550} of 1.7.

Folding modulator	**Promoter module**	**Total soluble FabZ concentration [mg/L] (EoF)**	**OD_{550} (EoF)**	**Intracellular ratio FabZ / FM (EoF)**
w/o gene	Ci	3.8	2.0	-
	C8	3.9	2.0	-
	C2	4.0	2.0	-
DsbA	Ci	4.2	2.5	4.0
	C8	4.7	8.4	0.9
	C2	5.2	9.4	0.8
DsbC	Ci	3.9	4.3	-
	C8	1.5	9.2	-
	C2	1.0	10.2	-
FkpA	Ci	10.7	5.3	10.4
	C8	13.2	10.5	0.9
	C2	11.5	8.9	0.7
PpiD	Ci	3.3	2.0	7.2
	C8	2.8	1.5	2.3
	C2	2.7	1.4	2.3
Skp	Ci	7.3	3.4	37.1*
	C8	17.0	8.5	5.4*
	C2	17.8	8.4	6.1*
SurA	Ci	8.0	4.8	1.8
	C8	8.6	9.0	0.5
	C2	8.9	10.0	0.5

The Application of Constitutive Promoter Modules Yielded an Improved Co-Expression System to Screen for Appropriate Folding Modulators. In a previous part of this project (Schuller 2015; Buettner 2016) the native T7 promoter and three T7 promoter mutants of various strength (3, 20 and 61 % in comparison to the native T7 promoter) were used to control the expression of the folding modulator genes. Severe drawbacks of the T7-promoter based co-expression system were observed as interference between the co-expression plasmid backbones and FabZ production was demonstrated. T7 promoters present in co-expression plasmids without gene exerted different effects on total soluble FabZ concentration, depending on the T7 promoter strength (see Figure 3-13). The application of the T7 promoter-based co-expression system prevented helper factors from exhibiting their full potential. Hence, in this study a co-expression system based on constitutive promoters of various strengths was established.

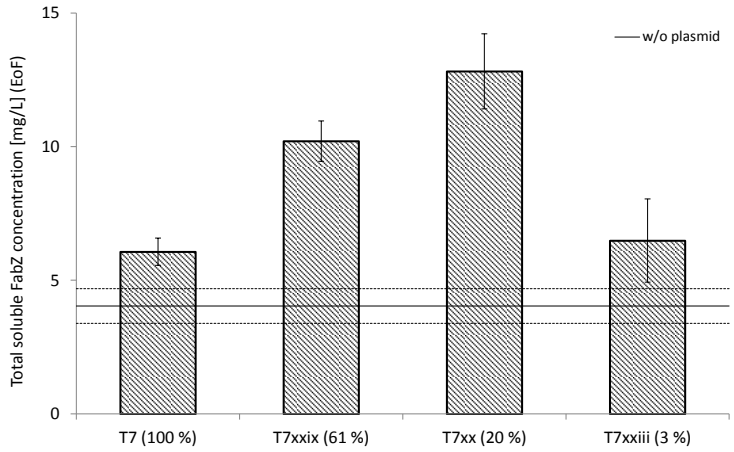

Figure 3-13: Influence of the T7 promoter-based co-expression system on soluble FabZ production. *E. coli* BL21(DE3) Tn7::<FabZ> cells, bearing the genome-integrated FabZ expression cassette, were transformed with four empty co-expression plasmids w/o folding modulator gene under control of a T7 promoter variant. Each used T7 promoter module exhibited a different expression strength (as indicated). Resulting strains were analysed for their FabZ production behaviour in shake flask experiments in a previous part of this project (Buettner 2016). Cell suspension samples were taken 12 h after inducing FabZ production with 1 mM IPTG (EoF). Respective samples were subjected to ELISA measurement to determine soluble FabZ concentrations of supernatant and sedimented cell samples at the EoF time points. Total soluble FabZ concentration was calculated by summing up the soluble FabZ content of both fractions and is shown on the y-axis. T7 promoter variants and their corresponding relative strength used for the co-expression system are shown on the x-axis. Error bars indicate standard deviations of biological duplicates or triplicates of the respective plasmid strain. w/o plasmid: FabZ production strain without a co-expression plasmid. Black line: Mean value of total soluble FabZ concentration (4.0 mg/L) determined by four-fold measurement of the production strain w/o plasmid. Respective error bars are indicated by dashed lines.

In this study the plasmid-free reference strain (w/o plasmid) yielded a total soluble FabZ concentration of 3.9 mg/L and an OD_{550} of 1.7 at EoF. Similar total soluble FabZ concentrations were determined in case of the reference strains carrying the empty co-expression plasmids with promoter modules Ci, C8 and C2. Also similar OD_{550} values were determined at EoF for the three reference strains w/o gene compared to the plasmid-free reference strain.

Apparently, the FabZ production and growth behaviour was comparable between the plasmid-free FabZ-producing strain and the plasmid strains carrying the empty co-expression plasmids. Therefore, it can be concluded that the presence of these basic co-expression plasmids had no significant impact on soluble FabZ production or the growth behaviour. This statement is valid, independent of the strength of the used constitutive promoter module. Thus, it can further be concluded that differences in FabZ concentration or OD_{550} at EoF of the analysed strains were caused by the presence and cellular level of the respective folding modulator. Opposed to the T7 promoter-based co-expression system, it could be shown that the newly established co-expression system based on constitutive promoter modules did not interfere with FabZ production. Hence, in this study a significant improvement of the basic co-expression system was achieved by application of constitutive promoter modules.

The Periplasmic Chaperone Skp Exerted the Strongest Positive Influence of All Examined Folding Modulators. The seventeen kilodalton Protein (Skp) is a periplasmic chaperone in *E. coli* that captures unfolded proteins after translocation via the Sec translocon. The primary function of Skp is to catalyse correct folding of outer membrane proteins and their insertion into the outer membrane (Schäfer et al. 1999). It was shown that Skp acts as a holdase and thereby prevents protein aggregation (Entzminger et al. 2012). The catalytic centre of Skp is composed of a central cavity in which folded proteins of a molecular mass of up to approximately 25 kDa can be accommodated. Unfolded proteins would have to be smaller to fit in the cavity of Skp. OmpA has a molecular mass of 18.8 kDa and is a well-characterized substrate of Skp and thus should fit in the central cavity in an unfolded state. It was observed that the central cavity of Skp is flexible and could therefore accommodate substrates that are significantly bigger than OmpA (Walton & M. C. Sousa 2004). Both monomers of FabZ are translocated via the Sec translocon and each monomer has a molecular mass of about 23 kDa. Hence, it was assumed that Skp might prevent aggregation of FabZ by binding the unfolded monomers or at least parts thereof in its central cavity. It was previously shown that Skp improved the production and secretion of difficult-to-express antibody fragments (Bothmann & A. Plückthun 1998; Hayhurst & Harris 1999; Lin et al. 2008).

As presented above (see Table 3-6 and Figure 3-11) Skp positively influenced soluble FabZ yields. The positive influence of Skp was seen at all applied synthesis rate. The highest positive effects of *skp* gene co-expression were determined for the strong promoter modules C8 (48 %) and C2 (71 %). The highest absolut total soluble FabZ titre in shake flask experiments of 17.8 mg/L (4.6-fold increase) was achieved by co-expression of *skp* under the control of the strongest promoter module C2. Skp co-synthesis also had a positive impact on EoF OD_{550} values. The beneficial effect on OD_{550} values at EoF was higher with increasing Skp levels. During SDS-PAGE analysis, detection of Skp was difficult and hence determination of the FabZ and Skp ratio was hardly possible.

In accordance with previous studies, the positive influence of Skp on soluble antibody fragment production was also shown in FabZ production experiments. Furthermore, Skp

overproduction exerted a positive effect on OD_{550} values at EoF. Apparently, Skp co-production could prevent cell lysis, which was detected in other strains. To examine the growth behaviour before EoF, growth curves of selected strains were recorded. *E. coli* BL21(DE3) Tn7::<FabZ> cells harbouring plasmid pBI4iSC8.3-skp and the corresponding empty reference plasmid pBI4iSC8.3 were used for this purpose. In shake flask experiments, which resembled the FabZ production experiments, OD_{550} was measured throughout the protein production phase to determine the respective growth curves (Figure 3-14).

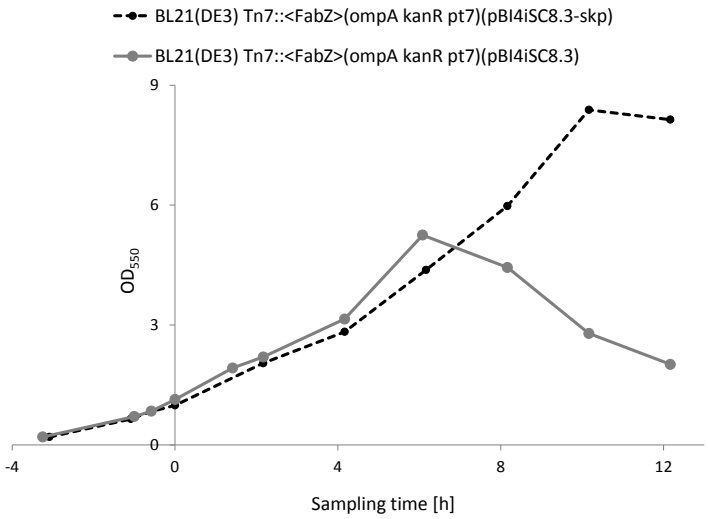

Figure 3-14: Influence of Skp co-synthesis on growth behaviour of FabZ production strain. Cell growth of *E. coli* BL21(DE3) Tn7::<FabZ> cells carrying plasmid pBI4iSC8.3-skp and its plasmid counterpart pBI4iSC8.3 w/o folding modulator gene was analysed in shake flask experiments. The experiment was conducted in the same way as FabZ production experiments. Samples of cell suspensions were taken at different time points. After preparation, samples were subjected to OD_{550} measurement. Sampling time at 0 h on x-axis refers to the time of IPTG addition.

Both strains showed comparable growth behavior within the first 6 h after induction of FabZ production. However, significant differences were observed during the remaining incubation period. Cell density of the production strain harboring the empty plasmid pBI4iSC8.3 reached its OD_{550} peak of 5.3 approximately 6 h after FabZ induction. In the remaining 6 h of cultivation, OD_{550} values decreased continuously until at EoF an OD_{550} value of 2.0 was measured. Apparently, growth of pBI4iSC8.3-bearing cells ceased 6 h after FabZ induction. Further reductions of OD_{550} indicated cell lysis. The production strain carrying plasmid pBI4iSC8.3-skp showed a different growth behaviour in the last 6 h of cultivation and reached a final OD_{550} of 8.1. In this case OD_{550} values increased continuously until 10 h after IPTG addition. For the last 2 h of incubation growth stagnation was observed.

Protein aggregation was previously reviewed to have a toxic effect on cells and promote cell lysis (A. DeMarco 2013). Hence, lysis of pBI4iSC8.3-bearing cells could be potentially caused by accumulation of incorrectly folded FabZ. Too high synthesis rates of FabZ might overload the periplasmic folding machinery leading to periplasmic protein aggregation. Apparently, continuous expression of *skp* improved growth behaviour of the FabZ production strain. The

improvement in cell growth could be attributed to a reduction in periplasmic FabZ aggregates. Improved capacities of the periplasmic folding machinery due to Skp overproduction could be a potential factor in enhancing soluble FabZ production. On the other hand also FabZ synthesis rate could be lowered by competitive co-expression of *skp*. SDS-PAGE analysis revealed that constitutive *skp* expression reduced total intracellular FabZ levels by 39 %, indicating a reduction in the synthesis rate of the antibody fragment. Previous studies revealed that a reduction in synthesis rates of recombinant proteins decreased the cells' metabolic burden and thereby improved folding quality (Hoffmann & Rinas 2004). Lowering the synthesis rate of FabZ by *skp* co-expression would result in slower secretion. Therefore, improved FabZ folding in the periplasm could be enabled and the formation of periplasmic aggregates could be reduced. In conclusion, increased Skp levels and/or reduction of FabZ synthesis rate prevented cell lysis and resulted in higher OD_{550} values at EoF.

Individual Co-Synthesis of the Thiol-Disulfide Oxidoreductases DsbA and DsbC Exerted No Positive Influence on Soluble FabZ Production. DsbA and DsbC are enzymes of the disulfide bond (Dsb) family and are representatives of bacterial thiol-disulfide oxidoreductases. DsbA and DsbC catalyse disulfide bond formation and isomerization in the oxidizing environment of the *E. coli* periplasm. DsbA is a periplasmic protein of 21 kDa which interacts with unfolded proteins upon translocation. DsbA catalyses *de novo* formation of disulfide bonds between two reduced cysteine residues and thereby has the tendency to oxidize cysteines in a consecutive manner (Kadokura et al. 2004). After reaction, the reduced DsbA is re-oxidized by the inner membrane protein DsbB (Jander et al. 1994). The 23 kDa disulfide bond protein DsbC catalyses disulfide isomerization in the periplasm by supporting rearrangement of incorrectly formed disulfides (Hiniker & Bardwell 2003). In order to remain reduced, DsbC requires the action of the inner membrane protein DsbD (Rietsch et al. 1997). As the heterodimeric FabZ contains one intermolecular and two intramolecular disulfide bonds per monomer, overexpression of *dsbA* or *dsbC* could be beneficial for correct folding of the antibody fragment.

Co-expression of *dsbA* had no significant effect on soluble FabZ production, independent of the intracellular level (see Table 3-6 and Figure 3-11). On the other hand, an influence on cell growth was observed with DsbA co-production as OD_{550} values at EoF were significantly higher compared to the plasmid-free FabZ production strain. The positive effect on OD_{550} values at EoF was stronger with increasing expression levels of *dsbA*. Apparently, co-production of DsbA could prevent cell lysis. An influence of the *dsbA* expression rate on total intracellular FabZ levels was also observed. The ratio of intracellular FabZ and DsbA levels was shifted towards DsbA with increasing synthesis rates of the folding modulator. The mere overproduction of DsbA could not enhance total soluble FabZ yields. DsbB, required for re-oxidation of DsbA, was not addressed in the here tested co-expression system. Since DsbB remained at a native level, re-oxidation of DsbA might be limited. Thus, a limited presence of DsbB might prevent the DsbA/DsbB system from exerting a positive influence on soluble

FabZ production. Hence, co-expression of both, *dsbA* and *dsbB* could be required to further improve soluble FabZ yields. The beneficial effect of increasing synthesis rates of DsbA on OD_{550} values at EoF could be explained by a reduction of the FabZ production rate due to competitive production and secretion of DsbA. Reduced secretion of FabZ would than lead to less FabZ aggregation in the periplasm and thereby prevent cell lysis.

Like DsbA, the second disulfide bond protein DsbC had also no significant effect on soluble FabZ production when the weakest promoter module was employed for its co-synthesis (see Table 3-6 and Figure 3-11). However, increasing expression levels of *dsbC* affected total soluble FabZ yields negatively. As already observed for DsbA, overproduction of DsbC had a positive influence on cell growth and led to higher OD_{550} values at EoF with increasing synthesis rates. The ratio of intracellular FabZ and DsbC levels could not be determined, due to the very similar molecular weights of DsbC and FabZ. Differentiation of the corresponding bands during SDS-PAGE analysis was not possible. Previous studies revealed that DsbC activity is not required for proteins in which disulfide bonds between consecutive cysteines are present in the native structure (Joly & Swartz 1997). Hence, the absence of a positive effect of DsbC on FabZ folding can be explained, since the native structure of FabZ consists only of disulfide bonds formed between consecutive cysteines. The negative effect on total soluble FabZ production of increasing periplasmic DsbC levels might be attributed to the reaction mechanism of DsbC. Periplasmic overabundance of DsbC could lead to the reduction of correctly folded disulfides. Correctly folded disulfide bonds in FabZ might potentially be rearranged and thus lead to increased levels of misfolded FabZ molecules. As seen for DsbA, the co-production of DsbC led to a reduction in FabZ synthesis and had a positive effect on EoF OD_{550} values. The prevention of cell lysis could again be caused by a reduction in periplasmic aggregates associated with a lowered FabZ synthesis rate.

In conclusion, it seemed that the mere co-synthesis of DsbA and DsbC is not useful to enhance total soluble FabZ yields in shake flask experiments under the applied cultivation conditions. However, it was shown in some review articles that the co-production of DsbA and DsbC could enhance the soluble production of other recombinant proteins (Kolaj et al. 2009; François Baneyx & Mujacic 2004; A. DeMarco 2009). As a direct cooperation between DsbA and DsbC was found (Vertommen et al. 2008), effects of simultaneous co-expression of both, *dsbA* and *dsbC* could be addressed in further co-production attempts using other target proteins. For example, combined co-expression of *dsbA* and *dsbC* was found to positively affect the production of a functional scFv (Sandee et al. 2005). To avoid electron transfer imbalances, *dsbA* and *dsbC* over-expression should be accompanied by an increased level of its inner membrane-bound counterparts DsbB and DsbD. As previously reviewed combined co-synthesis of DsbA, DsbB, DsbC and DsbD had a stronger positive influence on production of several recombinant proteins like human nerve growth factor, brain-derived neurophilic factor and horseradish peroxidase than co-synthesis of individual or pairs of Dsb proteins (Kolaj et al. 2009). Thus, combined co-expression of *dsbA*, *dsbB*, *dsbC* and *dsbD*

appears to constitute a valuable approach in improving soluble production of recombinant proteins and could be addressed in further co-expression attempts.

Of the Examined PPIases, FkpA and SurA Exerted a Positive Effect on Soluble Periplasmic FabZ Production. Peptidyl-prolyl isomerases (PPIases) catalyse the cis-trans isomerization of peptidyl-prolyl bonds (see Figure 3-15) of periplasmic and outer membrane proteins (Pliyev & Gurvits 1999). PPIases in the *E. coli* periplasm can be grouped into three distinct families of cyclopholins (e.g. PpiA), FK506 binding proteins (e.g. FkpA) and parvulins (e.g. PpiD and SurA) (Pliyev & Gurvits 1999). As FabZ contains 11 proline residues in its heavy chain and 12 in its light chain, increased levels of FkpA, PpiA, PpiD and SurA were assumed to improve folding and thus soluble production of FabZ. Previous studies showed that the overproduction of PpiA failed to improve expression of scFv fragments (Bothmann & A. Plückthun 2000) and had no effect on periplasmic protein folding (Kleerebezem et al. 1995). Due to lack of positive results, PpiA was not addressed in the co-expression system established in this work. Hence, only the effects of co-production of the PPIases FkpA, PpiD and SurA on soluble FabZ production were examined. Both, PPIase and chaperone activities were demonstrated for FkpA (Bothmann & A. Plückthun 2000), SurA (Behrens et al. 2001) and also for PpiD (Antonoaea et al. 2008). Chaperones assist polypeptides to attain their native conformation and thus prevent aggregation of incorrectly or incompletely folded polypeptide chains (Feldman & Frydman 2000). Hence, increasing periplasmic chaperone activities introduced by co-production of FkpA, SurA and PpiD might exert a positive effect on the soluble FabZ production by preventing aggregation.

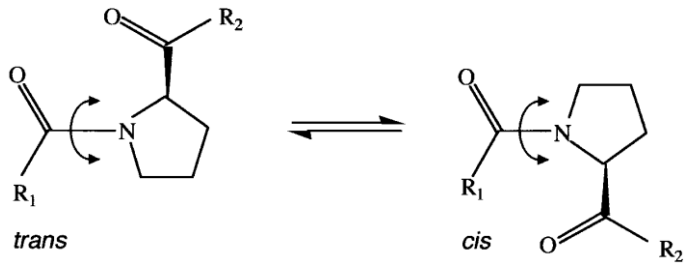

Figure 3-15: Cis-trans isomerization of a peptidyl-prolyl bond. This figure was copied from a review article (Göthel & Marahiel 1999).

FkpA co-synthesis had a significant positive influence on total soluble FabZ yields. The positive influence of FkpA was seen for all applied synthesis rate (see Table 3-6 and Figure 3-11). In addition, OD_{550} values at EoF were significantly increased by *fkpA* co-expression. The positive effect on OD_{550} values at EoF was dependent on the strength of the promoter module controlling *fkpA* expression. The use of promoter modules C8 and C2 led to highest OD_{550} values at EoF. The synthesis rate of FkpA also had an effect on cell growth during pre-culture incubation. Expression of *fkpA* controlled by the stronger constitutive promoter modules C8 and C2 led to cell lysis during pre-culture incubation at 37 °C. Regular growth behaviour was restored by reducing pre-culture incubation temperature to 33 °C. A previous

study showed improved yields of a wide range of scFv fragments due to co-synthesis of the 26 kDa PPIase FkpA (Bothmann & A. Plückthun 2000). In addition, *fkpA* co-expression led to reduced periplasmic aggregation of other recombinant proteins (Arié et al. 2001; Gunnarsen et al. 2010). In summary, findings of previous studies concerning FkpA's positive influence on soluble target protein production were confirmed in this work. Increased OD_{550} values at EoF indicated an influence of FkpA co-production on cell lysis. At 25 °C increased expression levels by C8 and C2 promoter modules of *fkpA* prevented cell lysis during main culture incubation. However, these expression levels of *fkpA* resulted in cell lysis when incubated at 37 °C during pre-culture cultivation. Possibly, expression levels of *fkpA* at 37 °C were enhanced and thus exerted a negative effect on cell growth. A further increase in *fkpA* expression could overload the secretion apparatus and thus limit the secretion of native periplasmic proteins. The reduced secretion of native periplasmic proteins potentially prevented cell growth and caused cell lysis.

In our experimental setup the 45 kDa PPIase SurA had a positive effect on total soluble FabZ yields. The positive effect of SurA was seen for all three synthesis rates. However, the synthesis rate of SurA had an influence on the OD_{550} values at EoF and the overall FabZ levels including insoluble fractions. The higher the expression level of *surA*, the more beneficial was the effect on OD_{550} at EoF. In previous studies improved folding of aggregation-prone proteins in the periplasm was shown upon SurA co-production (Missiakas et al. 1996). In this study a positive effect of SurA overproduction on total soluble FabZ yields could also be shown in shake flask experiments. SurA preferentially recognizes peptides containing *Ar*-X-*Ar* motifs, whereby "*Ar*" is an aromatic and "X" may be any proteinogenic amino acid (Bitto & McKay 2003). The monomers of FabZ contain several *Ar*-X-*Ar* motifs which could explain the positive influence of *surA* co-expression on total soluble FabZ yields. However, the positive effect on soluble FabZ yields was independent of the synthesis rate of SurA. The overproduction of SurA also led to reduced total FabZ levels. The reduction in total FabZ content affected OD_{550} values at EoF positively. Hence, cell lysis was prevented due to decreased FabZ synthesis rates.

The 68 kDa protein PpiD exerted no significant effect on total soluble FabZ yields and OD_{550} values at EoF, independent of its synthesis rate. Compared to DsbA, FkpA, Skp and SurA a lower decrease in the ratio between intracellular FabZ and folding modulator level was observed with increasing synthesis rates of PpiD. Apparently, PpiD had no significant influence on soluble FabZ production in shake flask experiments. PpiD is an inner membrane protein which promotes the folding and release of newly translocated proteins exiting the Sec tanslocon (Antonoaea et al. 2008). Although the single monomers of FabZ are translocated into the periplasm via the Sec pathway, no improvement of soluble FabZ production was demonstrated with *ppiD* co-expression. In a review article published in 2009, it was stated that no work was published so far which addressed the co-production of PpiD as an approach to improve recombinant target protein production in *E. coli* (Kolaj et al. 2009). Apparently, *ppiD* co-expression had a rather weak influence on the overall production

of FabZ compared to co-production of the other analysed folding modulators. The low OD_{550} values at EoF indicated cell lysis. As discussed earlier, this might be caused by FabZ aggregation in the periplasm.

In conclusion the PPIases FkpA, PpiD and SurA exerted different influences on total soluble FabZ yields and OD_{550} values at EoF in shake flask experiments. FkpA and SurA overproduction had a positive influence on total soluble FabZ concentration. The positive influence of FkpA and SurA was seen for all three synthesis rates. The positive influence of on OD_{550} values at EoF was stronger, with increasing synthesis rates of FkpA and SurA. PpiD co-production exerted no effect on total soluble FabZ yields and OD_{550} values at EoF, independent of the synthesis rate. PpiD differs from FkpA and SurA in its cellular localization. PpiD is anchored in the inner membrane near the SecYEG translocon (Antonoaea et al. 2008) while FkpA and SurA are located in the periplasm. PpiD has a molecular weight of 66.8 kDa which is higher than the one of FkpA (26.2 kDa) and SurA (45.1 kDa). It is not known whether these factors may contribute to differences between PpiD and the other PPIases FkpA and SurA.

Simultaneous Co-Expression of Folding Modulator Genes Present on Co-Expression Plasmid pTUM4 Showed a Negative Effect on Soluble FabZ Production. In this work a co-expression system based on three constitutive promoter modules of different strength was established for the co-production of the periplasmic folding modulators DsbA, DsbC, FkpA, PpiD, Skp and SurA. Further, the effect of individual co-production of the six periplasmic folding modulators at three different levels on soluble recombinant protein production was analysed. In contrast to the approach pursued in this work, it has previously been shown that combinations of folding modulators on a co-expression plasmid could positively affect soluble periplasmic protein production. For example, the co-expression plasmid pTUM4 (see Figure 1-7) which bears four folding modulator genes (*dsbA*, *dsbC*, *fkpA* and *surA)* showed a positive influence on cell viability, increased soluble periplasmic protein yields and induced efficient disulfide bond formation of a human plasma retinol-binding protein (RBP) and the human dendritic cell membrane receptor DC-SIGN in previous studies (Schlapschy et al. 2006). The presence of the co-expression plasmid pTUM4 could also raise the yield of a soluble, functional Fab fragment by a factor > 100 (Friedrich et al. 2010). To examine its influence on soluble FabZ production capability, *E. coli* BL21(DE3) Tn7::<FabZ> cells were transformed with the co-expression plasmid pTUM4. The resulting strains were analysed in shake flask experiments as described in 2.3.3.

Total soluble FabZ concentration was decreased from 3.9 mg/L to 1.5 mg/L (2.6-fold reduction) compared to the plasmid-free FabZ-producer strain. A decrease in total intracellular FabZ level of approximately 50 % was observed by pTUM4-mediated folding modulator co-synthesis using SDS-PAGE analysis. pTUM4-bearing cells reached an OD_{550} value of 9.8 at EoF while an OD_{550} value of 1.7 was determined for the plasmid-free FabZ-producing strain. Apparently, as seen in the system established in this work, also presence of pTUM4 prevented cell lysis until EoF.

In contrast to the above mentioned publications, presence of pTUM4 exerted a negative influence on soluble FabZ production analysed in this study. This fact proves the assumption that the success of folding modulator gene co-expression appears to be very target protein specific. Reduced total intracellular FabZ content in the presence of pTUM4 indicated a decrease in FabZ gene expression rates. This reduction in FabZ synthesis rates could be caused by competition of pTUM4-mediated folding modulator gene expression and the FabZ gene expression. Reduced production and thus secretion of FabZ potentially led to a lower amount of periplasmic FabZ aggregates. This reduction in periplasmic protein aggregates could prevent cell lysis and thus explain the positive effect of pTUM4 on OD_{550} values at EoF. In addition, the reduction in FabZ secretion would also be a explanation for the low total soluble FabZ yield. The negative effect of pTUM4 on total soluble FabZ yields might also be explained by the co-production of DsbC. As shown above, co-production of DsbC exerted a significant negative effect on total soluble FabZ yields. Furthermore, constitutive promoters driving gene expression on pTUM4 might be too strong and thus lead to high levels of DsbA, DsbC, FkpA and SurA. Simultaneous co-production of four folding modulators at once might exert an increased negative effect on FabZ synthesis. The co-expression system established in this work would be a better option to screen for an appropriate folding modulator type and its synthesis rate. If several folding modulator genes are combined on one co-expression plasmid it should be kept in mind that some periplasmic folding modulators could be redundant in their function. For example, a previous study showed functional redundancy in protein folding of the chaperone activity of the Skp and SurA pathway (Rizzitello et al. 2001).

Different Effects of Folding Modulators and Their Synthesis Rate on Soluble FabZ Production Were Demonstrated in Shake Flask Experiments. In conclusion, it was shown that under the applied cultivation conditions (200 mL reaction volume, 25 °C and 12 h of cultivation after induction with 1 mM IPTG) folding modulator type and synthesis rate affected soluble FabZ production differently. Co-expression of the PPIases *fkpA* and *surA* and of the generic chaperone *skp* influenced soluble periplasmic FabZ concentrations at EoF positively. On the other hand, co-synthesis of DsbA, DsbC and PpiD exerted no significant or had a negative effect on total soluble FabZ yields at EoF. Folding modulator type and synthesis rate also influenced OD_{550} values at EoF and thus cell lysis tendencies differently. DsbA, DsbC, FkpA, Skp and SurA exerted a positive effect on OD_{550} values at EoF. The beneficial effect on OD_{550} values at EoF was higher with increasing synthesis rates of these folding modulators. Apparently, co-production of these folding modulators could prevent cell lysis. On contrary, PpiD overproduction had no effect on OD_{550} values at EoF, independent of the applied synthesis rate. DsbA, FkpA and SurA co-production had an impact on overall FabZ production. Increasing expression rates of these folding modulator genes resulted in a significant decrease in intracellular FabZ levels. The ratio of intracellular FabZ and folding modulator was similar when the C8 and C2 promoter modules were employed. Overexpression of PpiD at different synthesis rates influenced the reduction of intracellular FabZ levels only to a minor extend.

The results of the shake flask experiments revealed the importance of testing all six periplasmic folding modulators at all three synthesis rates. By application of the developed co-expression system, a maximum increase in soluble FabZ concentration by a factor of 4.6 was observed with co-expression of *skp* controlled by the C2 promoter module. Selected plasmid strains were further employed in a 5 L fed-batch fermentation process which was developed in the course of another part of this project (Buettner 2016). In doing so, the selected strains can be analysed in realistic production conditions. All plasmid strains bearing Ci-promoter based co-expression plasmids were subjected to 5 L fed-batch fermentation experiments. In addition, folding modulators which exerted a positive effect on total soluble FabZ yields in shake flask experiments were analysed. Hence, FkpA, Skp and SurA were analysed at all three synthesis rates in the fed-batch fermentation experiments.

3.2.3. Positive Impact of Selected Co-expression Plasmids Could Not Be Shown in Fed-Batch Fermentation Process

Large-scale production of biopharmaceuticals is commonly conducted under controlled cultivation conditions in industrial fermentation processes (Walsh 2003). In a previous part of this project a fed-batch fermentation process for the production strain *E. coli* BL21(DE3) Tn7::<FabZ>, bearing the genome-integrated FabZ expression cassette, was developed (Buettner 2016). This fed-batch fermentation process should be applied as production process for FabZ and should enable a potential scale-up to industrial production scale. In these initial fermentation experiments large quantities of periplasmic FabZ aggregates but rather low levels of soluble FabZ were produced. To enhance soluble production of target proteins including FabZ, a co-expression system based on different periplasmic folding modulators (DsbA, DsbC, FkpA, PpiD, Skp and SurA) was established in this work. The co-expression system was applied in shake flask experiments and revealed promising results as total soluble FabZ yields were increased in this small-scale setup up to 4.6-fold (see Chapter 3.2.2). Here, it was analysed if the application of the co-expression system could also enhance soluble FabZ yields in the developed fed-batch fermentation process. Hence, the soluble FabZ production behaviour of co-expression plasmid-bearing strains was analysed in upscaled 5 L fed-batch fermentation experiments in accordance with the method described in 2.4. All fed-batch fermentation experiments were conducted in the course of the practical work of a PhD thesis. A more detailed description of the process can be found therein (Buettner 2016).

Briefly, fed-batch fermentations with a maximum volume of 5 L were carried out in stirred-bioreactors. The temperature was kept constant at 37 °C and the pH was maintained at 6.8. The dissolved oxygen level was adjusted to ≥20 % and an overpressure of 1000 mbar was applied. After cultivation of cells in semi-defined Preculture Medium, the preculture broth was used to inoculate a defined Batch Medium. After a batch phase, a glucose containing feed solution was added in an exponential feeding mode (calculated growth rate:

μ = 0.177/h). After 12 h of exponential feeding, a constant feed rate was employed for another 15 h maintaining the final feed rate of the exponential phase. In case of glucose accumulation (> 0.5 g/L), the feed rate was manually adjusted. FabZ production was fully induced 14 h after feed start by bolus addition of IPTG (1 mM referring to final volume). During the protein production phase, OD_{550}, dry cell weight (DCW) and glucose concentration was determined periodically. Cell samples and cell-free culture supernatant were prepared prior to and in regular intervals after IPTG addition. Intracellular, soluble FabZ concentrations and FabZ content of the cell-free culture supernatant were determined by ELISA analysis (2.5.2). Total soluble FabZ concentrations were obtained by addition of soluble FabZ content of both fractions at the corresponding point of time. Maximum total soluble FabZ concentration and DCW values determined during fermentation experiments were used to evaluate the expression strains. In the course of this study fermentation experiments were performed only once. In previous experiments maximum total soluble FabZ and DCW values were determined in replicated fed-batch fermentation experiments under similar cultivation conditions (Buettner 2016). The ranges between minimum and maximum values were calculated based on these biological replicate measurements. The calculated range (in %) was used to estimate the positive and negative error bars presented in this work. In the fed-batch fermentations FabZ production strains bearing co-expression plasmids without any folding modulator gene (w/o gene) and the plasmid-free strain (w/o plasmid) were used as references. All FabZ production strains bearing co-expression plasmids on which folding modulator gene expression is controlled by weak Ci promoter module were analysed in fed-batch fermentation experiments. Figure 3-16 depicts the maximum total soluble FabZ concentrations detected in these fermentation experiments. FkpA, Skp and SurA co-production exerted a positive effect on total soluble FabZ yields in shake flask experiments, independent of the synthesis rate (see Chapter 3.2.2 and Figure 3-11). Hence, co-production of these folding modulators was analysed in fed-batch fermentation experiments at all three synthesis rates. Figure 3-17 shows maximum total soluble FabZ concentrations and maximum DCW values of FkpA, Skp and SurA co-synthesis at all three levels in fed-batch fermentation experiments. Table 3-7 summarizes the results of fed-batch fermentation experiments for the production of FabZ.

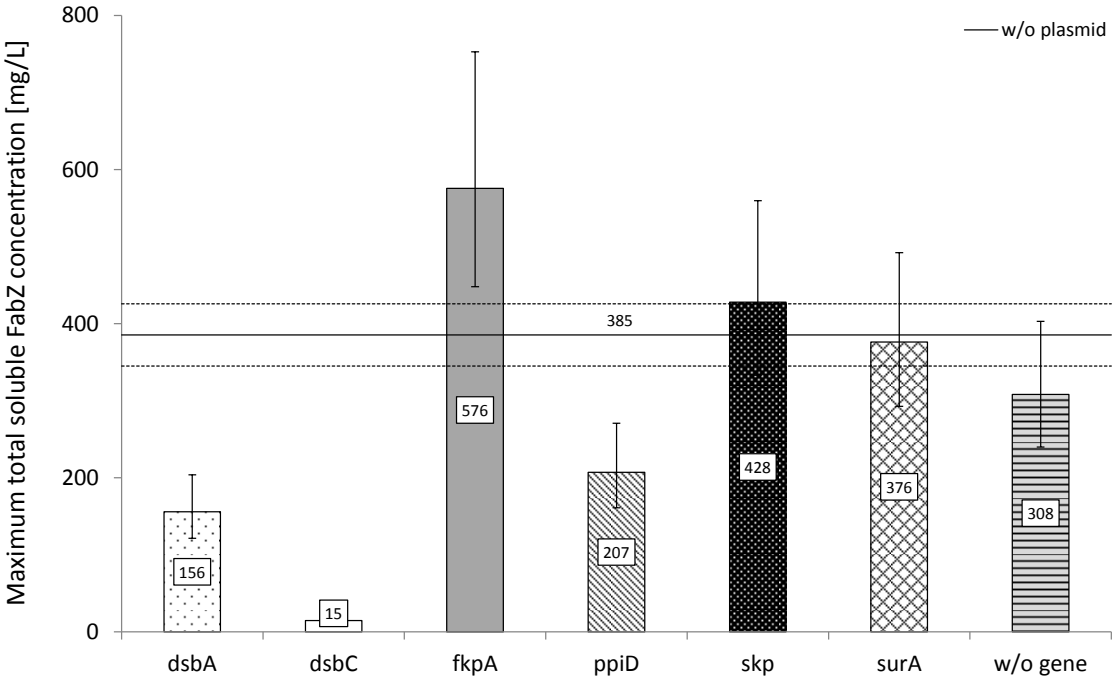

Figure 3-16: Influence of low level folding modulator co-production on soluble FabZ yields in fed-batch fermentation experiments. FabZ production strains bearing co-expression plasmids on which *dsbA*, *dsbC*, *fkpA*, *ppiD*, *skp* or *surA* expression is controlled by the weak Ci promoter module were employed in fed-batch fermentation experiments in accordance with the method described in 2.4. FabZ product concentrations were determined by ELISA analysis (see 2.5.2). Total soluble FabZ concentration was calculated by summing intracellular soluble FabZ content and FabZ concentration of the cell-free culture supernatant samples. The maximum total soluble FabZ concentration is presented in dependence of the respective co-produced folding modulator. Numbers within bars indicate maximum total soluble FabZ concentrations in mg/L. Error bars were calculated based on the range between minimum and maximum values of previously performed fed-batch fermentation experiments. w/o gene: FabZ production strain carrying the empty co-expression plasmid (pBI4iSCi.3). w/o plasmid: Plasmid-free FabZ production strain (BL21(DE3) Tn7::<FabZ>(ompA kanR pt7)). The mean total soluble FabZ concentration calculated from biological triplicate measurements of the plasmid-free FabZ production strain is indicated by the black line. Dashed lines indicate the corresponding standard deviation.

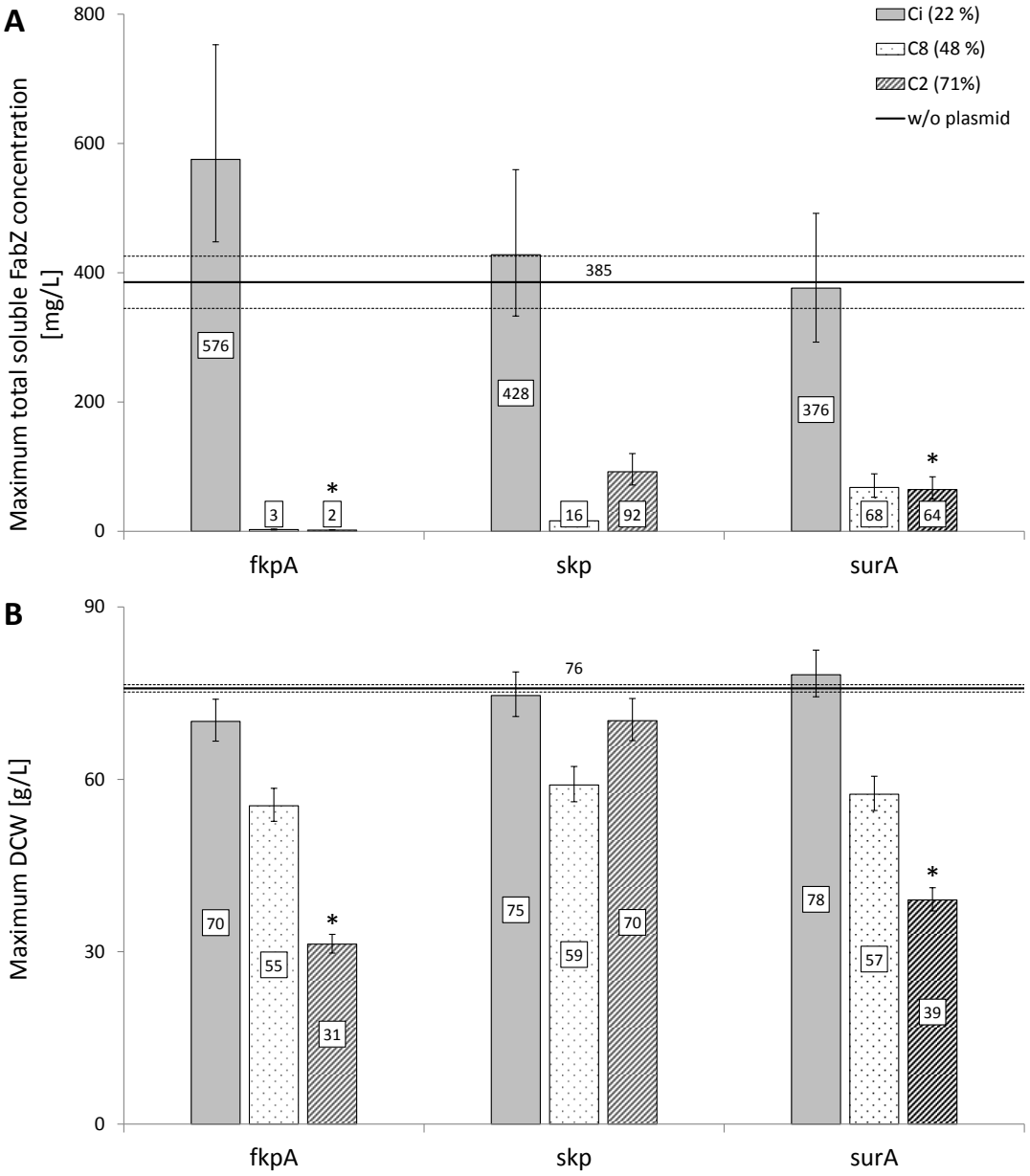

Figure 3-17: Influence of various levels of *fkpA*, *skp* and *surA* co-expression on soluble FabZ yields and DCW values in fed-batch fermentation experiments. FabZ production strains bearing co-expression plasmids on which *fkpA*, *skp* or *surA* expression is controlled by Ci, C8 and C2 promoter modules were employed in fed-batch fermentation experiments in accordance with the method described in 2.4. FabZ product concentrations were determined by ELISA analysis (see 2.5.2). Total soluble FabZ concentration was calculated by summing intracellular soluble FabZ content and FabZ concentration of the cell-free culture supernatant samples. The maximum total soluble FabZ concentration (A) or the maximum dry cell weight (DCW) values (B) are presented in dependence of the respective co-produced folding modulator. Different bar designs refer to the three different expression levels of the folding modulator genes mediated by the promoter modules Ci, C8 or C2 with a relative strength of 22, 48 and 71%, respectively. Numbers within bars indicate the maximum total soluble FabZ concentrations in mg/L (A) or maximum DCW values in g/L (B). Error bars of all values (FabZ concentration and DCW values) were calculated based on the range between minimum and maximum values of previously performed fed-batch fermentation experiments. w/o plasmid: Plasmid-free FabZ production strain (BL21(DE3) Tn7::<FabZ>(ompA kanR pt7)). Black lines indicate mean maximum total soluble FabZ concentration (A) and maximum DCW value (B) calculated from biological triplicate measurements of the FabZ production strain w/o plasmid. Dashed lines indicate corresponding standard deviation values. Asterisks indicate fed-batch fermentation experiments which were characterized by unplanned accumulation of glucose and in which manual adjustments of glucose feed rate were necessary.

Table 3-7: Maximum total soluble FabZ concentration and maximum DCW values in fed-batch fermentation experiments determined of strains co-producing FabZ and a folding modulator. DsbA, DsbC, FkpA, PpiD, Skp, SurA: Co-produced folding modulators. Ci, C8, C2: Constitutive promoter modules with a respective relative strength of 22, 48 and 71 % controlling the folding modulator gene expression. w/o gene: Empty co-expression plasmid lacking a folding modulator gene. Maximum total soluble FabZ concentration: Sum of soluble FabZ content of sedimented cell and FabZ concentration of cell-free culture supernatant samples determined by ELISA measurement (2.5.2). The maximum total soluble FabZ concentration determined during fermentation experiments is presented. Maximum dry cell weight (DCW) is presented in g/L. Asterisks indicate cultivations which were characterized by unplanned accumulation of glucose and where manual adjustment of the glucose feed rate was necessary. The FabZ production strain (BL21(DE3) Tn7::<FabZ>) w/o plasmid was used as a reference and yielded a maximum total soluble FabZ concentration of 385 mg/L and a maximum DCW value of 76 g/L.

Folding modulator	**Promoter module**	**Maximum Total soluble FabZ concentration [mg/L]**	**Maximum DCW values [g/L]**
w/o gene	Ci	308	75
	C8	296	75
	C2	-	-
DsbA	Ci	156	74
	C8	-	-
	C2	-	-
DsbC	Ci	15	83
	C8	-	-
	C2	-	-
FkpA	Ci	576	70
	C8	3	55
	C2	2*	31*
PpiD	Ci	207	69
	C8	-	-
	C2	-	-
Skp	Ci	428	75
	C8	16	59
	C2	92	70
SurA	Ci	376	78
	C8	68	57
	C2	64*	39*

A maximum total soluble FabZ concentration of 385 mg/L and a DCW value of 76 g/L were determined as mean values from biological triplicate fermentation experiments of the plasmid-free production strain BL21(DE3) Tn7::<FabZ>. Slightly lower FabZ concentrations of approximately 300 mg/L were determined for the reference strains carrying empty co-expression plasmids with either promoter modules Ci or C8. Also similar maximum DCW values were determined for the two reference strains w/o gene compared to the plasmid-free reference strain. Therefore, it can be concluded that the presence of empty co-

expression plasmids did not significantly interfere with FabZ gene expression in the fed-batch fermentation process. Similar as in shake flask experiments, the strength of the constitutive promoter modules present on the empty co-expression plasmids had no significant impact on soluble FabZ yields. By contrast, empty plasmids harbouring T7 promoter modules for co-expression of folding modulator genes, which were developed in a previous part of this project, influenced the FabZ production significantly (Buettner 2016). The influence exerted by this T7 promoter-based co-expression system was dependent on both, the T7 promoter strength and the scale of the experiment (shake flask or fed-batch fermentation experiment). The minimal effect on soluble FabZ production of empty co-expression plasmids based on constitutive promoter modules was rather independent of the applied production scale. Hence, the co-expression system developed in this work appears as a valuable tool to screen for appropriate folding modulators and their respective synthesis rate also in the fed-batch fermentation process.

Different effects on total soluble FabZ yields were exerted by Ci promoter module-controlled co-expression of *dsbA*, *dsbC*, *fkpA*, *ppiD*, *skp* and *surA* in fed-batch fermentation experiments. Weak *fkpA* overexpression had a significant positive influence on soluble FabZ production, yielding a maximum total soluble FabZ concentration of 576 mg/L. This was the highest maximum total soluble FabZ yield which was determined during all fed-batch fermentation experiments so far. The co-production of Skp and SurA seemed to have no significant impact on soluble FabZ production as similar soluble FabZ yields were obtained compared to the plasmid-free reference strain. The co-production of DsbA, DsbC and PpiD led to lowered soluble FabZ yields. While *dsbA* and *ppiD* co-expression resulted in an approximately 50 % reduction of soluble FabZ yields, co-production of DsbC had an even more pronounced negative effect on the FabZ production behaviour. Summarizing, similar tendencies for shake flask and fed-batch fermentation experiments were observed concerning the weak Ci-controlled overexpression of folding modulator genes. In both production scales co-expression of *fkpA* resulted in high total soluble FabZ yields. A slight increase in total soluble FabZ concentrations was determined for the co-production of Skp and SurA in shake flask experiments. The overproduction of these folding modulators exerted at least no negative effect on total soluble FabZ yields in fed-batch fermentation experiments. Compared to FkpA, Skp and SurA, the co-production of DsbA, DsbC and PpiD led to lower total soluble FabZ yields in both production scales. DsbC co-production had no significant effect on total soluble FabZ yields in shake flask experiments. However, the overexpression of this folding modulator exerted a highly negative effect on the FabZ production behaviour in the fermentation process.

Increased expression levels of *fkpA*, *skp* and *surA* obtained by control with C8 and C2 promoter modules exerted a negative influence on soluble FabZ production in fed-batch fermentation experiments (see Figure 3-17). With the exception of C2-controlled *skp* co-expression, increasing cellular levels of FkpA, Skp and SurA had also a negative impact on maximum DCW values. Accumulation of glucose was observed during the fed-batch

fermentations of FkpA and SurA co-producing strains employing the C2 promoter module. Under such glucose excess conditions, the FabZ production potential of these strains might be severely impaired. This might be the cause why the positive effect of increasing synthesis rates of FkpA, Skp and SurA observed in shake flask experiments could not be shown in the fed-batch fermentation processes. Soluble FabZ production in fed-batch fermentation experiments might also be disturbed by too high intracellular levels of the respective folding modulator. The higher production temperature of 37 °C in the fed-batch fermentation process might be a potential trigger which increased the expression levels of the folding modulator genes. An increased level of folding modulators might further raise the metabolic burden for the cell which might result in cell lysis. Some cell lysis effects were already observed during pre-culture incubation at 37 °C when *fkpA* expression was controlled by either the C8 or the C2 promoter module. Hence, the production temperature of 37 °C might exert a negative effect on some co-expression plasmid-bearing strains.

In conclusion, the positive influence of folding modulator co-production on soluble FabZ formation observed in shake flask experiments could not be reproduced in the fed-batch fermentation process. However, a similar trend for both scales was observed for soluble FabZ yield during co-production of folding modulator genes controlled by the weak Ci promoter module in both production scales. Contrary to the shake flask results, increased synthesis rates of FkpA, Skp and SurA exerted a negative influence on total soluble FabZ yields in fed-batch fermentation experiments. Hence, the shake flask screening system should be optimized to better predict the behaviour in the defined fed-batch fermentation process. On the basis of a new screening system it should be possible to predict the FabZ production behaviour of co-expression plasmid-bearing strains in the fed-batch fermentation processes.

4. Conclusion

In this work a co-expression system for different periplasmic folding modulator genes should be established which can be used to improve the soluble production of recombinant target proteins in the periplasm of *E. coli*. The system should enable a quick screening for appropriate folding modulators and their co-production levels to improve production of different target proteins. In this work it was specially focussed on improving the soluble productivity of the model protein FabZ, which is an antibody fragment containing five disulfide bonds. In a previous part of the project the periplasmic folding machinery was identified as the main bottleneck in soluble production of FabZ (Buettner 2016). Increased levels of molecular elements of the periplasmic folding machinery have frequently been reviewed to exert positive effects on soluble target protein production (Kolaj et al. 2009; François Baneyx & Mujacic 2004; A. DeMarco 2009). Increased soluble product yields due to folding modulator co-synthesis have also been demonstrated for Fab fragments in particular (Levy et al. 2001; Lin et al. 2008). However, the success of co-expression approaches appears to be depended on the target protein (A. DeMarco & V. DeMarco 2004; Schaefer & Andreas Plückthun 2010). This means that a trial-and-error approach is required to identify folding modulators which can improve soluble production of a target protein (Martínez-Alonso et al. 2010; Overton 2014). In this study a system for the individual co-production of the periplasmic folding modulators DsbA, DsbC, FkpA, PpiD, Skp and SurA at different co-production levels should be established.

A Co-Expression System Enabling Screening of Six Different Periplasmic Folding Modulators at Three Different Levels Was Established. Nine different constitutive promoter sequences providing different transcription rates were obtained from two synthetic promoter collections (Anderson 2006; Davis et al. 2010). The promoters are based on the consensus sequence of a σ^{70} promoter and are thus recognized by the major *E. coli* σ factor. In order to achieve independence of promoter strength and its genetic context, 3' and 5' insulation sequences flanking the core promoter region were added. After some optimization steps, the basic plasmid for co-expression of folding modulator genes was obtained consisting of a streptomycin resistance cassette, a p15A origin of replication (*ori*) and the tZenit terminator (Witwer 2010) for transcription termination. The presence of this basic vector system seemed to exert a reduced negative effect on *E. coli* cells during creation of co-expression plasmids. Since also a plasmid stability of 100 % was shown for the vector backbone, it was identified to be suitable as basis for the co-expression vectors. After several plasmid cloning attempts and promoter tests, only the weakest insulated promoter (Ci) was identified to have an appropriate promoter strength for the co-expression of folding modulator genes. Expression levels of all other insulated promoter modules were too high and exerted a negative effect on cell growth. After removal of the insulation sequence and replacement of the RBS, synthesis rates of the respective new promoter modules were significantly decreased. The two weakest modules of these Second Generation promoters (C8 and C2)

were successfully used for the generation of folding modulator gene co-expression plasmids. A promoter test revealed significantly different synthesis rates for the promoter modules Ci, C8 and C2. Hence, a co-expression system based on these three promoter modules should facilitate a fine-tuned expression of folding modulator genes.

Application of the New Co-Expression System Revealed Favourable Combinations of Folding Modulators and Synthesis Rates in Shake Flask and Fermentation Experiments. The newly developed co-expression system based on three constitutive promoter modules of different strength and six different periplasmic folding modulator genes was employed in FabZ production experiments. Experiments were conducted in shake flasks and under production process conditions using a fed-batch fermentation process. As opposed to the T7 co-expression systems which were applied previously in this project (Schuller 2015; Buettner 2016), the new co-expression system did not interfere with target gene expression. Increased levels of DsbA, DsbC and PpiD showed no significant effect on soluble FabZ production in shake flask experiments, independent of the synthesis rate. On the other hand, co-production of the PPIases FkpA and SurA and of the generic chaperone Skp exerted a positive influence on total soluble FabZ yields. A positive effect of co-production of these folding modulators was seen for all applied synthesis rates. A maximum increase in soluble FabZ concentration (4.6-fold) in shake flask experiments was observed when co-expression of *skp* was controlled by the C2 promoter module. The most promising folding modulators and their respective co-production levels were further verified in fed-batch fermentation experiments. Under these process conditions many co-expression attempts had no positive influence on total soluble FabZ yields. Contrary to shake flask experiments, higher synthesis rates in case of FkpA, Skp and SurA exerted a negative influence on total soluble FabZ yields in the fed-batch fermentations. However, Ci promoter module-mediated expression of *fkpA* increased the maximum total soluble FabZ yields 1.5-fold in the fermentation experiments.

The new co-expression system based on constitutive promoters exhibits a significantly improved behaviour compared to previous T7 promoter-based systems, as it did not interfere with target gene expression. Hence, this constitutive promoter-based plasmid system is suitable to control the expression of folding modulator genes. As the level of the folding modulator gene co-expression needs to be optimized for each target protein, fine-tuned co-expression of different folding modulator genes is required. With the newly developed co-expression system the effect of six periplasmic folding modulators at three levels on soluble target protein production can quickly be estimated. Application of the new co-expression system in two production scales revealed that the results of the applied shake flask approach are not predictive for the outcome of the fermentation process. Hence, further studies are planned to establish an optimized small-scale system with higher predictive power. In addition, the co-expression system established in this work will further be tested with other target proteins. Moreover, the positive effect of Ci-controlled *fkpA* co-expression in fermentation experiments will be verified in other process set-ups to identify even better suited process conditions.

5. References

Addgene, 2014. Plasmid modification by annealed oligo cloning.

Ahmad, Z.A. et al., 2012. scFvantibody: Principles and clinical application. *Clinical and Developmental Immunology*, pp.1-16.

Alanen, H.I. et al., 2015. Efficient export of human growth hormone, interferon α2b and antibody fragments to the periplasm by the *Escherichia coli* Tat pathway in the absence of prior disulfide bond formation. *Biochimica et Biophysica Acta*, 1853, pp.756-763.

Alper, H. et al., 2005. Tuning genetic control through promoter engineering. *Proc. Natl. Acad. Sci.*, 102, pp.1-8.

Anderson, J.C., 2006. Promoters Catalog Anderson. *Registry of Standard Biological Parts*. Available at: http://parts.igem.org/Promoters/Catalog/Anderson.

Antonoaea, R. et al., 2008. The Periplasmic Chaperone PpiD Interacts with Secretory Proteins Exiting from the SecYEG Translocon. *Biochemistry*, 47(20), pp.5649-5656.

Arié, J.P., Sassoon, N. & Betton, J.M., 2001. Chaperone function of FkpA, a heat shock prolyl isomerase, in the periplasm of *Escherichia coli*. *Molecular Microbiology*, 39, pp.199-210.

Baneyx, François & Mujacic, M., 2004. Recombinant protein folding and misfolding in *Escherichia coli*. *Nature Biotechnology*, 22(11), pp.1399-1408.

Barrett, C.M. et al., 2003. Quantitative export of a reported protein, GFP, by the twin-arginine translocation pathway in *Escherichia coli*. *Biochem Biophys Res Commun*, 304, pp.279-284.

Behrens, S. et al., 2001. The SurA periplasmic PPIase lacking its parvulin domains functions *in vivo* and has chaperone activity. *The EMBO Journal*, 20, pp.285-294.

Bentley, W.E. et al., 1990. Plasmid-encoded protein: The principal factor in the “metabolic burden” associated with recombinant bacteria. *Biotechnology and Bioengineering*, 35(7), pp.668-681.

Bird, R.E. et al., 1988. Single-Chain Antigen-Binding Proteins. *Science*, 242, pp.423-426.

Bitto, E. & McKay, D.B., 2003. The periplasmic molecular chaperone protein SurA binds a peptide motif that is characteristic of integral outer membrane proteins. *Journal of Biological Chemistry*, 278, pp.49316-49322.

Bogsch, E.G. et al., 1998. An Essential Component of a Novel Bacterial Protein Export System with Homologues in Plastids and Mitochondria. *Journal of Biological Chemistry*, 273(29), pp.18003-18006.

Bothmann, H. & Plückthun, A., 1998. Selection for a periplasmic factor improving phage display and functional periplasmic expression. *Nature Biotechnology*, 16, pp.376-380.

Bothmann, H. & Plückthun, A., 2000. The Periplasmic *Escherichia coli* Peptidylprolyl *cis,trans*-Isomerase FkpA. *Journal of Biological Chemistry*, 275(22), pp.17100-17105.

Brewster, R.C., Jones, D.L. & Phillips, R., 2012. Tuning Promoter Strength through RNA Polymerase Binding Site Design in *Escherichia coli*. *PLoS Computational Biology*, 8(12), pp.1-10.

Buettner, A., 2016. *Genetic Strategies to Improve Folding and Secretion of Recombinant Proteins in Escherichia coli*, Technical University of Munich.

Burgess, R.R. et al., 1969. Factor stimulating transcription by RNA polymerase. *Nature*, 221, pp.43-46.

Chen, H., Lin, M. & Hou, S., 2008. Multiple-copy-gene integration on chromosome of *Escherichia coli* for beta-galactosidase production. *Korean J. Chem. Eng.*, 25, pp.1082-1087.

Chou, C.P. et al., 1999. Effect of SecB chaperone on production of periplasmic penicillin acylase in *Escherichia coli*. *Biotechnol. Prog.*, 15, pp.439-445.

Cormack, B.P., Valdivia, R.H. & Falkow, S., 1996. FACS-optimized mutants of the green fluorescent protein (GFP). *Gene*, 173, pp.33-38.

Datta, S., Costantino, N. & Court, D.L., 2006. A set of recombineering plasmids for gram-negative bacteria. *Gene*, (379), pp.109-115.

Davis, J.H., Rubin, A.J. & Sauer, R.T., 2010. Design, construction and characterization of a set of insulated bacterial promoters. *Nucleic Acids Research*, 39, pp.1131-1141.

DeLeeuw, E. et al., 2002. Oligomeric Properties and Signal Peptide Binding by *Escherichia coli* Tat Protein Transport Complexes. *Journal of Molecular Biology*, 322, pp.1135-1146.

DeLisa, M.P. et al., 2004. Phage Shock Protein PspA of *Escherichia coli* Relieves Saturation of Protein Export via the Tat Pathway. *Journal of Bacteriology*, 186, pp.366-373.

DeMarco, A., 2011. Biotechnological applications of recombinant single-domain antibody fragments. *Microbial Cell Factories*, 10, pp.1-14.

DeMarco, A., 2013. Recombinant polypeptide production in *E. coli*: towards a rational approach to improve the yields of functional proteins. *Microbial Cell Factories*, 12, pp.1-8.

DeMarco, A., 2009. Strategies for successful recombinant expression of disulfide bond-dependent proteins in Escherichia coli. *Microbial Cell Factories*, 8(1), p.26.

DeMarco, A. & DeMarco, V., 2004. Bacteria co-transformed with recombinant proteins and chaperones cloned in independent plasmids are suitable for expression tuning. *Journal of Biotechnology*, 109, pp.45-52.

DeMey, M. et al., 2007. Construction and model-based analysis of a promoter library for *E. coli*: an indispensable tool for metabolic engineering. *BMC Biotechnology*, 7, pp.1-14.

DelSolar, G. & Espinosa, M., 2000. Plasmid copy number control: an ever-growing story. *Molecular Microbiology*, 37(3), pp.492-500.

DeSmit, M.H. & van Duin, J., 1994. Control of Translation by mRNA Secondary Structure in *Escherichia coli*. *J. Mol. Biol.*, 244, pp.144-150.

Dombroski, A.J. et al., 1992. Polypeptides containing highly conserved regions of transcription initiation factor sigma 70 exhibit specificity of binding to promoter DNA. *Cell*, 70, pp.501-512.

Driessen, A.J., Fekkes, P. & van der Wolk, J.P., 1998. The Sec system. *Curr Opin Microbiol*, 1, pp.216-222.

Driessen, A.J.M. & Nouwen, N., 2008. Protein Translocation Across the Bacterial Cytoplasmic Membrane. *Annual Review of Biochemistry*, 77(1), pp.643-667.

Economou, A., 1999. Following the leader: bacterial protein export through the Sec pathway. *Trends in Microbiology*, 7, pp.315-320.

Einhorn, L., 2013. *Specific Determination of Hinge Disulfide Connectivity Region of Recombinant Human Fabs by the Development of a generic Homogeneous Time-Resolved Fluorescence (HTRF) Immuno Assay*, University of Natural Resources and Life Sciences Vienna.

Elgert, K.D., 2009. Immunology. In *Understanding the Immune System*. Antibody Structure and Function, pp. 58 - 78.

Entzminger, K.C. et al., 2012. The Skp Chaperone Helps Fold Soluble Proteins *in Vitro* by InhibitingAggregation. *Biochemistry*, (51), pp.4822-4834.

Estrem, S.T. et al., 1999. Bacterial promoter architecture: subsite structure of UP elements and interactions with the carboxy-terminal domain of the RNA polymerase alpha subunit. *Genes Dev*, 13, pp.2134-2147.

FDA, 1982. Human insulin receives FDA approval. *FDA Drug Bull*, 3, pp.18-19.

Feldman, D.E. & Frydman, J., 2000. Protein folding *in vivo*: the importance of molecular chaperones. *Current Opinion in Structural Biology*, 10, pp.26-33.

Ferrer-Miralles, N. et al., 2009. Microbial factories for recombinant pharmaceuticals. *Microbial Cell Factories*, 8(1), p.17.

Frenzel, A., Hust, M. & Schirrmann, T., 2013. Expression of recombinant antibodies. *Frontiers in Immunology*, 4, pp.1-20.

Friedrich, L. et al., 2010. Bacterial production and functional characterization of the Fab fragment of the murine IgG1/λ monoclonal antibody cmHsp70.1, a reagent for tumour diagnostics. *Protein Engineering, Design & Selection*, 23(4), pp.161-168.

Friehs, K., 2004. Plasmid Copy Number and Plasmid Stability. *Advances in Biochemical Engineering*, 86, pp.47-82.

García-Ortega, L. et al., 2000. The solubility of the ribotoxin α-sarcin, produced as arecombinant protein in*Escherichia coli*, is increased in the presence of thioredoxin. *Letters in Applied Microbiology*, 30, pp.298-302.

Giacomelli, G. & Depetris, A., 2012. Part:BBa_K731721. *Registry of Standard Biological Parts*. Available at: http://parts.igem.org/Part:BBa_K731721?title=Part:BBa_K731721.

Graumann, K. & Premstaller, A., 2006. Manufacturing of recombinant therapeutic proteins in microbial systems. *Biotechnology Journal*, 1, pp.164-186.

Gross, C.A. et al., 1998. The Functional and Regulatory Roles of Sigma Factors in Transcription. *Cold Spring Harbor Symposia on Quantitative Biology*, 63, pp.141-155.

Gunnarsen, K.S. et al., 2010. Periplasmic expression of soluble single chain T cell receptors is rescued by the chaperone FkpA. *BMC Biotechnology*, 10.

Göthel, S.F. & Marahiel, M.A., 1999. Peptidyl-prolyl cis-trans isomerases, a superfamily of ubiquitous folding catalysts. *Cellular and Molecular Life Sciences*, (55), pp.423-436.

Hammer, K., Mijakovic, I. & Jensen, P.R., 2006. Synthetic promoter libraries - tuning of gene expression. *Trends in Biotechnology*, 24, pp.1-3.

Harley, C.B. & Reynolds, R.P., 1987. Analysis of *E. coli* promoter sequences. *Nucleic Acids Research*, 15, pp.2343-2361.

Harrison, J.S. & Keshavarz-Moore, E., 1996. Production of Antibody Fragments in *Escherichia coli*. *Annals of the New York Academy of Sciences*, 782(1), pp.143-158.

Hayhurst, A. & Harris, W.J., 1999. *Escherichia coli* Skp Chaperone Coexpression Improves Solubility and Phage Display of Single-Chain Antibody Fragments. *Protein Expression and Purification*, 15(3), pp.336-343.

Hiniker, A. & Bardwell, J.C.A., 2003. Disulfide Bond Isomerization in Prokaryotes. *Biochemistry*, 42, pp.1179-1185.

Hoffmann, F. & Rinas, U., 2004. Stress Induced by Recombinant Protein Production in *Escherichia coli*. *Advances in Biochemical Engineering*, 89, pp.73-92.

Holliger, P. & Hudson, P.J., 2005. Engineered Antibody Fragments and the Rise of Single Domains. *Nature Biotechnology*, 23, pp.1126-1136.

Holt, L.J. et al., 2008. Anti-Serum Albumin Domain Antibodies for Extending the Half-Lives of Short Lived Drugs. *Protein Engineering, Design & Selection*, 21(5), pp.283-288.

Huang, C., Lin, H. & Yang, X., 2012. Industrial production of recombinant therapeutics in *Escherichia coli* and its recent advancements. *Journal of Industrial Microbiology & Biotechnology*, 39(3), pp.383-399.

Invitrogen, 2006. Subcloning Efficiency DH5α Competent Cells., pp.1-4.

Iserentant, D. & Fiers, W., 1980. Secondary structure of mRNA and efficiency of translation initiation. *Gene*, 9, pp.1-12.

Itakura, K. et al., 1977. Expression In *Escherichia Coli* of aChemically Synthesized Gene For The Hormone Somatostatin. *Science*, 198, pp.1056-1063.

Jain, A. & Jain, S.K., 2008. PEGylation: an approach for drug delivery. A review. *Crit Rev Ther Drug Carrier Syst*, (25), pp.403-447.

Jander, G., Martin, N.L. & Beckwith, J., 1994. Two cysteines in each periplasmic domain of the membrane protein DsbB are required for its function in protein disulfide bond formation. *The EMBO Journal*, 13, pp.5121-5127.

Janeway, C., Travers, P. & Walport, M., 2001. *Immunobiology* 5 ed., Garland Science.

Jensen, P.R. & Hammer, K., 1998. The Sequence of Spacers between the Consensus Sequences Modulates the Strength of Prokaryotic Promoters. *Applied and Environmental Microbiology*, 64, pp.82-87.

Jeong, K.J., Jang, S.H. & Velmurugan, N., 2011. Recombinant antibodies: Engineering and production in yeast and bacterial hosts. *Biotechnology Journal*, 6(1), pp.16-27.

Joly, J.C. & Swartz, J.R., 1997. *In Vitro* and *in Vivo* Redox States of the *Escherichia coli* Periplasmic Oxidoreductases DsbA and DsbC. *Biochemistry*, 36, pp.10067-10072.

Kadokura, H. et al., 2004. Snapshots of DsbA in Action: Detection of Proteins in the Process of Oxidative Folding. *Science*, 303, pp.534-537.

Kamionka, M., 2011. Engineering of Therapeutic Proteins Production in *Escherichia coli*. *Current Pharmaceutical Biotechnology*, 12, pp.268-274.

Kelly, J.R. et al., 2009. Measuring the activity of BioBrick promoters using an *in vivo* reference standard. *Journal of Biological Engineering*, 3, pp.1-13.

Kleerebezem, M., Heutink, M. & Tommassen, J., 1995. Characterization of an *Escherichia coli rotA* mutant, affected in periplasmic peptidyl-prolyl *cis/trans* isomerase. *Molecular Microbiology*, 18, pp.313-320.

Kolaj, O. et al., 2009. Use of folding modulators to improve heterologous protein production in *Escherichia coli*. *Microbial Cell Factories*, 8(9), pp.1-17.

Larson, S.M. et al., 1983. Localization of ^{131}I-Labeled p97-Specific Fab Fragments in Human Melanoma as a Basis for Radiotherapy. *The Journal of Clinical Investigation*, 72, pp.2101-2114.

Lebendiker, M. & Danieli, T., 2014. Production of prone-to-aggregate proteins. *FEBS Letters*, 588, pp.236-246.

Lee, G.H. et al., 2006. The economics of inclusion body processing. *Bioprocess Biosyst Eng*, 29, pp.73-90.

Levy, R. et al., 2001. Production of Correctly Folded Fab Antibody Fragment inthe Cytoplasm of *Escherichia coli trxB gor* Mutants viathe Coexpression of Molecular Chaperones. *Protein Expression and Purification*, 23, pp.338-347.

LifeTechnologies, 2010. The Molecular Probes Handbook. In *A GUIDE TO FLUORESCENT PROBES AND LABELING TECHNOLOGIES*. Antibodies, Avidins and Lectins, pp. 241-298.

Lin, B. et al., 2008. A step-wise approach significantly enhances protein yield of a rationally-designed agonist antibody fragment in *E. coli*. *Protein Expression and Purification*, 59(1), pp.55-63.

Macdonald, L.E. et al., 1994. Characterization of two types of termination signal for bacteriophage T7 RNA polymerase. *J. Mol. Biol.*, 238, pp.145-158.

Mairhofer, J. et al., 2013. Comparative Transcription Profiling and In-Depth Characterization of Plasmid-Based and Plasmid-Free *Escherichia coli* Expression Systems under Production Conditions. *Applied and Environmental Microbiology*, 79(12), pp.3802-3812.

Mairhofer, J. et al., 2014. Preventing T7 RNA Polymerase Read-through Transcription-A Synthetic Termination Signal Capable of Improving Bioprocess Stability. *ACS Synthetic Biology*, 4, pp.265-273.

Marston, F.A., 1986. The purification of eukaryotic polypeptides synthesized in *Escherichia coli*. *Biochem. J.*, 240, pp.1-12.

Martínez-Alonso, M. et al., 2010. Side effects of chaperone gene co-expression in recombinant protein production. *Microbial Cell Factories*, 9, pp.4-6.

Mendoza-Vargas, A. et al., 2009. Genome-Wide Identification of Transcription Start Sites, Promoters and Transcription Factor Binding Sites in *E. coli*. *PLoS ONE*, 4(10), pp.1-19.

Mergulhao, F.J.M., Summers, D.K. & Monteiro, G.A., 2005. Recombinant protein secretion in *Escherichia coli*. *Biotechnology Advances*, 23, pp.177-202.

Missiakas, D., Betton, J. & Raina, S., 1996. New components of protein folding in extracytoplasmic compartments of *Escherichia coli* SurA, FkpA and Skp/OmpH. *Molecular Microbiology*, 21(4), pp.871-884.

Nagai, K. et al., 2003. Structure, function and evolution of the signal recognition particle. *The EMBO Journal*, 22, pp.3479-3485.

Nelson, A.L. & Reichert, J.M., 2009. Development trends for therapeutic antibody fragments. *Nature Biotechnology*, 27, pp.331-337.

Nossal, N.G. & Heppel, L.A., 1966. The release of enzymes by osmotic shock *from Escherichia coli* in exponential phase. *The Journal of Biological Chemistry*, 241, pp.3055-3062.

Otto, R., Santagostino, A. & Schrader, U., 2014. Rapid growth in biopharma: Challenges and opportunities. *McKinsey & Company*. Available at: http://www.mckinsey.com/insights/health_systems_and_services/rapid_growth_in_biopharma.

Overton, T.W., 2014. Recombinant protein production in bacterial hosts. *Drug Discovery Today*, 19, pp.590-601.

Pan, S.H. & Malcolm, B.A., 2000. Reduced background expression and improved plasmid stability with pET vectors in BL21 (DE3). *Biotechniques*, 29, pp.1234-1238.

Patzelt, H. et al., 2001. Binding specificity of *Escherichia coli* trigger factor. *Proc. Natl. Acad. Sci.*, 98, pp.14244-14249.

Pliyev, B.K. & Gurvits, B.Y., 1999. Peptidyl-prolyl *cis-trans* isomerases: structure and functions. *Biochemistry (Mosc.)*, 64, pp.738-751.

Rietsch, A. et al., 1997. Reduction of the Periplasmic Disulfide Bond Isomerase, DsbC, Occurs by Passage of Electrons from Cytoplasmic Thioredoxin. *Journal of Bacteriology*, 179, pp.6602-6608.

Rizzitello, A.E., Harper, J.R. & Silhavy, T.J., 2001. Genetic Evidence for Parallel Pathways of Chaperone Activity in the Periplasm of *Escherichia coli*. *Journal of Bacteriology*, 183, pp.6794-6800.

Roberts, T.M., Kacich, R. & Ptashne, M., 1979. A general method for maximizing the expression of a cloned gene. *Proc. Natl. Acad. Sci.*, 76, pp.760-764.

Rosano, G.L. & Ceccarelli, E.A., 2014. Recombinant protein expression in *Escherichia coli*: advances and challenges. *Frontiers in Microbiology*, 5, pp.1-17.

Ross, W., Ernst, A. & Gourse, R.L., 2001. Fine structure of *E. coli* RNA polymerase-promoter interactions: alpha subunit binding to the UP element minor groove. *Genes Dev*, 15, pp.491-506.

Sahdev, S., Khattar, S.K. & Saini, K.S., 2008. Production of active eukaryotic proteins through bacterial expression systems: a review of the existing biotechnology strategies. *Molecular and Cellular Biochemistry*, 307, pp.249-264.

Salis, H.M., Mirsky, E.A. & Voigt, C.A., 2009. Automated design of synthetic ribosome binding sites to control protein expression. *Nature Biotechnology*, 27, pp.946-950.

Samuelson, J., 2011. Expression Systems. In *Production of Membrane Proteins: Strategies for Expression and Isolation*. Wiley-VCH Verlag GmbH & Co. KGaA, pp. 11-36.

Sandee, D. et al., 2005. Combination of Dsb coexpression and an addition of sorbitol markedly enhanced soluble expression of single-chain Fv in *Escherichia coli*. *Biotechnology and Bioengineering*, 91, pp.418-424.

Sanz, L. et al., 2005. Antibody engineering: facing new challenges in cancer therapy. *Acta Pharmacologica Sinica*, 26(6), pp.641-648.

Schaefer, J.V. & Plückthun, Andreas, 2010. *Improving Expression of scFv Fragments by Co-expression of Periplasmic Chaperones*, Antibody Engineering.

Schein, C.H. & Noteborn, M.H.M., 1988. Formation of Soluble Recombinant Proteins in *Escherichia Coli* is Favored by Lower Growth Temperature. *Nature Biotechnology*, 6, pp.291-294.

Schlapschy, M., Grimm, S. & Skerra, A., 2006. A system for concomitant overexpression of four periplasmic folding catalysts to improve secretory protein production in *Escherichia coli*. *Protein Engineering, Design & Selection*, 19, pp.385-390.

Schlegel, S. et al., 2013. Optimizing heterologous protein production in the periplasm of *E. coli* by regulating gene expression levels. *Microbial Cell Factories*, 12, p.24.

Schuller, A., 2015. *Improving Soluble Periplasmic Fab Production in Escherichia coli by Fine-tuned Folding-Modulator Co-Production*, Universität für Bodenkultur.

Schäfer, U., Beck, K. & Müller, M., 1999. Skp, a Molecular Chaperone of Gram-negative Bacteria, Is Required for the Formation of Soluble Periplasmic Intermediates of Outer Membrane Proteins. *Journal of Biological Chemistry*, 274(35), pp.24567-24574.

Sekhon, B.S., 2010. Biopharmaceuticals: an overview. *The Thai Journal of Pharmaceutical Sciences*, 34, pp.1-19.

Selzer, G. et al., 1983. The Origin of Replication of Plasmid p15A and Comparative Studies on the Nucleotide Sequences around the Origin of Related Plasmids. *Cell*, 32, pp.119-129.

Sharan, S.K. et al., 2009. Recombineering: a homologous recombination-based method of genetic engineering. *Nature Protocols*, 4, pp.206-223.

Simmons, L.C. & Yansura, D.G., 1996. Translational level is a critical factor for the secretion of heterologous proteins in Escherichia coli. *Nature Biotechnology*, 14, pp.629-634.

Singh, S.M. & Panda, A.K., 2005. Solubilization and Refolding of Bacterial Inclusion Body Proteins. *Journal of Bioscience and Bioengineering*, 99, pp.303-310.

Snyder, L. et al., 2010. *Molecular Genetics of Bacteria* 4 ed., Bacterial Cell Biology and Development.

Sousa, R., Patra, D. & Lafer, E.M., 1992. Model for the mechanism of bacteriophage T7 RNAP transcription initiation and termination. *Journal of Molecular Biology*, 224(2), pp.319-334.

Spadiut, O. et al., 2014. Microbials for the production of monoclonal antibodies and antibody fragments. *Trends in Biotechnology*, 32, pp.54-60.

Stewart, E.J., Åslund, F. & Beckwith, J., 1998. Disulfide bond formation in the *Escherichia coli*cytoplasm: an *in vivo* role reversal for thethioredoxins. *The EMBO Journal*, 17, pp.5543-5550.

Striedner, G. et al., 2010. Plasmid-free T7-based *Escherichia coli* expression systems. *Biotechnology and Bioengineering*, 105, pp.786-794.

Studier, F.W., 1991. Use of bacteriophage T7 lysozyme to improve an inducible T7 expression system. *Journal of Molecular Biology*, 219(1), pp.37-44.

Summers, D.K. & Sherratt, D.J., 1988. Resolution of ColE 1 dimers requires a DNA sequence implicated in the three-dimensional organization of the *cer* site. *The EMBO Journal*, 7, pp.851-858.

Swamy, K.H.S. & Goldberg, A.L., 1982. Subcellular distribution of various proteases in *Escherichia coli*. *Journal of Bacteriology*, 149, pp.1027-1033.

Sørensen, H.P. & Mortensen, K.K., 2005. Soluble expression of recombinant proteins in the cytoplasm of *Escherichia coli*. *Microbial Cell Factories*, 4, pp.1-8.

Talmadge, K. & Gilbert, W., 1982. Cellular location affects protein stability in *Escherichia coli. Proc. Natl. Acad. Sci.*, 79, pp.1830-1833.

Telesnitsky, A.P. & Chamberlin, M.J., 1989. Sequences linked to prokaryotic promoters can affect the efficiency of downstream termination sites. *J. Mol. Biol.*, 205, pp.315-330.

Vasina, J.A. & Baneyx, F., 1997. Expression of aggregation-prone recombinant proteins at low temperatures: a comparative study of the *Escherichia colicspA* and *tac* promoter systems. *Protein Expr. Purif.*, 9, pp.211-218.

Vera, A. et al., 2007. The conformational quality of insoluble recombinant proteins is enhanced at low growth temperatures. *Biotechnology and Bioengineering*, 96(6), pp.1101-1106.

Vertommen, D. et al., 2008. The disulfide isomerase DsbC cooperates with the oxidase DsbA in a DsbD-independent manner. *Molecular Microbiology*, 67, pp.336-349.

Villaverde, A. & Carrió, M.M., 2003. Protein aggregation in recombinant bacteria: biological role of inclusion bodies. *Biotechnology Letters*, 25, pp.1385-1395.

Voskuil, M.I., Voepel, K. & Chambliss, G.H., 1995. The -16 region, a vial sequence for the utilization of a promoter in *Bacillus subtilis* and *Escherichia coli*. *Molecular Microbiology*, 17(2), pp.271-279.

Walsh, G., 2010. Biopharmaceutical benchmarks 2010. *Nature Biotechnology*, 28, pp.917-926.

Walsh, G., 2014. Biopharmaceutical benchmarks 2014. *Nature Biotechnology*, 32, pp.992-1002.

Walsh, G., 2003. *Biopharmaceuticals* 2nd ed., John Wiley & Sons.

Walton, T.A. & Sousa, M.C., 2004. Crystal Structure of Skp, a Prefoldin-like Chaperone that Protects Soluble and Membrane Proteins from Aggregation. *Molecular Cell*, 15, pp.367-374.

Warsaw, 2010. RBS measurement. *Registry of Standard Biological Parts*. Available at: http://2010.igem.org/Team:Warsaw/Stage1/RBSMeas.

Winograd, E., Pulido, M.A. & Wasserman, N., 1993. Production of DNA-recombinant polypeptides by *tac*-inducible vectors using micromolar concentrations of IPTG. *Biotechiques*, 14, pp.886-890.

Witwer, A., 2010. *A novel transcriptional termination signal capable to terminate T7 polymerase mediated transcription more efficiently*, Universität Wien.

Wösten, M.M.S.M., 1998. Eubacterial sigma-factors. *FEMS Microbiology Reviews*, 22, pp.127-150.

Yahr, T.L. & Wickner, W.T., 2001. Functional reconstitution of bacterial Tat translocation *in vitro*. *The EMBO Journal*, 20, pp.2472-2479.

6. List of Figures

7. List of Tables